Geologic Controls on Reservoir Quality of the Viola Limestone in Newbury Field, Wabaunsee County, Kansas

by

Creenen Ceddell McGuire

B.S., Northwest Missouri State University, 2016

A THESIS

submitted in partial fulfillment of the requirements for the degree

MASTER OF SCIENCE

Department of Geology
College of Arts and Sciences

KANSAS STATE UNIVERSITY
Manhattan, Kansas

2019

Approved by:

Co-Major Professor
Dr. Matthew Totten

Approved by:

Co-Major Professor
Dr. Abdelmoneam Raef

Copyright

Abstract

The focus of this study was Newbury field, Wabaunsee County, Kansas, and the geologic controls that allow for economic oil production from the Viola formation. Newbury field has produced 507,894 barrels of oil from the Viola formation between 1965 and 2018 (Newbury—Oil and Gas Production, 2018). The Viola formation's favorable reservoir characteristics have drawn production interest in Nebraska, Kansas, and Oklahoma, with 50 fields producing oil along the boundary of the Forest City basin and Nemaha ridge (Dolton and Finn, 1989). The Viola formation is a Middle to Upper Ordovician age carbonate composed of dolomite, chert, and limestone (Adkinson, 1972).

South of Newbury field are the Davis Ranch and John Creek fields. Davis Ranch and John Creek are the two largest fields along the western boundary of the Forest City basin in northeastern Kansas. Davis Ranch and John Creek have produced 9,084,020 and 10,305,259 barrels of oil, respectively, from the Viola formation (Davis Ranch—Oil and Gas Production, 2018; John Creek—Oil and Gas Production, 2018). So, what geologic controls allow for such variation in production from the Viola formation within the Forest City basin of northeastern Kansas?

Two previous studies of the Soldier and Leach fields, which are northeast of the Newbury field, showed that production there has been less than that of Newbury field (Jensik, 2013; Rennaker, 2016). These studies reported that Viola reservoir quality is controlled by dolomitization (Jensik, 2013; Rennaker, 2016), because areas of dolomitization showed greater porosity and permeability, which in turn results in more favorable reservoir characteristics (Jensik, 2013; Rennaker, 2016).

To understand this variation in production quality from the same formation, geologic controls of the Viola formation in Newbury field were identified using well log analysis; binocular and petrographic microscopy; alizarin red staining, subsurface mapping, and reserve calculations.

Several conclusions that will aid geologists to more easily identify economically viable Viola formation reservoirs along the western edge of the Forest City basin were drawn from this study. Production variation between fields in the Forest City basin is controlled not only by structure, but also by porosity. Viola formation porosity varies with spatial distribution due to varying degrees of dolomitization. Degree of dolomitization controls dolomite crystal size and dolomite texture, and thus controls porosity. Porosity is also affected by large scale fracture networks due to the proximity of the Nemaha Uplift. Production within Newbury field varies due to structure, but also from differences in dolomite crystal size and texture, and thus porosity. Wells in Newbury field with smaller dolomite crystal size ranges and euhedral to subhedral textures have slower, but longer production, while wells with large dolomite crystal size ranges, and euhedral to anhedral textures have short lived production.

Table of Contents

List of Figures

List of Tables

Acknowledgements

I would like to thank Ken Walker of Stoke of Luck Energy & Exploration, LLC for reaching out to the Department of Geology for this study. Without Ken's permission and personal financing, this study would not have been possible. I am also grateful for Ryan Keast, Adam Lane, Victor Cimino, Billy Hagood, Christian Tucci, Spencer Brower, Zachary Van Ornam, Austin Schuck, and Luke Rijfkogel for passing on their wisdom and being supportive of my endeavors. I will be forever grateful for my advisors Dr. Matthew Totten and Dr. Abdelmoneam Raef for giving me this opportunity and providing guidance and advice during my journey. Finally, I want to thank my wonderful mother, Tammy McGuire, for her undying support in all my educational pursuits and for always pushing me to strive and achieve my dreams.

Dedication

I would like to dedicate this thesis to my mother as she has helped me achieve my dreams in so many ways that I could never repay her.

Chapter 1 - Introduction

With the Forest City basin of northeastern Kansas becoming the target of increased exploration, how might geologists better understand the large variation in historical production between oil fields, so future exploration can be more successful? Certain fields within the Forest City basin have been known producers since the 1950's, producing large amounts of hydrocarbons. To the southwest of Newbury field are two of the largest producing fields on the western edge of the Forest City basin, Davis Ranch field and John Creek field. Davis Ranch has produced 9,084,020 barrels of oil and John Creek has produced 10,305,259 barrels of oil (Davis Ranch—Oil and Gas Production, 2018; John Creek—Oil and Gas Production, 2018). However, some fields in the Forest City basin have produced less than Newbury field. Northeast of Newbury field are some of the lower producing fields on the western edge of the Forest City basin. Only one of 17 fields to the northeast has produced over one million barrels of oil from the Viola formation (McClain—Oil and Gas Production, 2018). So, what geologic controls allow for such variation in production from the Viola formation within the Forest City basin of northeastern Kansas?

Chapter 2 - Background

Newbury Field

Newbury field, located in Newbury Township, is in north central Wabaunsee County, Kansas (Figure 1). The western boundary of the Forest City basin cuts through Wabaunsee County, with the eastern three-fourths of the county within the Forest City basin. Newbury field lies within the Forest City basin along the boundary between the basin and the Nemaha ridge. The field encompasses the southern half of section two and all of section eleven, T11S R11E.

Skelly Oil Company discovered Newbury field as they were drilling the Fearon 1 well for structural information in October of 1950 (Lewis, 1960). The field covers an area of 160 acres and was developed using 20 acres spacing in a staggered pattern (Lewis, 1960). Oil is produced from the coarsely crystalline, dolomitic, Viola formation in the upper 15 feet of a small concentric anticline (Lewis, 1960). At the time, only one well completely penetrated the Viola formation, G. Reiners 1, which determined that the Viola formation is 106 feet thick in Newbury field (Lewis, 1960). Oil production from Newbury field is driven by a natural water drive that produces a black crude with an API gravity of 24° (Lewis, 1960).

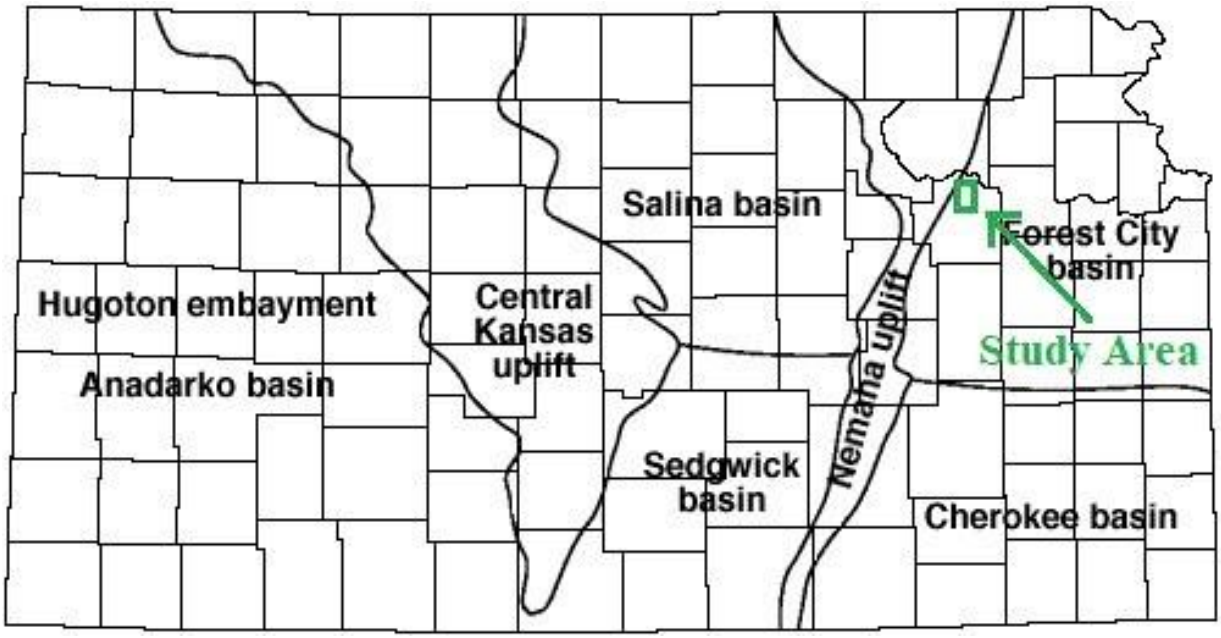

Figure 1: A map of Kansas showing county boundaries as well as the major basins and geologic structures. The area of study is indicated by the green square. Modified from Baars et al. (1989).

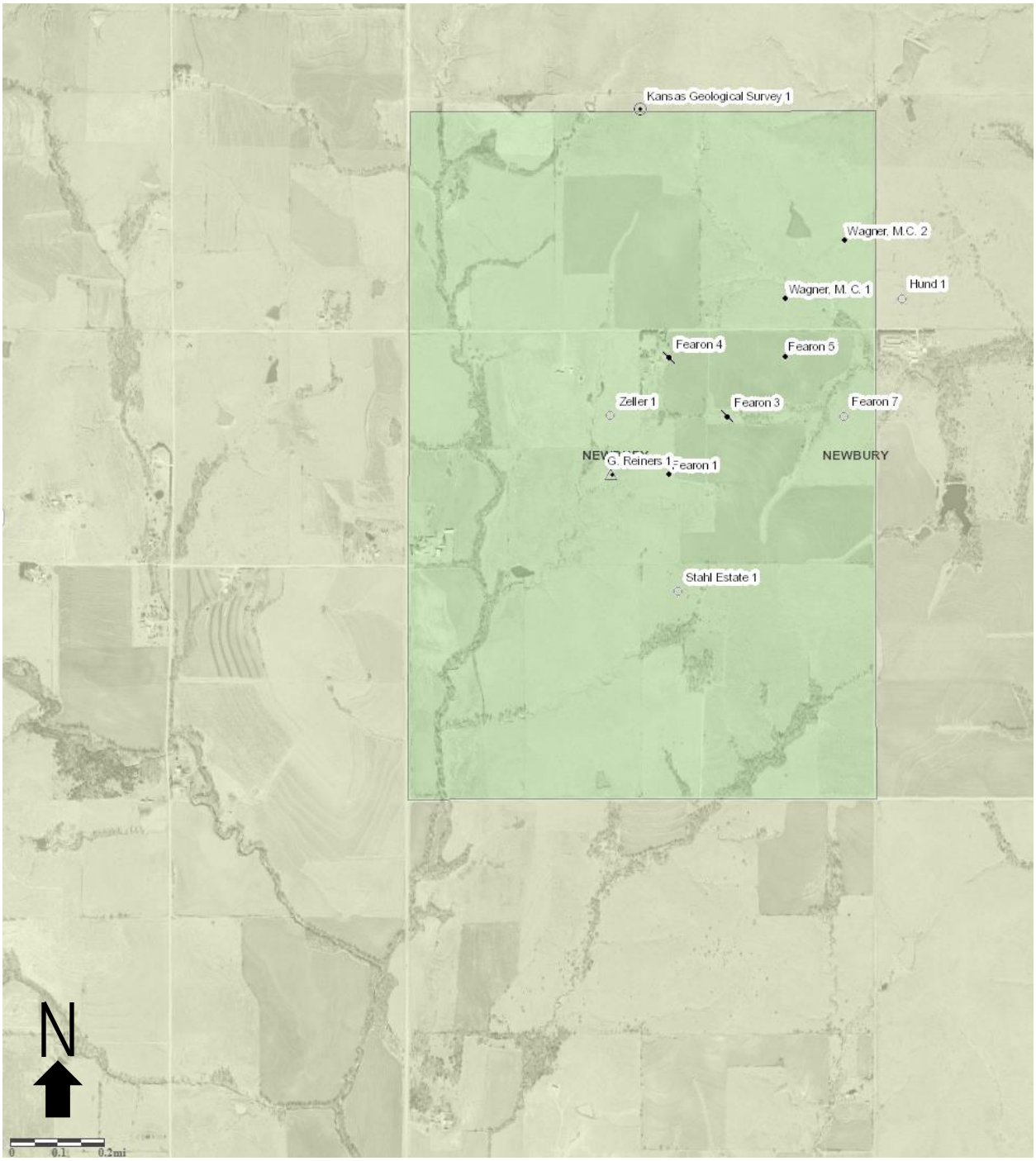

Figure 2: Aerial map showing the study area inside of the shaded green box as well as the location of wells in this study. Wells of interest are Fearon 1, Fearon 3, Fearon 4, Fearon 5, Wagner M.C 1, and Wagner M.C 2. Modified from Kansas Geological Survey Interactive Oil and Gas Wells and Fields (2018).

Well Name	NAD27 Longitude	NAD27 Latitude
Fearon 1	-96.1581159	39.1117669
Fearon 3	-96.1558046	39.1136392
Fearon 4	-96.1581292	39.1154382
Fearon 5	-96.1534783	39.1154873
Wagner M.C 1	-96.1534747	39.1172611
Wagner M.C 2	-96.1511352	39.1190783

Table 1: Table showing the NAD27 longitude and latitude of each of the wells in the study.

Between 1950 and 2018, Newbury field produced 507,894 barrels of oil from the Viola formation (Newbury—Oil and Gas Production, 2018). Newbury field is a unique occurrence in the immediate vicinity with the only other oil production at Paxico field two miles to the south. Production at Paxico field lasted one-year totaling 1,898 barrels of oil from the Hunton formation (Paxico—Oil and Gas Production, 2018). Ken Walker, owner and operator of Stroke of Luck Energy and Exploration LLC, holds leases in Newbury field and selected it as an area for future hydrocarbon exploration. This research aimed to understand the geologic controls that affect Viola formation reservoir quality at Newbury field and the disparity in production between fields located in the Forest City basin. It is also the goal of this study to evaluate the remaining production potential of Newbury field.

Geologic Setting

The Forest City basin is a shallow basin comprised of structural and depositional features that encompass portions of Iowa, Kansas, Missouri, and Nebraska (Adler et al., 1971). The basin is structurally bounded on the west by the Nemaha ridge, the south by the Bourbon arch, the north by the Thurman-Redfield fault, and on the east by the Cherokee Group outcrop (Figure 3) (Adler et al., 1971).

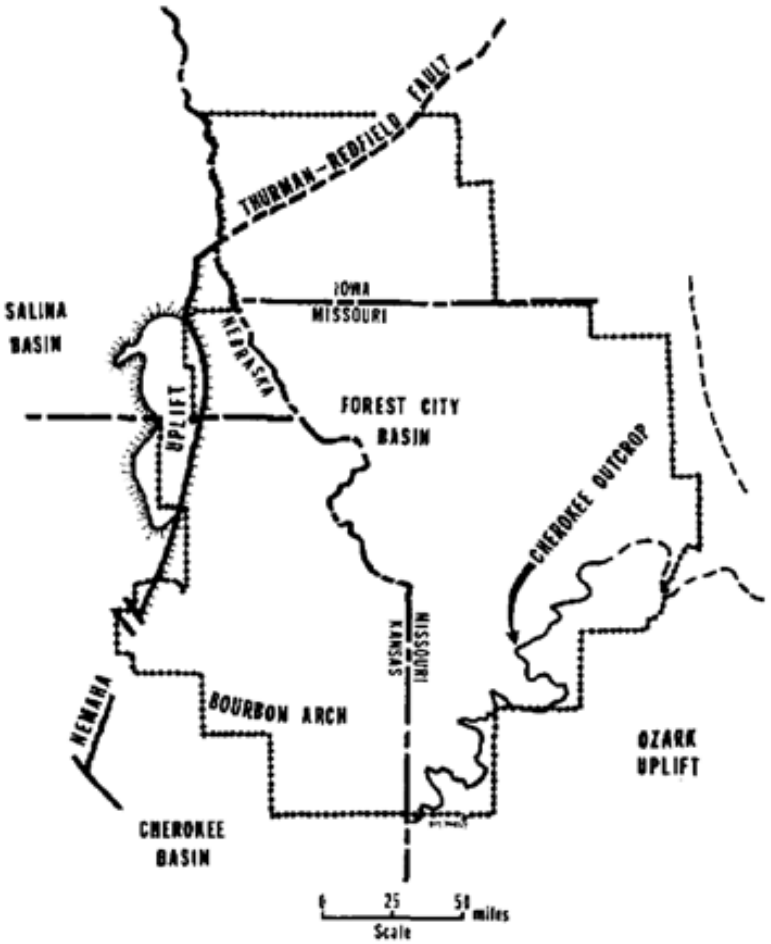

Figure 3: Map of Iowa, Kansas, Missouri, and Nebraska showing the structural and depositional boundaries of the Forest City basin (Adler et al., 1971).

During the Late Middle Ordovician the basin began forming when the Chautauqua arch formed in southeastern Kansas and southern Missouri (Adler et al., 1971). Introduction of the

Chautauqua arch and Ozark uplift formed an area of higher elevation creating a sedimentary basin to the north known as the Iowa Basin (Adler et al., 1971). During the Late Mississippian and Early Pennsylvanian, movement along the Nemaha ridge split the Iowa Basin in two, creating the Forest City basin to the east and Salina basin to the west (Figure 4) (Adler et al., 1971). Faulting and downwarping to the east of the Nemaha ridge created the asymmetrical shape of the basin, with the deepest portion of the basin near the Nemaha ridge (Adler et al., 1971) Sediment from the Nemaha ridge first began to fill the Forest City basin during Atokan time (308 – 311.7 Ma), but this stage of deposition was interrupted due to flooding from rising sea levels. During this period of high sea level, the Nemaha ridge remained exposed at the surface marking the start of a transgressive sequence that included the Cherokee, Marmaton, and Pleasant formations (Adler et al., 1971). The transgressive sediment deposition persisted until the Nemaha ridge was flooded during early Missourian time (305 – 306.5 Ma). This period of flooding marked a new stage of deposition that buried the Nemaha ridge (Adler et al., 1971)

Two structural trends are observed in the basin. A northwest to southeast trend formed during the Cambrian and Early Ordovician, and a northeast to southwest trend that developed during and after the Mississippian (Adler et al., 1971). The intersection of these trends created the doming effect, anticlinal structures, present within the basin strata (Adler et al., 1971).

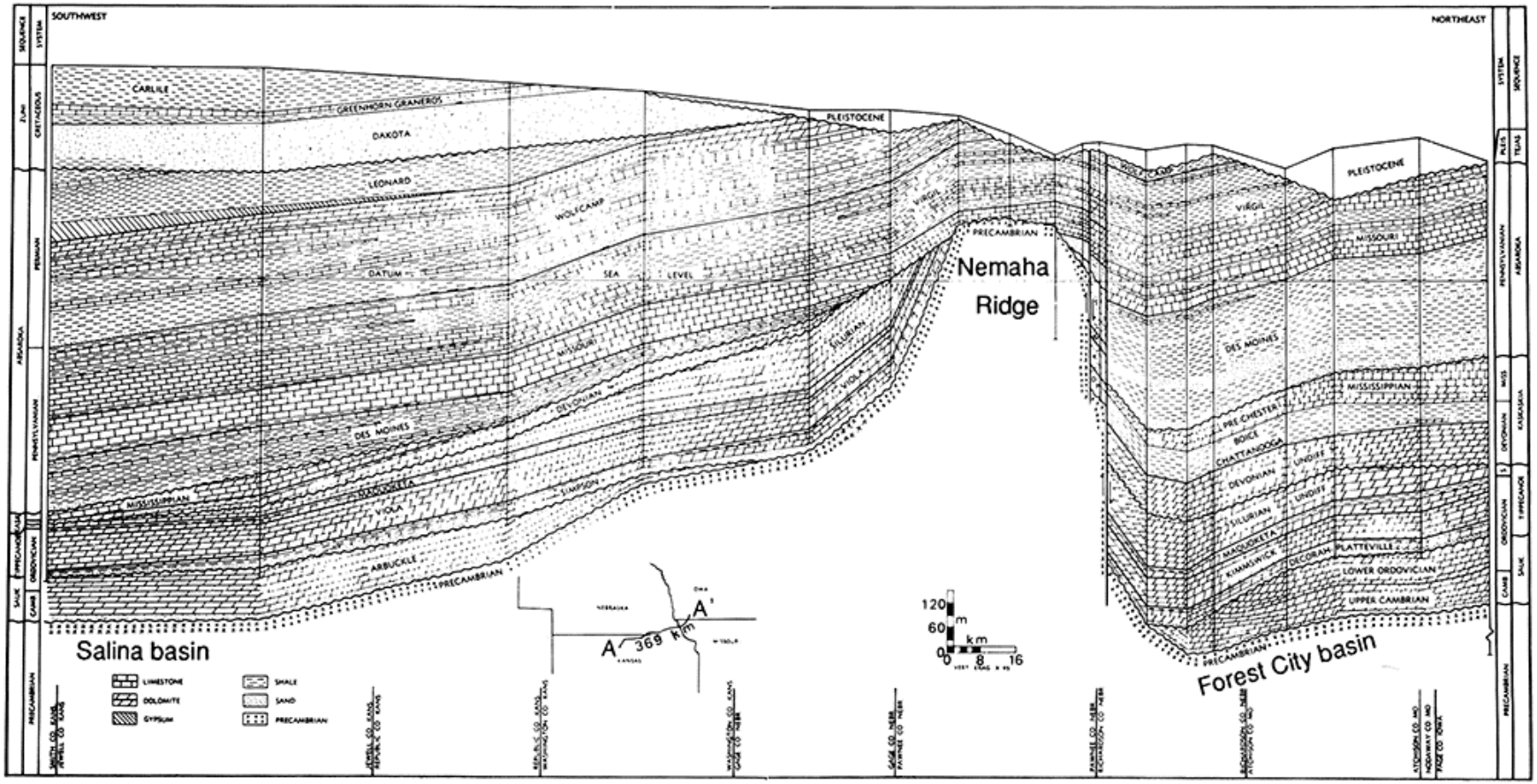

Figure 4: Basin profile showing the Nemaha Ridge splitting what was the Iowa basin into the Salina basin on the left and the Forest City basin on the right (Steeples, 1982)

Forest City Basin Oil Production and History

Oil and gas fields within the Forest City Basin cluster into three groups based on their location, oil geochemistry, trapping mechanism, and reservoir. The first group is made up of structural-stratigraphic and stratigraphic traps in Middle to Upper Pennsylvanian lenticular sandstones located along the eastern boundary of the basin, extending from Kansas City down to northeastern Oklahoma (Hatch and Newell, 1999). The second group is located on the western edge of the basin along the boundary with the Nemaha ridge (Hatch and Newell, 1999). This group extends along the northeast to southwest axis of the basin with hydrocarbons accumulated in anticlinal traps comprised of Paleozoic reservoirs (Hatch and Newell, 1999). High viscosity oil trapped in near surface Pennsylvanian sand lenses along the eastern and southern edges of the basin in Missouri and Kansas make up the third group (Figure 5) (Hatch and Newell, 1999).

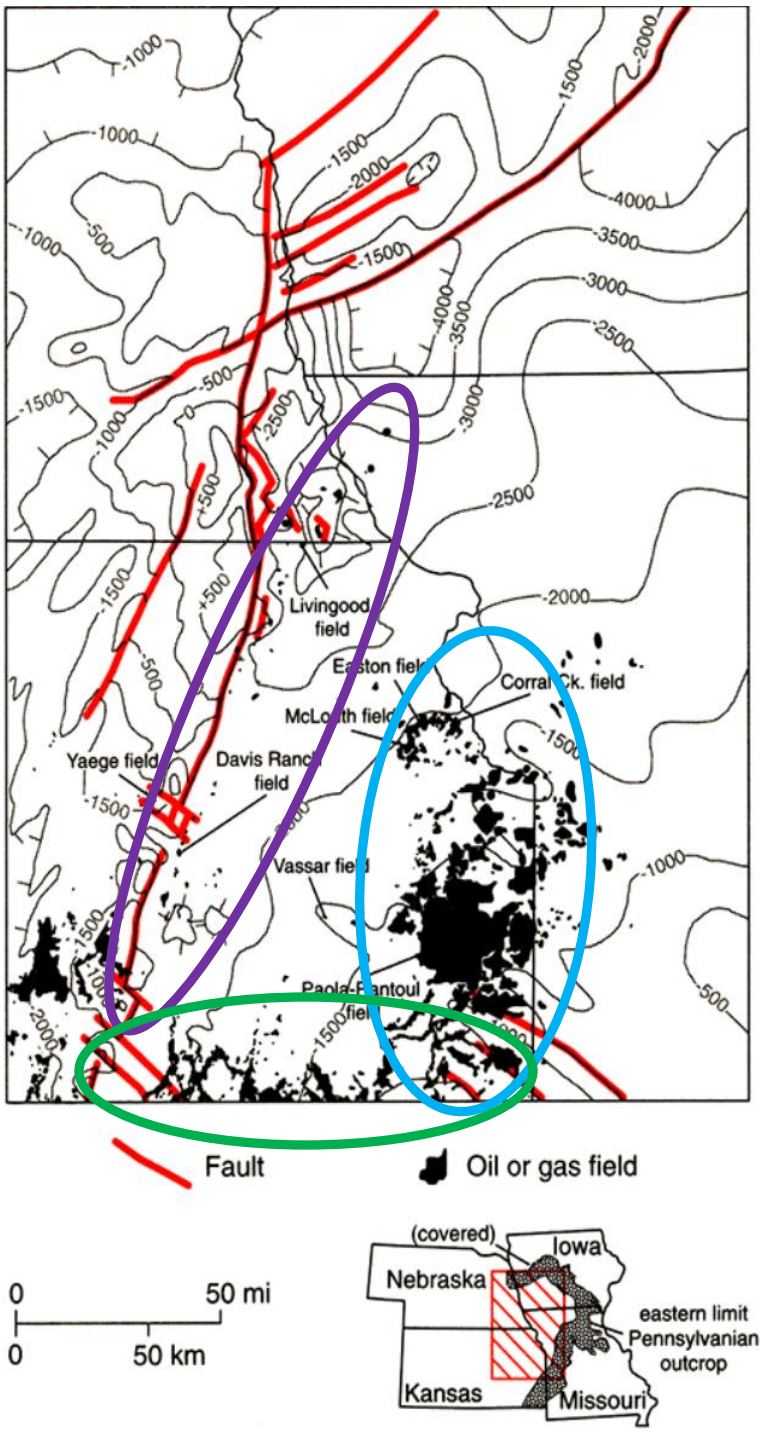

Figure 5: Map showing the three distinct groups of oil and gas fields in the Forest City basin. The first group of oil and gas fields is outlined by the blue oval, the second group by the purple oval, and the third group by the green oval. Groups one and three have some overlap, but the oil and gas fields in this overlapping area are classified into the correct group by their oil geochemistry, trapping mechanism, and reservoir type. Modified from Hatch and Newell (1999).

Oil and gas exploration in the Forest City basin began in 1860 with the drilling of the first well west of the Mississippi River near Paola, Kansas, which was a dry non-producing well (Anderson and Wells, 1960). Later that same year, near Paola, the first successful well was drilled and encountered oil at 275 feet below the surface in lenticular Middle to Upper Pennsylvanian sandstones (Anderson and Wells, 1960). The successful well marked the beginning of the Paola field, which has gone on to produce 100 million barrels of oil and 6.6 billion cubic feet of gas (Newell et al., *Hydrocarbon Potential,* 1987; Powers, 1994). Since the first successful discovery, oil fields along the western edge of the Forest City basin along the boundary of the Nemaha ridge have produced ~32 million barrels of oil from Paleozoic reservoirs (Newell et al., *Hydrocarbon Potential,* 1987). The United States Geological Survey (USGS) (1995) estimated undiscovered, conventional hydrocarbon plays to have ~20 million barrels of oil, ~70 billion cubic feet of gas, and less than 10 million barrels of gas liquids still recoverable within the Forest City basin (USGS, 1995). Although 24 years have passed since the USGS made their predictions, there are still economic amounts of undiscovered oil and gas within the Forest City basin, but there is not a definitive exploration model to aid in locating high quality drilling sites.

Formation of Interest

The upper Viola formation, due to its good porosity, permeability, and production history, is the principle formation of study for Newbury field. More than 50 fields in Oklahoma, Nebraska, and Kansas that border the Nemaha ridge have produced oil from the Viola formation (Dolton and Finn, 1989). Newbury field's cumulative 507,894 barrels of oil produced is more than average, but also less than several of the surrounding fields. Fields to the northeast of

Newbury field such as Leach, Soldier, and Casey have produced 394,345 barrels, 30,983 barrels, and 181,162 barrels of oil, respectively, from the Viola and Hunton formations (Figure 6) (Leach—Oil and Gas Production, 2018; Soldier—Oil and Gas Production, 2018; Casey—Oil and Gas Production, 2018). To the southwest of Newbury field, fields such as Davis Ranch and John Creek have produced 9,084,020 and 10,305,259 barrels of oil, respectively, from the Kansas City, Hunton, and Viola formations, with the Viola accounting for most of the production.

Heterogeneous oil recovery between fields in northeastern Kansas characterizes the Viola formation. Therefore, two questions arise: What are the geologic controls at Newbury field that allow for greater oil recovery compared to some fields to the northeast, and what are the possibilities that other locations in northeastern Kansas also feature these conditions?

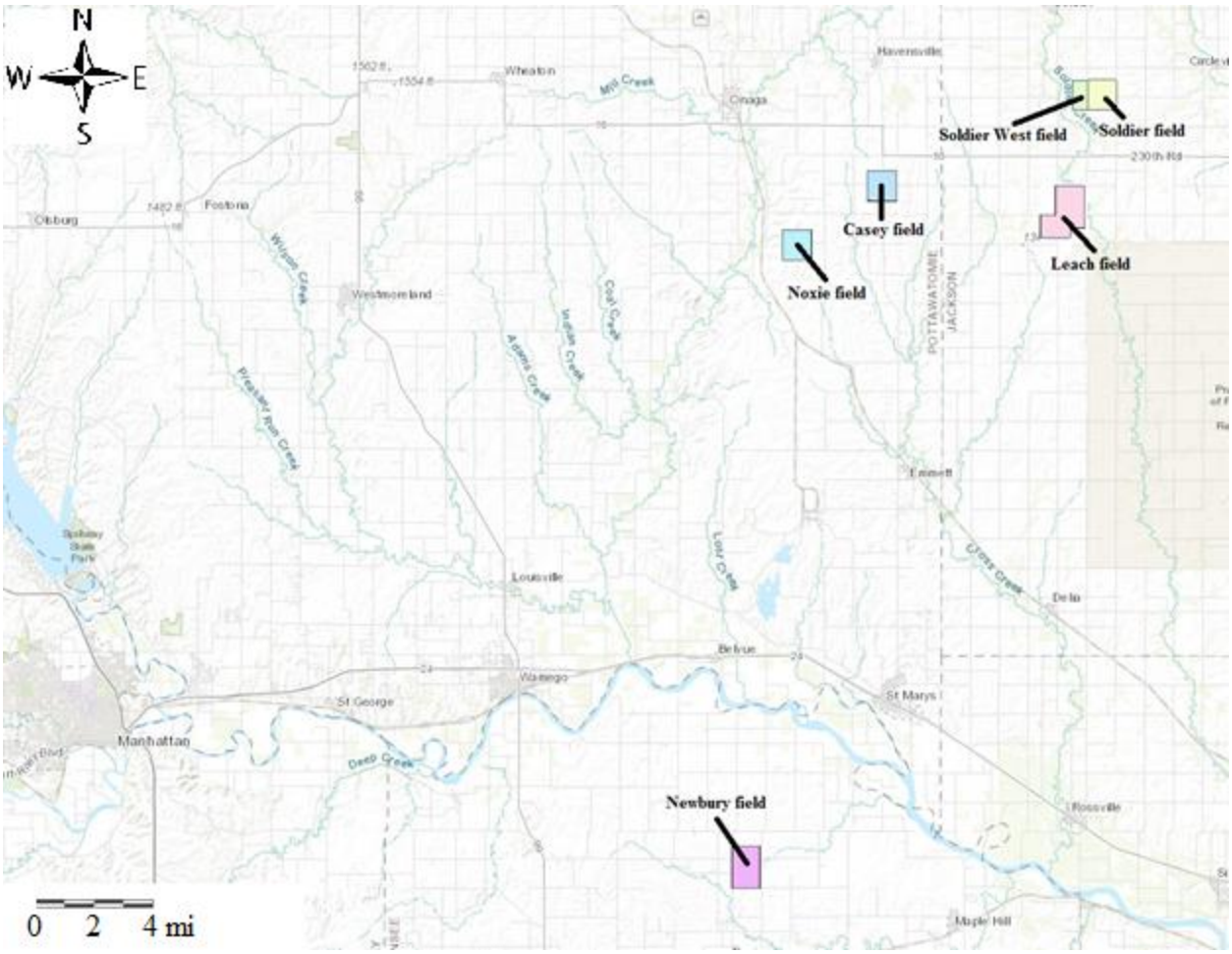

Figure 6: Terrain map showing the location of Newbury field in relation to Soldier, Soldier West, Casey, Leach, and Noxie fields. Modified from Kansas Geological Survey Interactive Oil and Gas Wells and Fields (2018).

Viola Formation

The Viola formation is characterized as a carbonate of Middle to Upper Ordovician age that is bounded below by the Simpson Group and unconformably overlain by the Maquoketa Shale (Figure 7) (Adkinson, 1972). In northeastern Kansas the Viola formation is primarily dolomite north of Douglas, Johnson, Osage, and Lyon counties, and limestone to the south of these counties (Lee, 1943). Three distinct zones comprise the Viola formation in northeastern Kansas (Lee, 1943): an upper dolomitic layer, cherty middle layer, and sparsely cherty bottom

layer (Lee, 1943); however, this study only provided descriptions for the upper dolomitic zone of the Viola formation, because of limited well penetrations. Minimum thickness of the Viola formation is <1 foot in southwestern Kansas and maximum thickness is 310 feet in Washington County in northeastern Kansas (Zeller, 1968). In Wabaunsee County, Kansas, the Viola formation is 106 feet thick in one well that completely drilled through the zone (Lee, 1943). Large variations in thickness and the absence of the Viola formation in several locations of Kansas are due to extensive erosion, as evidenced by the unconformity on top of the Viola formation (Adkinson, 1972).

The upper zone of the Viola formation in northeastern Kansas is primarily dolomitic but may include limestone in some areas (Lee, 1943). It is thin toward the southern edge of the Forest City basin at just 5-10 feet thick but increases in thickness toward the north with values varying between 20-40 feet thick (Lee, 1943). Chert is not present in the upper layer of the Viola limestone in Kansas but drusy, vesicular, and fibrous semi-opaque quartz is present in small quantities ranging from three to ten percent (Lee, 1943). Porosity types within the Viola formation include fracture, vuggy, moldic, and intergranular (Newell et al., *Stratigraphic and Spatial,* 1987).

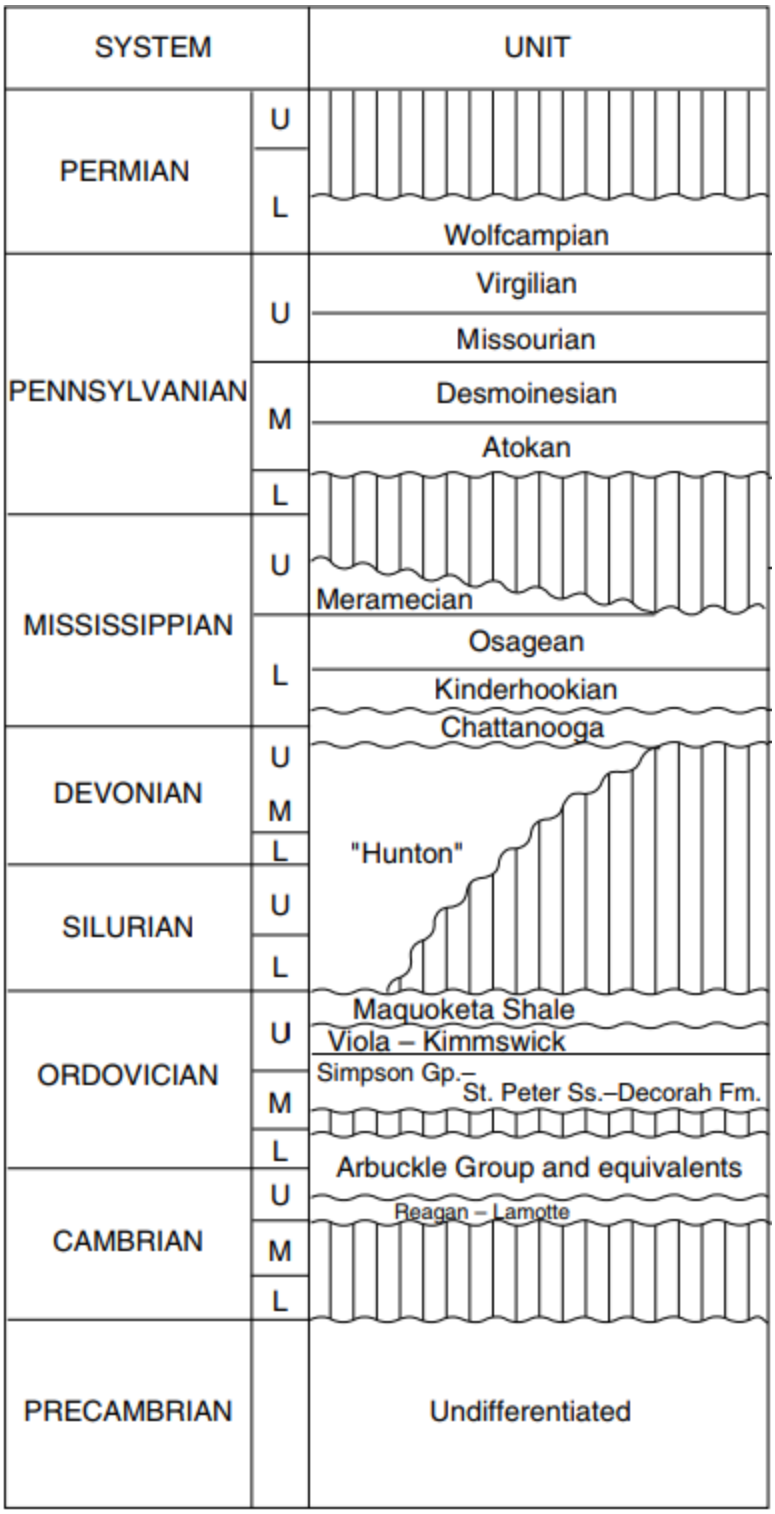

Figure 7: Stratigraphic column for northeast Kansas showing the Ordovician Viola formation above the Simpson Group and unconformably overlain by the Maquoketa Shale (Charpentier, 1995).

Dolomitization

Dolomite ($CaMg(CO_3)_2$) reservoirs in the United States hold most of the recoverable oil and gas that is found in carbonate rocks, making dolomitization an important process in this study (Qing Sun, 1995). Dolomite can either form as primary or secondary dolomite, with secondary dolomite being much more common (Al-Awadi et al., 2009). Primary dolomite is created from the precipitation of aqueous solutions in the form of dolostone or as dolomite cement (Al-Awadi et al., 2009). Secondary dolomite is created by the replacement of limestone ($CaCO_3$) with dolomite, which occurs when magnesium rich waters percolate through limestone, and some of the calcium ions in the limestone are substituted with magnesium ions to form dolomite (Al-Awadi et al., 2009). The formation of dolomite through replacement of limestone theoretically increases the porosity by as much as 13% (Qing Sun, 1995). This porosity increase occurs because the volume of calcite dissolved is greater than the volume of dolomite that precipitates and replaces it (Weyl, 1960). This is not always achieved, as several dolomite units have been discovered that are nonporous (Qing Sun, 1995). A study by Powers (1962) in the Arabian Upper Jurassic dolomites provided additional insight into dolomitization's effect on porosity. Powers (1962) concluded that permeability decreases in carbonate rocks that have 10-80% dolomite replacement. Powers (1962) also found that when carbonate rocks have been replaced by 80-90% dolomite, there is a significant increase in intercrystalline porosity as well as permeability (Powers, 1962). Carbonate rocks with greater than 90% dolomite replacement start to decrease in porosity and permeability (Powers, 1962). At and above 95% dolomite replacement, the effective porosity and permeability begin to decrease to the point that the rock nears impermeability (Qing Sun, 1995). Also, dolomite achieves greater porosity over limestone at depth due to grain supported fabric (Al-Awadi et al., 2009). Grain-supported dolomite is better

suited than limestone to resist compaction due to overburden, thus preserving porosity at depth (Al-Awadi et al., 2009). Grain-supported fabric is achieved when dolomite replacement reaches 80% (Al-Awadi et al., 2009). Dolomitization is also known to increase pore throat size and decrease pore roughness, allowing for better flow of hydrocarbons through reservoir rocks (Allan and Wiggins, 1993). These reasons are why dolomite holds most of the recoverable oil and gas reserves found in carbonate rocks within the United States.

Dolomite Porosity, Texture Types, and Crystal Size

Texture describes mineral constituents' shape and how they are aligned. There are three different dolomite textures: anhedral, euhedral, and subhedral (Sibley and Gregg, 1987). Texture plays a large role in dolomite porosity and was identified and described using a petrographic microscope, following dolomite texture descriptions by Sibley and Gregg (1987).

Porosity is all the void space within a rock. It is quantified by taking the amount of void space divided by the total rock volume. Porosity is one of the two main geologic controls that determines how viable a rock is as a reservoir. The higher the porosity of a rock the greater quantity of hydrocarbon that rock can store. Thus, it was important for this study to identify and determine the amount of porosity within the Viola formation. Porosity type was determined using a petrographic microscope, following the terminology proposed by Choquette and Pray (1970). Dolomite porosity types observed for the rocks in this study include: intercrystalline, moldic, fracture, or vuggy (Choquette and Pray, 1970).

Dolomite units can be made up of crystals that are homogeneous or heterogeneous in size. Differences in crystal size alter the reservoir properties of dolomitic reservoirs (Mazzulo, 2004). There are seven distinct dolomite crystal sizes presented by Scholle and Ulmer-Scholle

(2003). The crystal sizes groups determined by Scholle and Ulmer-Scholle (2003) were used to describe samples for this study.

Dolomite Textures

Anhedral – Anhedral texture is dolomite described as having irregular intercrystalline boundaries that is made up of serrated, curved, or lobate crystals closely packed together (Figure 8) (Sibley and Gregg, 1987). In an anhedral texture, the straight edges of dolomite crystal faces are not observed due to crowding of the dolomite crystals (Sibley and Gregg, 1987). Often undulatory extinction can be observed microscopically under cross polarized light (Sibley and Gregg, 1987).

Euhedral – Euhedral textured dolomite is described as grain-supported with distinct rhombohedral crystals that have well defined, straight-edge crystal faces (Figure 8) (Sibley and Gregg, 1987). The area in between dolomite rhombs is either filled with another mineral or porous (Sibley and Gregg, 1987).

Subhedral – Subhedral textured dolomite is described as having compromised crystal face edges, but some crystal face edges are preserved (Figure 8) (Sibley and Gregg, 1987). Subhedral texture is usually represented by limited intercrystalline matrix (Sibley and Gregg, 1987).

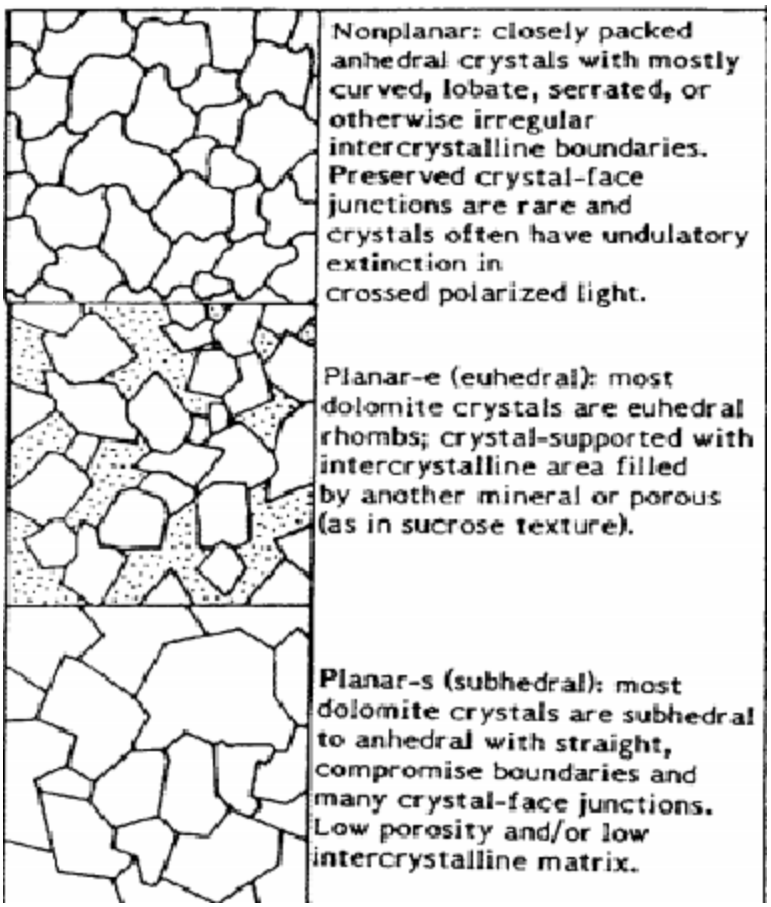

Figure 8: Diagram showing the three textures present in dolomite: anhedral, euhedral, and subhedral (Sibley and Gregg, 1987).

Porosity Types

Intercrystalline – Intercrystalline porosity is defined as porosity located in between individual crystals (Figure 9) (Choquette and Pray, 1970). In porous dolomite these crystals should be roughly equal in size (Choquette and Pray, 1970). Intercrystalline porosity can be found in primary and secondary dolomites (Choquette and Pray, 1970).

Moldic – Moldic porosity occurs where a crystal, shell fragment, fossil, or oolite has been removed due to dissolution (Figure 9) (Choquette and Pray, 1970). In dolomite, moldic porosity usually forms from the dissolution of original calcite or aragonite constituents (Choquette and Pray, 1970).

Fracture – Fracture porosity is any porosity that forms due to breaks in a rock (Figure 9) (Choquette and Pray, 1970). This porosity type is formed where there is enough displacement between different portions of a rock body that fractures occur (Choquette and Pray, 1970). Fractures in carbonate rocks can occur due to deformation, dissolution collapse, and slumping (Choquette and Pray, 1970).

Vuggy – Vuggy porosity is described as porosity that can be seen with the naked eye, is equant in shape, not stretched, and is not fabric selective (Figure 9) (Choquette and Pray, 1970). This means that vuggy porosity does not conform to any of the shapes represented by primary constituents (Choquette and Pray, 1970). Most commonly, vuggy porosity is created due to the dissolution of primary constituents. With extensive dissolution the original constituent shape is lost (Choquette and Pray, 1970).

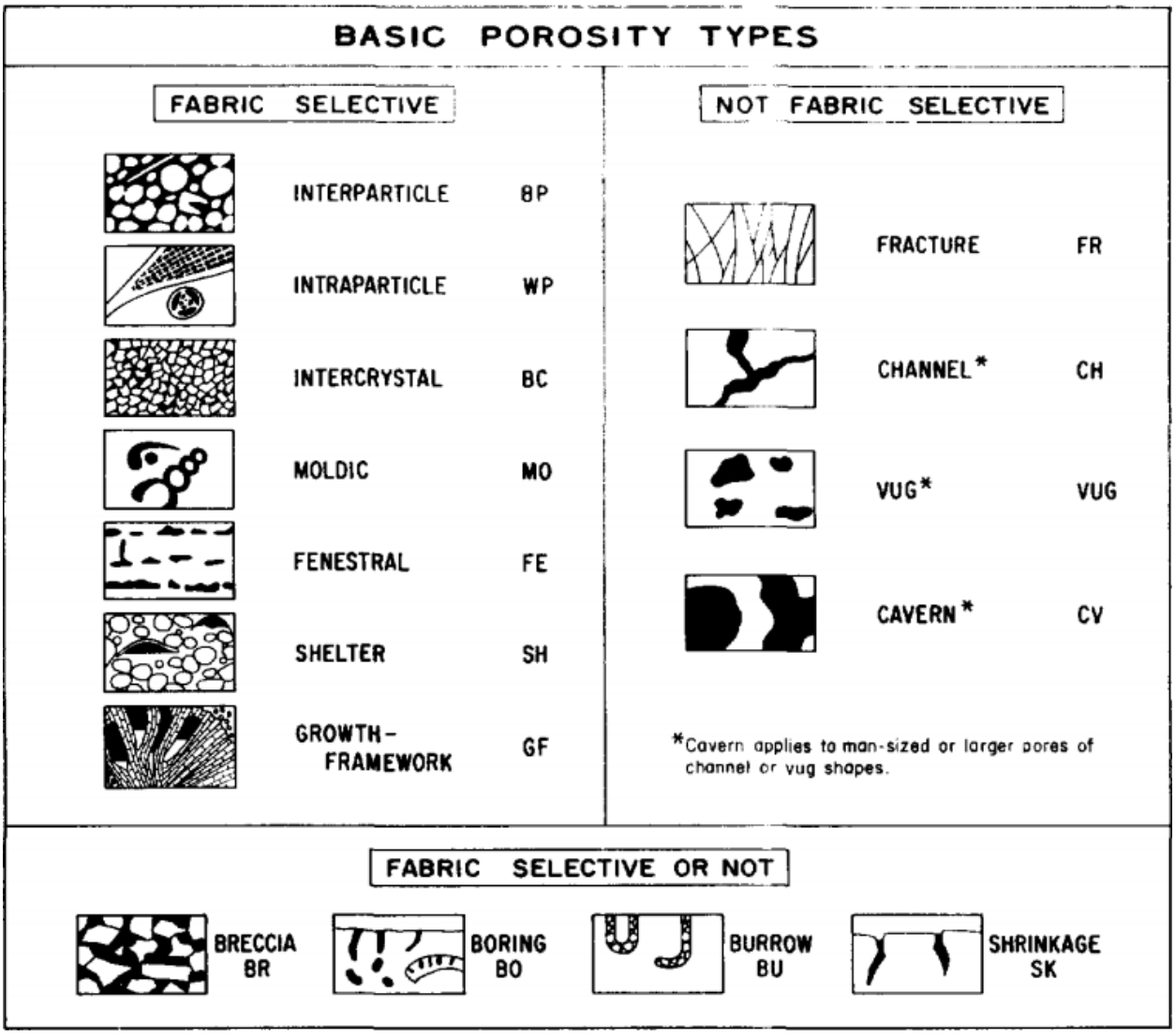

Figure 9: Diagram showing carbonate porosity types. Of importance to this study are intercrystalline (intercrystal), moldic, vuggy (vug), and fracture (Choquette and Pray, 2003).

Crystal Size

Crystal size will be reported following the scheme proposed by Scholle and Ulmer-Scholle (2003), as shown in figure 10.

Figure 10: Diagram showing the size ranges and designations for crystal size. Modified from Scholle and Ulmer-Scholle (2003).

Previous Studies

Oil fields flanking the Nemaha ridge along the western edge of the Forest City basin have been the focal point of two previous studies conducted at Kansas State University (Jensik, 2013; Rennaker, 2016). Jensik (2013) studied Soldier field and Rennaker (2016) studied Leach field, both in Jackson County, Kansas. Both studies worked on determining the geologic factors controlling oil production in the area. Jensik (2013) concluded that production is controlled by the fabric and size of dolomite crystals. He also noticed that porosity and permeability increase where large euhedral dolomite crystals are present in the Viola Limestone. This suggests that wells with coarsely crystalline, euhedral dolomite have higher porosity because the large dolomite crystals are unable to fit together tightly (Jensik, 2013). He also hypothesizes that

intercrystalline porosity observed in coarsely crystalline samples increases permeability by connecting vuggy pores, whereas the medium crystalline samples, due to the smaller crystal size, fill more of the pore spaces, cutting off the interconnectedness of the pores (Jensik, 2013).

The results of Rennaker (2016) are consistent with Jensik (2013). Both found that larger euhedral dolomite crystals were located on the downdip portion of the concentric anticlinal structures, suggesting that variability in crystal size between the top of the anticlinal structures and the flanks is due to deformation of the Viola formation soon after deposition (Jensik, 2013; Rennaker, 2016). This deformation created anticlinal structures that caused the Viola formation at the top and bottom of the structure to undergo dolomitization at differing times, duration, and number of events causing variability in crystal size and texture. (Jensik, 2013; Rennaker, 2016).

Chapter 3 - Methods

Reservoir characterization for this study consisted of analyzing well cuttings using binocular and petrographic microscopy, subsurface mapping, porosity analysis, carbonate mineralogy determination using alizarin iron cyanide red stain, and oil reserve estimations. Six wells were selected for analysis and chosen based on four key criteria: 1) availability of geological reports that included tops data; 2) penetration into the Viola formation; 3) availability of well cuttings including the interval of the Viola formation and held by the Kansas Geological Survey; and 4) availability of at least some type of record for production history. The six wells selected were the only wells that checked all four criteria at the time cuttings were collected and prepared. These six were all productive wells and thus, no dry wells were included in the study. These oil and gas wells include: Fearon 1, Fearon 3, Fearon 4, Fearon 5, Wagner M.C 1, and Wagner M.C 2 (Figure 2). Cuttings for the wells were collected from the Kansas Geological Survey's rotary-cutting samples library in Wichita, Kansas.

The methods used to characterize the reservoir for this study were limited due to the lack of core for examination, limited penetration of the Viola, lack of modern well logs, missing geological reports, limited number of wells, cuttings availability, and the general lack of information regarding the Forest City basin and oil and gas fields in northeastern Kansas.

Binocular Microscopy

A binocular microscope was used to examine and select cuttings that were subsequently used for thin section analysis. Cuttings for all six wells in the study were analyzed using the binocular microscope.

The open-hole completions within Newbury field required an unorthodox approach to examination and selection of cuttings. This is due to the lack of well log coverage across the Viola limestone in Newbury field, as the logging tool used did not measure the bottom of the hole. Normally, cuttings for a study of this type would be selected by determining the actual depth to the formation of interest. Actual depth to the formation of interest is decided by taking the lag time, the amount of time it takes for cutting samples from a certain depth to reach the surface, converting the lag time into feet, and then subtracting that value from the depth to the top of the formation of interest. The calculated depth is then compared to characteristic signatures that indicate the top of the formation found on well logs, usually the gamma ray log, to make sure that the calculated depth is correct. Unfortunately, well logs for the Viola formation were not available for any of the wells in this study. So, a different method had to be used to determine the depth range of Viola limestone cuttings.

None of the wells in Newbury field drilled completely through the Viola formation. Instead, they drilled into the top of the formation; each well then had a period during which cuttings were circulated and cleared from the hole at total depth. After a 45 to 60-minute circulation time period, the cuttings coming out of the hole were from the bottom of the well and contained the Viola formation. Knowing this information, cuttings were picked from the longest circulation time interval first, so that a good visual description of the Viola formation was formed.

The Viola limestone from Newbury field is distinctly sucrosic, whitish gray, when oil staining is not present, light tan to very dark brown, when oil staining is present, and exhibits visible crystals when looked at under the binocular microscope. Working backwards up the hole from that point, cuttings from the Viola formation were picked from different intervals, placed

into separate envelopes, and labelled. This was done until the interval containing Maquoketa shale was reached. The Maquoketa shale was easy to distinguish from the Viola limestone in cuttings due to it being primarily shale and its uniform greenish gray color.

Thin Section Preparation

Twenty one thin sections were created from cuttings that were handpicked under a binocular microscope. Each set of cuttings was placed into a single flat layer at the bottom of a medicine cup, so that resin blanks could be made. The medicine cups were labelled with the corresponding well name, depth, and circulation time interval. Fiberglass resin, hardener, and blue dye were mixed together and poured into each medicine cup, completely covering each cutting with the mixture. Blue dye was added to the mixture so ImageJ software could be used to estimate the porosity of cuttings. Each medicine cup was then placed in a vacuum chamber one at a time to remove air trapped in the pore spaces, and to ensure that resin had filled any pore spaces in the cuttings once the vacuum was released. Air was purged from the chamber three times for five seconds each time. The blanks were left to harden overnight at ambient temperature and pressure. The blanks were separated from the medicine cups by simply peeling the cups away from the hardened resin. Each blank was kept separated from the others and placed on a piece of paper that was labelled with the well name, depth, and circulation time interval. The topside of each blank was then made flat by firmly pressing it onto a piece of 220-grit sandpaper and moving it in a figure eight motion vigorously until the entire surface of the blank had been scuffed. Once the topsides were flattened, blanks were placed on a Hilquist grinder and the bottom side of the blank, where the cuttings are located, was ground down until all the cuttings were visible and flat. Blanks were mounted, bottom side down, onto petrographic

thin sections coated with a thin layer of fiberglass and hardener mixture. The thin sections were left to harden for a few hours at ambient temperature and pressure, and then the well name, depth, and circulation time interval were scribed into each thin section using a diamond tipped jewelry engraver. Thin sections were placed on the grinder and excess resin from the top of the thin sections was ground away in small incremental steps until the thickness was approximately 30 microns. The 30-micron thickness was achieved using a dial indicator attached to the grinder.

Thin sections were polished to remove or minimize scratches left behind during the grinding process. Each thin section was polished in a four-step process using a table top disk sander. First, 220-grit sand paper was placed on the disk sander and coated with a layer of water. Thin sections were placed onto the disk sander and firmly held in place while the disk sander was turned on to the lowest speed setting. Each thin section was held in place for 15-20 seconds. The 220-grit sand paper was removed once every thin section had been polished and replaced with 400-grit. The process was repeated until each thin section had been polished using 220, 400, 800, and 1000-grit sand paper. At this point the thin sections were ready to be analyzed using the petrographic microscope.

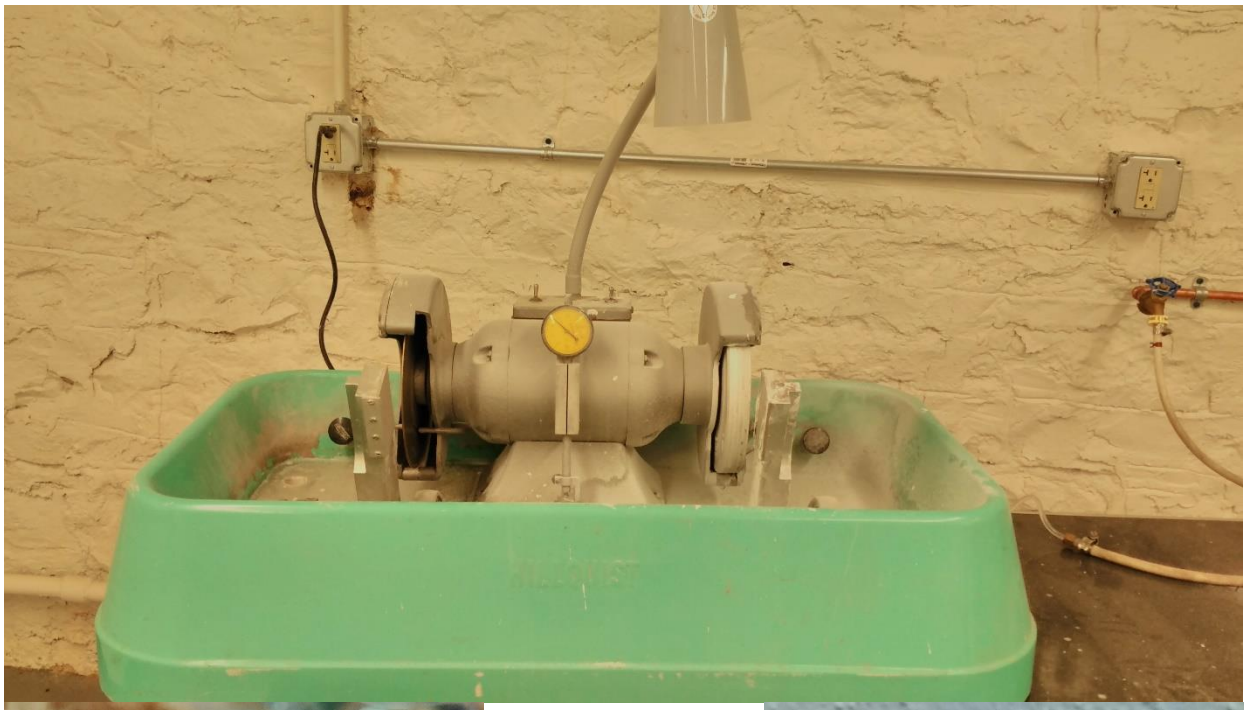

Figure 11: Images in order from top to bottom and left to right. Image of cutting blanks inside of pill cups and labelled by well name, depth, and circulation time. Image of cutting blank with the pill cup removed and the top side, the side with no cuttings, being flattened using sandpaper, preparing it to be placed on the Hilquist grinder. Image of blank placed

on the Hilquist grinder with the bottom side, the side with cuttings, facing the grinding disk. Wide view image of the Hilquist grinder. Image of a petrographic thin section with a thin coat of fiberglass resin and hardener mixture applied. Image of a blank glued onto a petrographic slide. Image of a blank applied to a thin section mounted to the Hilquist grinder with the top side of the blank facing the grinding disk. Finally, a completed thin section ground down to roughly 30 microns and ready to be polished.

Figure 12: Images in order from top to bottom and left to right. Image of a thin section mounted in the thin section holder. Image of the table top disk sander and the sand paper that is applied to the surface of the sander. Image of the sand paper after it had been applied to the disk sander. Image showing the faucet that was used to apply a thin layer of water onto the sand paper. Image showing the method that thin sections were held in place on the disk sander using the thin section holder. Image of the speed controller, speed was always set to I.

Petrographic Microscope

A petrographic microscope was used to examine each thin section so that crystal size, texture, and porosity type could be observed. Thin sections were also analyzed for other interesting features such as oil staining and the presence of ooids.

A Leica DM 2700 P petrographic microscope equipped with a camera and Leica Application Suite (LAS) was used to examine and photograph thin sections. Thin sections were placed on the sample stage and a general look at the entire thin section was completed using 2.5x

magnification in plane polarized light (PPL), as well as cross polarized light (XPL). Any significant feature was noted and then each thin section was looked at in more detail using various levels of magnification. Porosity type was determined first, and descriptions by Choquette and Pray (1970) were used to identify different porosity types (Figure 9). Every void space observed was classified as either intercrystalline (intercrystal), moldic, vuggy (vug), or fracture. Texture was determined using dolomite texture descriptions by Sibley and Gregg (1987) and the range of textures present was noted (Figure 8). Textures included anhedral, euhedral, and subhedral. Crystal size was determined next using size range values from Scholle and Ulmer-Scholle (2003). The smallest and largest dolomite crystal observed for each thin section was located and documented to give a range of crystal sizes present. Next maximum porosity was located, and a photomicrograph was taken at 5x magnification in PPL using LAS. The most representative cutting or cuttings for each thin section was located and a photomicrograph was taken at 2.5x magnification in PPL and XPL using LAS.

ImageJ Porosity Estimation

The Java-based image processing program ImageJ was used to determine porosity estimates from thin sections using photomicrographs taken in PPL at 5x magnification. ImageJ was opened on the computer and a photomicrograph was uploaded and opened in the program. Next the photomicrograph was converted into a 32-bit gray-scale image within ImageJ, and the program was set to measure area percentage (%Area). Photomicrographs were converted to 32-bit gray scale so that the pore spaces are represented as white hues and the mineral grains are represented as gray and black hues. The %Area calculation measures the area covered by a set threshold and is proportional to the porosity of the rock. Next, the threshold was set so that it included as much of the pore spaces while minimizing the amount of mineral grains included in

the threshold. The threshold works by filling in all the white hues and gray hues up to the set saturation threshold with a red color. Once this was completed a measurement of the %Area was calculated by ImageJ and recorded in Microsoft Excel. Most of the photomicrographs only showed cuttings, but some included portions of the thin section background. In this case, the portion of interest for porosity estimates was selected and isolated from the background to ensure an accurate porosity estimate. Also, the scale bar was excluded from the threshold, or was manually removed from the %Area calculation to avoid skewing of the results.

Alizarin Iron Cyanide Red Staining

Alizarin iron cyanide red stain mixed with a 0.2% hydrochloric acid solution was applied to selected thin sections to aid in differentiating between dolomite and calcite grains. The main goal is to determine the amount of calcite and dolomite present with the hopes of contributing to the explanation of variations in porosity estimations between thin sections.

The staining process works due to the carbonate minerals present in the thin sections reacting at different rates with the hydrochloric acid in the solution. Only the carbonate minerals that readily react with acid, i.e. calcite, are stained a pink to reddish pink color. Dolomite, which does not readily react with hydrochloric acid, remains unstained and allows for easy identification of calcite and dolomite in thin sections.

Thin sections to be stained were selected based on their porosity estimates. Six thin sections were selected, such that the entire range of porosity estimates for the study was represented. Two thin sections exhibiting the lowest porosity, medium porosity, and highest porosity estimates had stain applied.

A thin section was placed onto the Leica DM 2700 P petrographic microscope equipped with a camera and LAS. This allowed the reaction between any carbonates and the stain to be monitored in case there was a vigorous reaction that needed to be stopped prematurely. The thin section had a drop of alizarin iron cyanide red stain placed onto each individual grain. Each thin section sat for 60 seconds before the alizarin iron cyanide red stain was rinsed off with water. A paper towel was used to dry the thin section and then it was placed back on the petrographic microscope for examination. Each thin section was examined using 2.5x magnification in PPL and XPL for the presence of stained grains. Any stained grains were noted and documented in Microsoft Excel.

Subsurface Mapping

A base map, placing all the wells at their respective locations, of Newbury field was created using IHS Petra mapping software. Well data were downloaded from the Kansas Geological Survey and entered into a spreadsheet for wells in Newbury field. The spreadsheet was opened in Microsoft Excel, edited and formatted. IHS Petra was opened and the spreadsheet was uploaded. Values for X-Y coordinates, depths to the top of the Viola formation, kelly bushing/drill floor elevations, and well type for each well were selected from the spreadsheet and assigned specific distinctions within IHS Petra. IHS Petra calculated the depth to the top of the Viola formation from sea level by subtracting the kelly bushing/drill floor elevation from the depth to the top of the Viola formation. Using X-Y coordinates from the spreadsheet, each well was placed onto a township and range map and a structure map was generated based on the depths to the top of the Viola formation from sea level. Unfortunately, due to the small number of wells in Newbury field, IHS Petra was unable to generate an acceptable structure map for the

Viola formation. A structure map of the Viola formation was created by hand, contouring the Viola tops onto the base map generated by IHS Petra. The hand drawn structure map was gridded, scanned, and then digitized back into IHS Petra to give it a more refined look.

Oil Reserves Calculations

Oil reserves were calculated using several steps and different equations. First, an oil water contact was determined. Two oil water contacts were determined based on the deepest well that has produced oil. By looking at the drill stem tests provided on the geologic reports, Fearon 7 was determined to be the deepest producer in Newbury field's history at 1,776 to 1,780 feet below sea level. The first oil water contact was hypothesized to be at 1,785 feet and the second at 1,795 feet below sea level. The hypothesized oil water contacts were then subtracted from the shallowest depth to reach the top of the Viola limestone to determine the oil column. Oil columns of 23 and 33 feet, respectively, were calculated.

Next, the areal extent of the Viola formation above the two oil water contacts was determined using hand drawn subsurface maps and ImageJ software. Starting at 1,765 feet below sea level, an individual subsurface map was created for each contour at a 5-foot interval until the depth of the two oil-water contacts was achieved (Figure 13). Every subsurface map was then scanned and opened in Microsoft Paint, where the inner portion of the contour line of interest was filled in with a light gray color and saved as a JPEG file (Figure 14). ImageJ was then launched, and the scale was set using a known distance between two wells on the subsurface map. The measurement type was set to area and was limited to the threshold. One by one each JPEG file was uploaded to ImageJ, converted to a 32-bit gray scale image, and had a threshold set manually to only include the light gray area that was filled inside of the contour line (Figure

15). Each JPEG file was then analyzed and a measurement of area was calculated by multiplying the number of pixels inside the threshold by the scale that was input previously. Finally, dividing by 43,560 converted the area from square feet to acres.

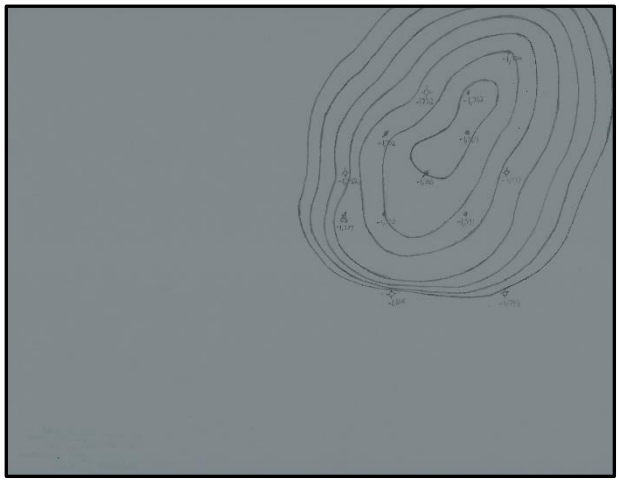

Figure 13: Structure maps showing each individual contour being added so the area of each contour can be calculated.

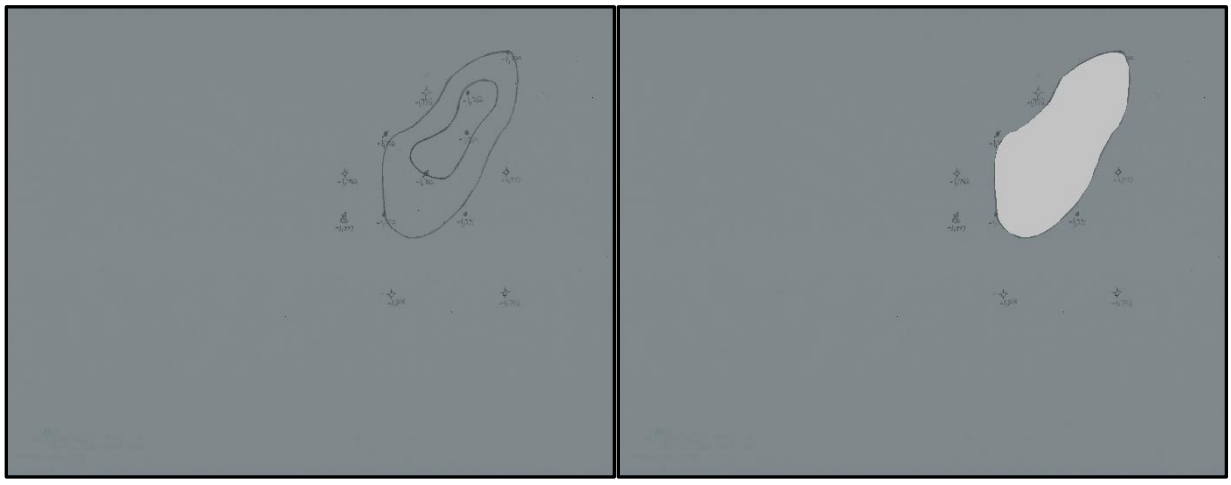

Figure 14: Structure map on the right and the same structure map with the inside of the contour line filled with a light gray color using Microsoft Paint on the left.

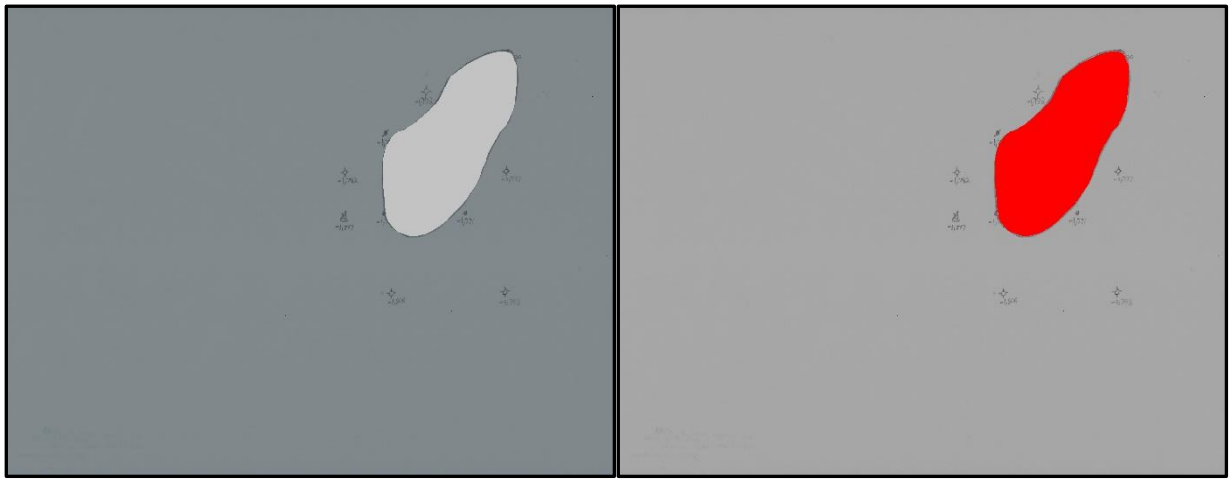

Figure 15: Structure map on the right and the same structure map after it has been converted to a 32-bit grayscale image and the threshold has been set in ImageJ on the left.

Volume of the reservoir above each of the oil-water contacts was determined next using area values determined by ImageJ and Simpson's rule (Figure 16). Simpson's rule is used to approximate volume under a curve over a known interval (Malvic et al., 2014). In the case of hydrocarbon reservoirs the anticlinal structure is representative of the curve, and the distance from the top of reservoir formation down to the oil-water contact is the known interval. In the Simpson's rule equation (Figure 16), h is equal to the contour interval in feet and $a_o \ldots a_1 \ldots a_2 \ldots$ are the areal extent in acres of each of the contour lines. Using this method, the volume in acre-feet was determined between the top and bottom contour lines, but the volume above the top contour line, top volume, still needed to be determined. Top volume, Vtop, is determined by taking the average of two equations, $Vtop_1$ and $Vtop_2$ (Figure 17). In these two equations, h_4 is the depth, in feet, from the top of Viola formation structure at 1,762 feet below sea level down to the 1,765-foot contour line. Also, a_4 is the area, in acres, inside of the 1,765-foot contour line. Finally, the volume determined using Simpson's rule was added to the Vtop volume to get the total volume of the Viola formation at Newbury field above the two oil water contacts.

$$V_{Simp} = \frac{h}{3}(a_0 + 4a_1 + 2a_2 + 4a_3 + a_4)$$

Figure 16: Simpson's rule in equation form (Malvic et al., 2014).

$$V_{top1} = \frac{h_4 a_4}{3}$$

$$V_{top2} = \frac{h_4^3 \pi}{6} + \frac{a_4 h_4}{2}$$

Figure 17: $Vtop_1$ and $Vtop_2$ equations (Malvic et al., 2014).

Finally, oil reserves were calculated using the volumetric method (Figure 18). In the equation below, (Figure 18), V is equal to the volume of the Viola formation within the oil column; 7758 is the number of barrels of oil there are in an acre-foot; Ø is the porosity, as a decimal, of the reservoir; S_o is the oil saturation, as a decimal, of pore spaces; R is the recovery factor, as a decimal, of the reservoir; and FVF is the formation volume factor, which is the ratio of oil to gas production (Hyne, 2001). Oil reserves were calculated using several combinations of different variables (Table 2). Reserves were calculated using two different volume values that represented an oil water contact at 1,785 and 1,795 feet below sea level. These values were 3,288.862 and 7,084.596 acre-feet, respectively. Porosity values using ImageJ average porosity of all the thin sections created, 4.27%, ImageJ average porosity of the highest porosity found at each well, 7.56%, visual porosity count average of each of the wells of 6.2%, and the average of the porosity at Davis Ranch field and John Creek field, 15.00% were evaluated. Oil saturation was calculated by taking the average of the oil saturations determined at two well developed fields, Davis Ranch and John Creek (Davis Ranch Field, 1960; John Creek Field, 1960). The oil saturation value calculated was 24.25%. A recovery factor for the Viola formation was estimated

at 70% (Richardson, 2016). Finally, an FVF of 1 was used, because there is such a small quantity of gas produced at Newbury field that it can be assumed that the formation volume factor is 1.

$$\text{stock tank bbls of oil} = \frac{V \times 7758 \times \emptyset \times S_o \times R}{FVF}$$

Figure 18: Equation for the volumetric method used to determine oil reserves (Hyne, 2001).

Oil Water Contact (Feet Below Sea Level)	Volume (Acre-Feet)	Porosity (%)	Oil Saturation (%)	Recovery Factor (%)
1,785	3,288.862	4.27	24.25	70
1,785	3,288.862	6.20	24.25	70
1,785	3,288.862	7.56	24.25	70
1,785	3,288.862	15.00	24.25	70
1,795	7,084.596	4.27	24.25	70
1,795	7,084.596	6.20	24.25	70
1,795	7,084.596	7.56	24.25	70
1,795	7,084.596	15.00	24.25	70

Table 2: Table showing the different combination of variables used to determine oil reserves at Newbury Field.

Chapter 4 - Results

The results for petrographic and porosity analyses are presented below. Discussion of each circulation interval, a group of cuttings that were collected within a specific amount of time as mud was allowed to circulate through the pipe, in which thin sections were created are grouped together with the well in which the cuttings originated. A brief written description of each thin section is provided, which includes: dolomite texture, crystal size, porosity type, and porosity estimates. Below every text description are four photomicrographs for each circulation interval analyzed for that well. The top left photomicrograph shows a general view of the thin section in plane polarized light (PPL), whereas the top right presents a general view of the thin section in cross-polarized light (XPL). The bottom left photomicrograph shows the highest porosity found within the thin section in PPL, but does not necessarily represent every porosity type observed for the thin section. The bottom right photo shows the same photomicrograph as the bottom left, but with the ImageJ threshold applied for porosity estimate determination. Below each set of images is a table that breaks down the information provided for the specific thin section in the text above. It includes the well name, depth, and circulation interval for the cuttings being discussed, as well as the dolomite texture, crystal size, porosity type, ImageJ porosity estimate, and visual porosity count estimate for the thin section.

A caveat must be made for the porosity estimates generated using ImageJ software. Porosity values from cuttings are notorious for giving mixed results due to the limited quantity of rock available for analysis and the nature in which the drill crushes the formation, creating cuttings. Cuttings also do not show large scale fracture and vuggy porosity as the scale of the porosity is larger than that of cuttings. The porosity values in this study are no exception, but these problems were further exasperated by issues that occurred while using ImageJ software.

There is a discrepancy in the visual estimation of porosity in thin sections, using visual porosity count methods, when compared to the estimated porosity calculated by ImageJ. It appears that ImageJ underestimates the porosity. This can be seen when looking at the photomicrographs that contain red coloration. The red represents the occurrence of porosity within the thin sections, and porosity values higher than those generated by ImageJ are encountered when a visual porosity count is done. The process of generating porosity estimates using ImageJ was completed on two separate occasions, getting the same results, offering no resolution for the problem. Because there are no cores and porosity logs penetrating the Viola formation for the wells studied, visual porosity counts were conducted to try and calibrate and correct the error produced by ImageJ. The magnitude of difference between ImageJ porosity estimates and visual porosity count estimates is not equal across all of the thin sections, but each of the thin sections saw an increase in porosity when using visual porosity counts. The magnitude of the error produced by ImageJ appears to be variable between thin sections to a small degree, but not variable enough to rearrange the hierarchy of porosity estimated for the thin sections. Visual porosity count estimates for each thin section was however higher than those generated by ImageJ proving that ImageJ underestimated porosity. Porosity estimates generated using ImageJ were reproducible, generated several times, showing precision, but lacking accuracy when compared to visual estimates of porosity that were determined, and thus were able to be used when comparing wells within the study, but accurately comparing the porosity values to those of surrounding fields was not possible.

Fearon 1

Geologic reports for Fearon 1 oil and gas well indicate a total depth of 2904 feet with the top of the Viola limestone occurring at 2901 feet. Based on the information from the geologic reports, well cuttings for Fearon 1 oil and gas well were collected from 2904 feet at the intervals of 15, 30, 45, and 60 minutes of circulation and thin sections were created from the selected cuttings. Petrographic analysis of the thin section created from cuttings at the 15-minute circulation interval revealed finely to very coarsely crystalline dolomite. The dolomite observed is euhedral to anhedral and exhibits intercrystalline porosity. Porosity for the 15-minute circulation interval was estimated at 1.7% using ImageJ software. Finely to very coarsely crystalline dolomite that is euhedral to anhedral was observed in the 30-minute circulation interval when looked at under the petrographic microscope. The 30-minute circulation interval has an estimated porosity of 8.8%, which includes intercrystalline and vuggy porosity. The 45-minute circulation thin section revealed finely to very coarsely crystalline dolomite that is subhedral. Intercrystalline porosity was observed when viewed under the petrographic microscope and porosity was estimated at 2.6%. Finally, finely to coarsely crystalline dolomite that is euhedral to anhedral was observed in the 60-minute circulation thin section. Intercrystalline porosity is present and ImageJ software estimated maximum porosity at 2.3%.

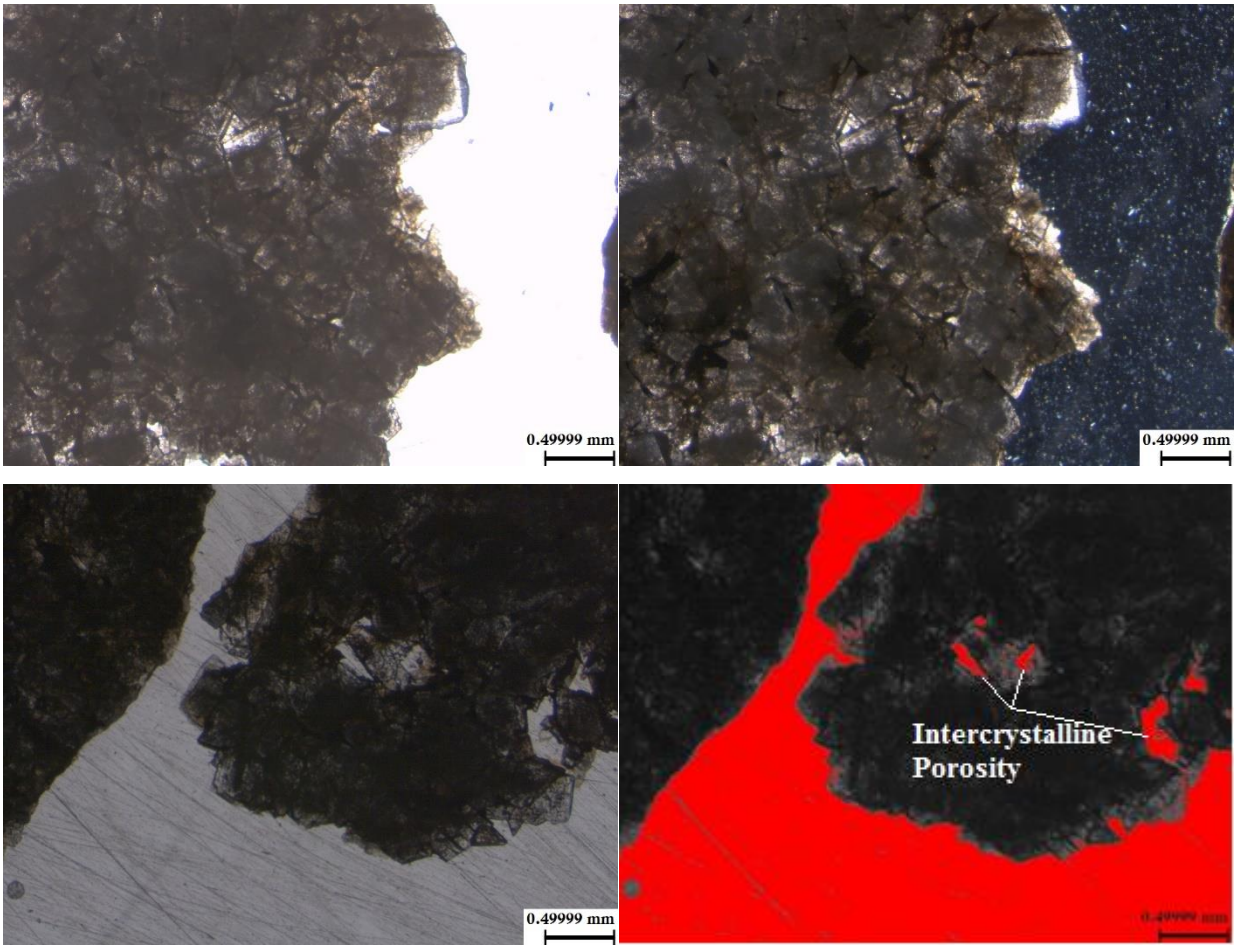

Figure 19: Optical PPL thin section (upper left), optical XPL thin section (upper right), optical PPL thin section (bottom left) and the corresponding ImageJ picture with threshold applied (bottom right) to estimate maximum porosity for Fearon 1 (2904 ft, 15 minutes circulation).

Well Name (Depth and Circulation Time)	Crystal Size	Texture	Porosity Type	ImageJ Porosity Estimate	Visual Porosity Count Estimate
Fearon 1 (2904 ft, 15 minutes)	Finely to Very Coarsely Crystalline	Euhedral to Anhedral	Intercrystalline	1.7%	5%

Table 3: Table summarizing thin section observations as well as maximum ImageJ porosity estimate and visual porosity count estimate for Fearon 1 (2904 ft, 15 minutes circulation).

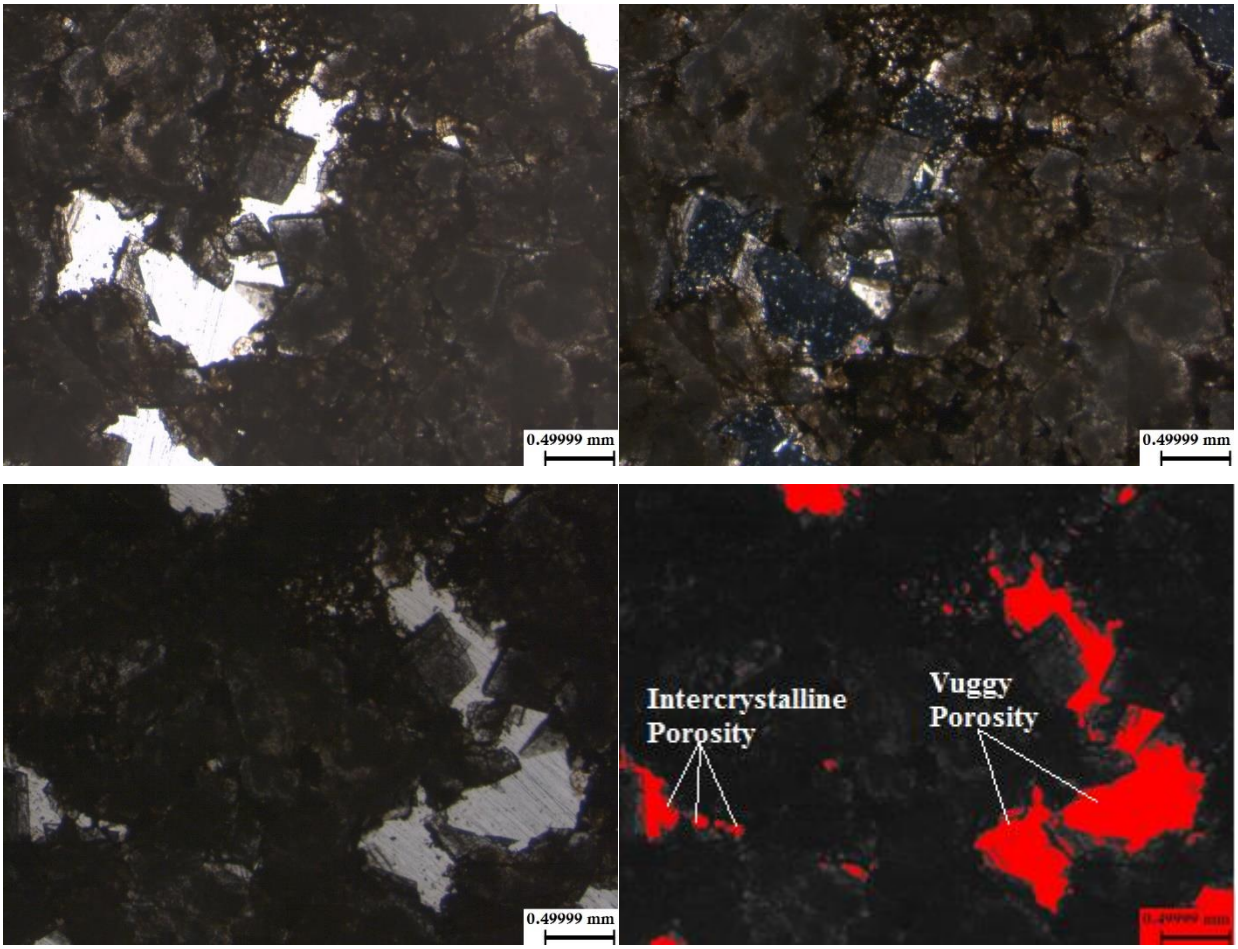

Figure 20: Optical PPL thin section (upper left), optical XPL thin section (upper right), optical PPL thin section (bottom left) and the corresponding ImageJ picture with threshold applied (bottom right) to estimate maximum porosity for Fearon 1 (2904 ft, 30 minutes circulation).

Well Name (Depth and Circulation Time)	Crystal Size	Texture	Porosity Type	ImageJ Porosity Estimate	Visual Porosity Count Estimate
Fearon 1 (2904 ft, 30 minutes)	Finely to Very Coarsely Crystalline	Euhedral to Anhedral	Intercrystalline, Vuggy	8.8%	10%

Table 4: Table summarizing thin section observations as well as maximum ImageJ porosity estimate and visual porosity count estimate for Fearon 1 (2904 ft, 30 minutes circulation).

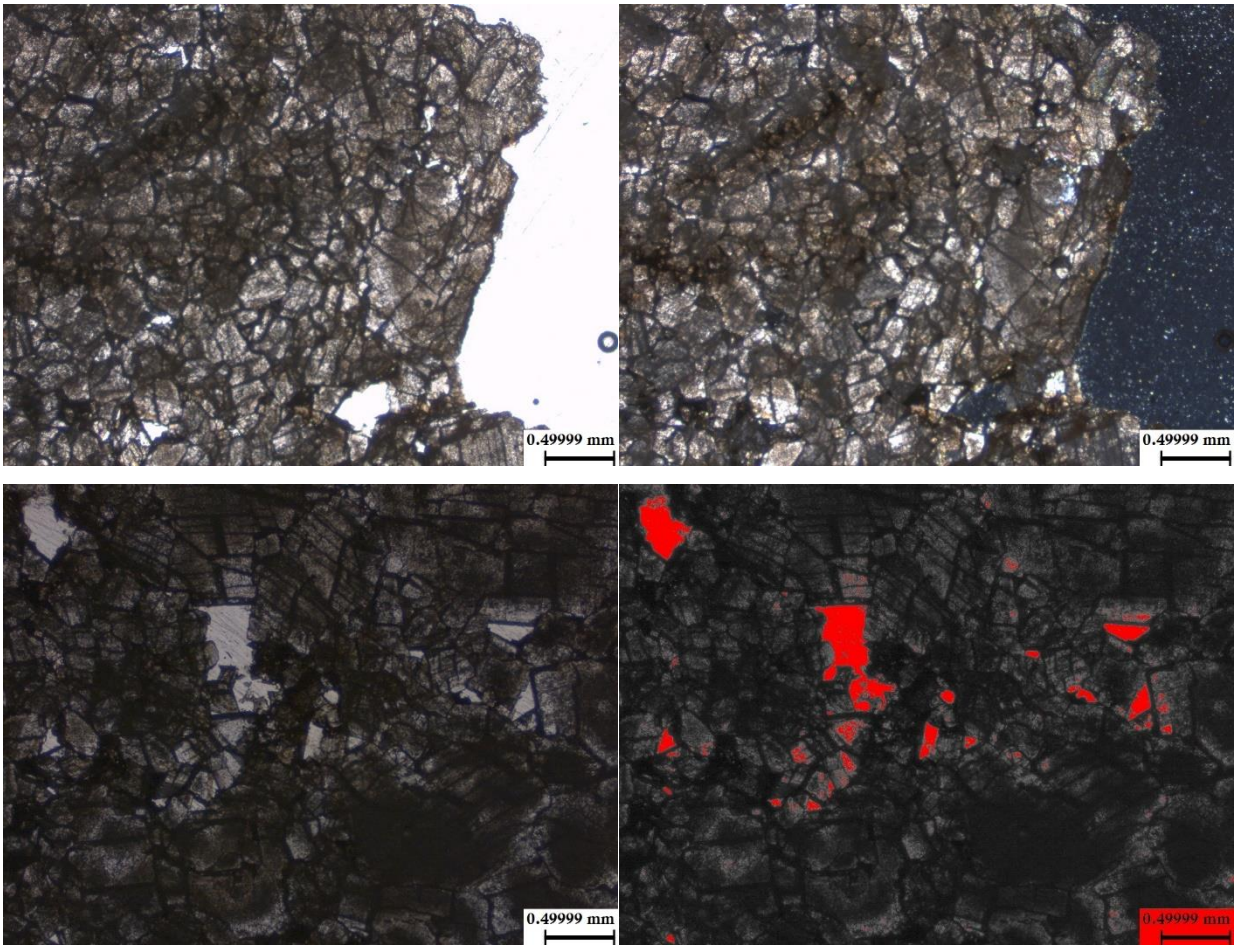

Figure 21: Optical PPL thin section (upper left), optical XPL thin section (upper right), optical PPL thin section (bottom left) and the corresponding ImageJ picture with threshold applied (bottom right) to estimate maximum porosity for Fearon 1 (2904 ft, 45 minutes circulation).

Well Name (Depth and Circulation Time)	Crystal Size	Texture	Porosity Type	ImageJ Porosity Estimate	Visual Porosity Count Estimate
Fearon 1 (2904 ft, 45 minutes)	Finely to Very Coarsely Crystalline	Subhedral	Intercrystalline	2.6%	5%

Table 5: Table summarizing thin section observations as well as maximum ImageJ porosity estimate and visual porosity count estimate for Fearon 1 (2904 ft, 45 minutes circulation).

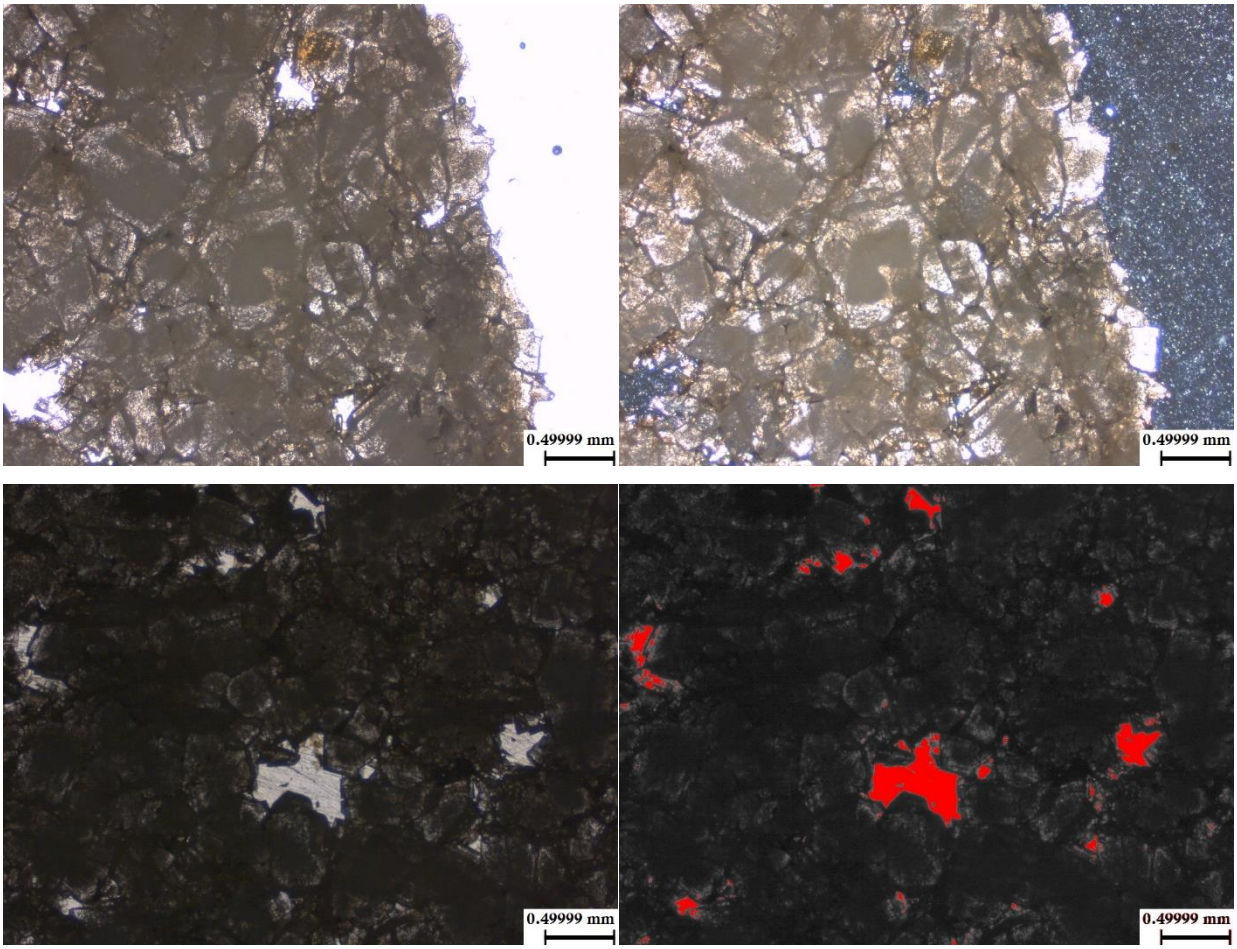

Figure 22: Optical PPL thin section (upper left), optical XPL thin section (upper right), optical PPL thin section (bottom left) and the corresponding ImageJ picture with threshold applied (bottom right) to estimate maximum porosity for Fearon 1 (2904 ft, 60 minutes circulation).

Well Name (Depth and Circulation Time)	Crystal Size	Texture	Porosity Type	ImageJ Porosity Estimate	Visual Porosity Count Estimate
Fearon 1 (2904 ft, 60 minutes)	Finely to Coarsely Crystalline	Euhedral to Anhedral	Intercrystalline	2.3%	8%

Table 6: Table summarizing thin section observations as well as maximum ImageJ porosity estimate and visual porosity count estimate for Fearon 1 (2904 ft, 60 minutes circulation).

Fearon 3

Geologic reports for Fearon 3 oil and gas well indicate that the bottom of the well is at 2885 feet, with the top of the Viola limestone occurring at 2882 feet. Well cuttings were collected from 2889 feet at the 15, 30, and 45 minutes of circulation intervals based on the information provided in the geologic reports. Thin sections were created using cuttings from the 15, 30, and 45-minutes circulation intervals and analyzed using a petrographic microscope. Analysis of the 15-minute circulation thin section revealed finely to coarsely crystalline dolomite that is euhedral to anhedral. Porosity is exhibited as intercrystalline and estimated at 6.7% using ImageJ software. Looking at the 30-minute circulation interval thin section exposed finely to coarsely crystalline dolomite. The dolomite present in the 30-minute circulation interval is euhedral to anhedral with intercrystalline porosity. ImageJ software estimated a maximum porosity of 2.2%. Lastly, the 45-minute circulation thin section exhibits very finely to very coarsely crystalline dolomite that is euhedral to anhedral. Intercrystalline and vuggy porosity is present, with porosity being estimated at 2.6%.

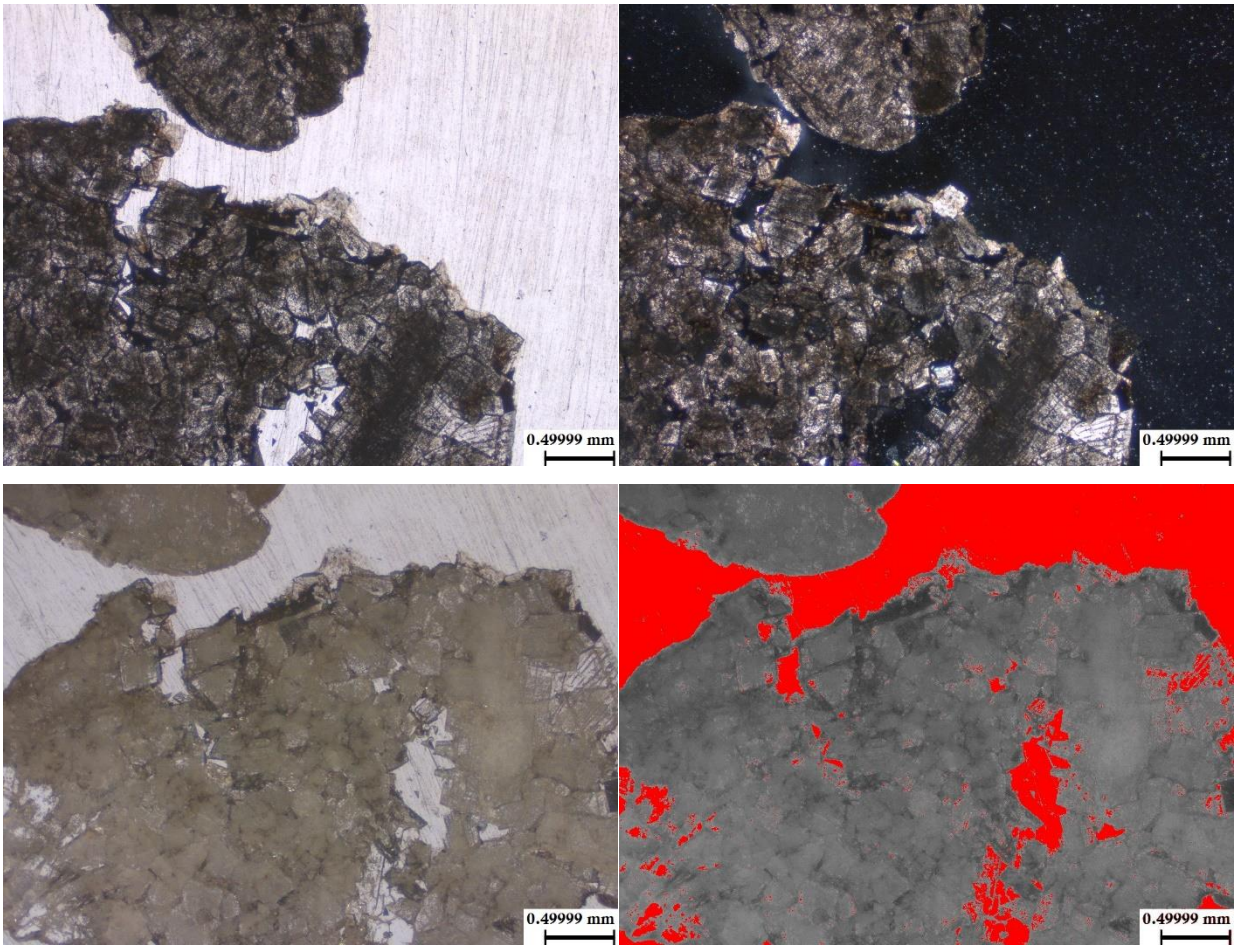

Figure 23: Optical PPL thin section (upper left), optical XPL thin section (upper right), optical PPL thin section (bottom left) and the corresponding ImageJ picture with threshold applied (bottom right) to estimate maximum porosity for Fearon 3 (2889 ft, 15 minutes circulation).

Well Name (Depth and Circulation Time)	Crystal Size	Texture	Porosity Type	ImageJ Porosity Estimate	Visual Porosity Count Estimate
Fearon 3 (2889 ft, 15 minutes)	Finely to Coarsely Crystalline	Euhedral to Anhedral	Intercrystalline	6.7%	10%

Table 7: Table summarizing thin section observations as well as maximum ImageJ porosity estimate and visual porosity count estimate for Fearon 3 (2889 ft, 15 minutes circulation).

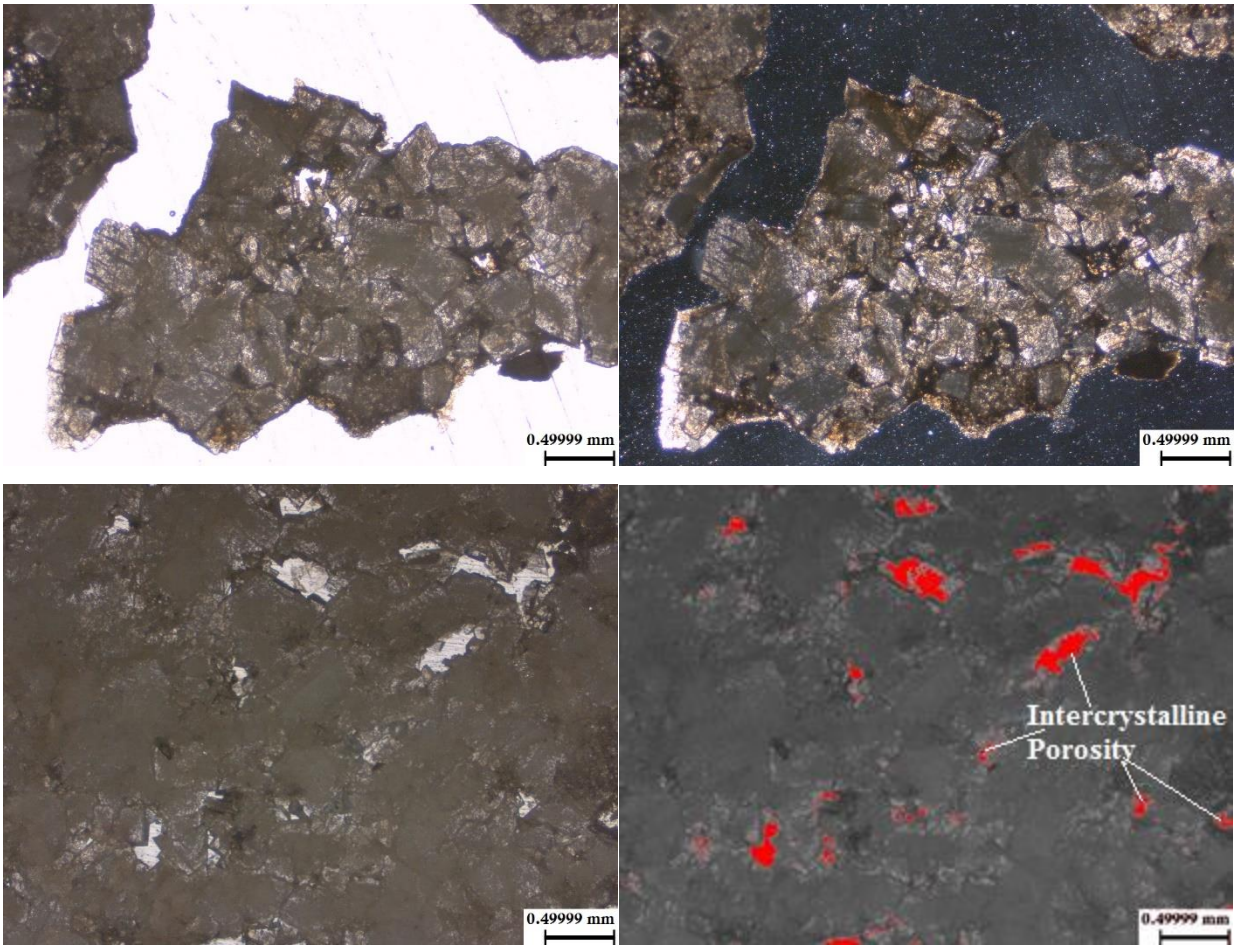

Figure 24: Optical PPL thin section (upper left), optical XPL thin section (upper right), optical PPL thin section (bottom left) and the corresponding ImageJ picture with threshold applied (bottom right) to estimate maximum porosity for Fearon 3 (2889 ft, 30 minutes circulation).

Well Name (Depth and Circulation Time)	Crystal Size	Texture	Porosity Type	ImageJ Porosity Estimate	Visual Porosity Count Estimate
Fearon 3 (2889 ft, 30 minutes)	Finely to Coarsely Crystalline	Euhedral to Anhedral	Intercrystalline	2.2%	8%

Table 8: Table summarizing thin section observations as well as maximum ImageJ porosity estimate and visual porosity count estimate for Fearon 3 (2889 ft, 30 minutes circulation).

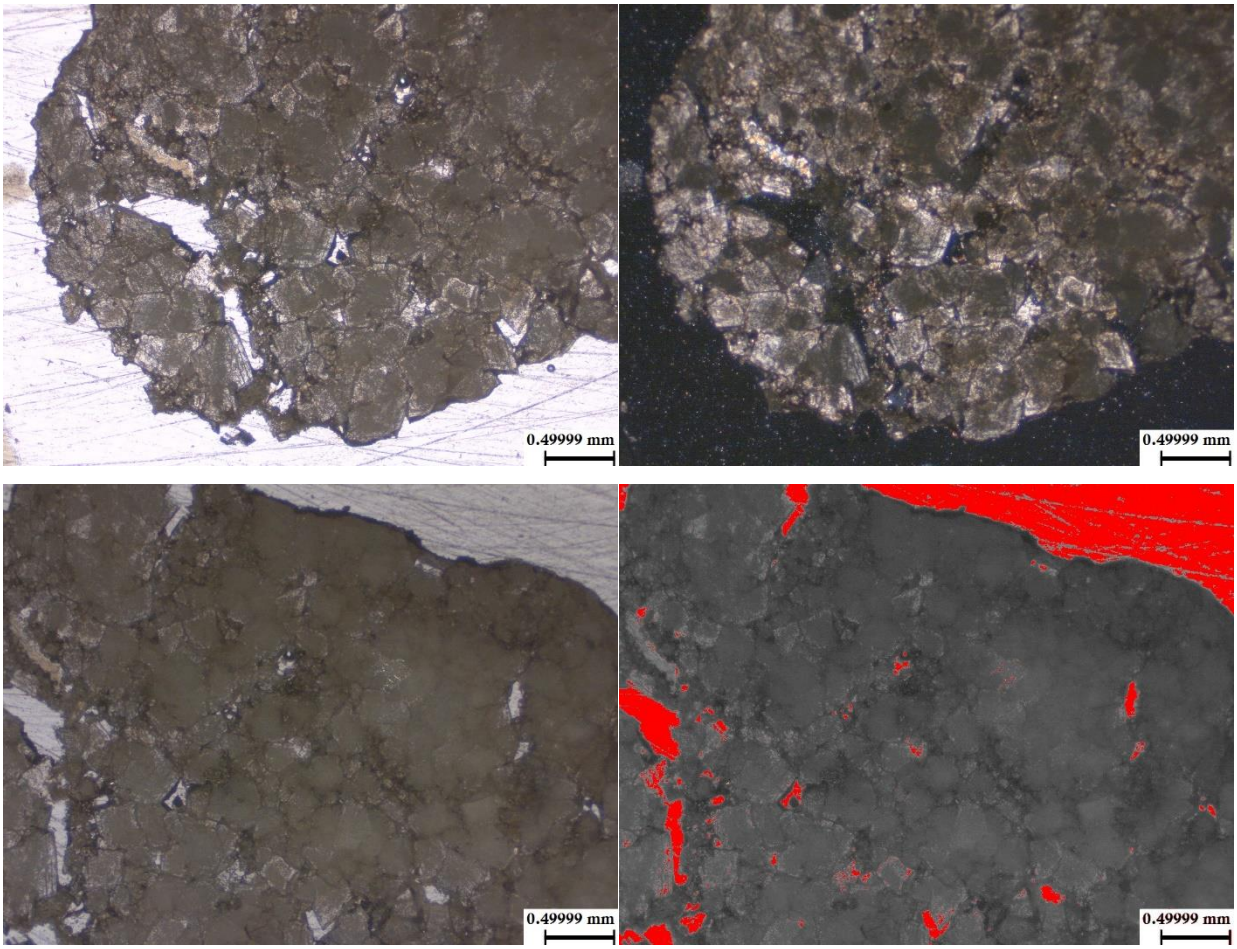

Figure 25: Optical PPL thin section (upper left), optical XPL thin section (upper right), optical PPL thin section (bottom left) and the corresponding ImageJ picture with threshold applied (bottom right) to estimate maximum porosity for Fearon 3 (2889 ft, 45 minutes circulation).

Well Name (Depth and Circulation Time)	Crystal Size	Texture	Porosity Type	ImageJ Porosity Estimate	Visual Porosity Count Estimate
Fearon 3 (2889 ft, 45 minutes)	Very Finely to Very Coarsely Crystalline	Euhedral to Anhedral	Intercrystalline, Vuggy	2.6%	5%

Table 9: Table summarizing thin section observations as well as maximum ImageJ porosity estimate and visual porosity count estimate for Fearon 3 (2889 ft, 45 minutes circulation).

Fearon 4

Well cuttings for Fearon 4 oil and gas well were collected from 2911 feet at the 20, 30, and 45-minutes of circulation intervals based on information disclosed in the geologic reports. Geologic reports state 2911 feet as the bottom of the hole with the top of the Viola limestone being at 2904 feet. Thin sections were created for each of the 20, 30, and 45-minute circulation intervals and analyzed using a petrographic microscope. Analysis of the thin section for the 20-minute circulation interval revealed heavy oil staining of very finely to coarsely crystalline dolomite that is euhedral to anhedral. Porosity types for the 20-minute circulation interval include intercrystalline, fracture, and vuggy with a porosity estimate of 7.4%. Potential oolitic grains were also observed in the 20-minute circulation interval thin section. The 30-minute circulation interval thin section exhibited heavy oil staining, exceptional porosity, and finely to very coarsely crystalline dolomite that is euhedral to anhedral. Porosity was estimated at 15.2% and included intercrystalline and vuggy porosity types. Finally, finely to coarsely crystalline dolomite that is euhedral to anhedral was observed in the 45-minute circulation interval thin section. These grains are heavily oil stained and exhibit intercrystalline porosity. ImageJ software estimated the maximum porosity to be 7.4%.

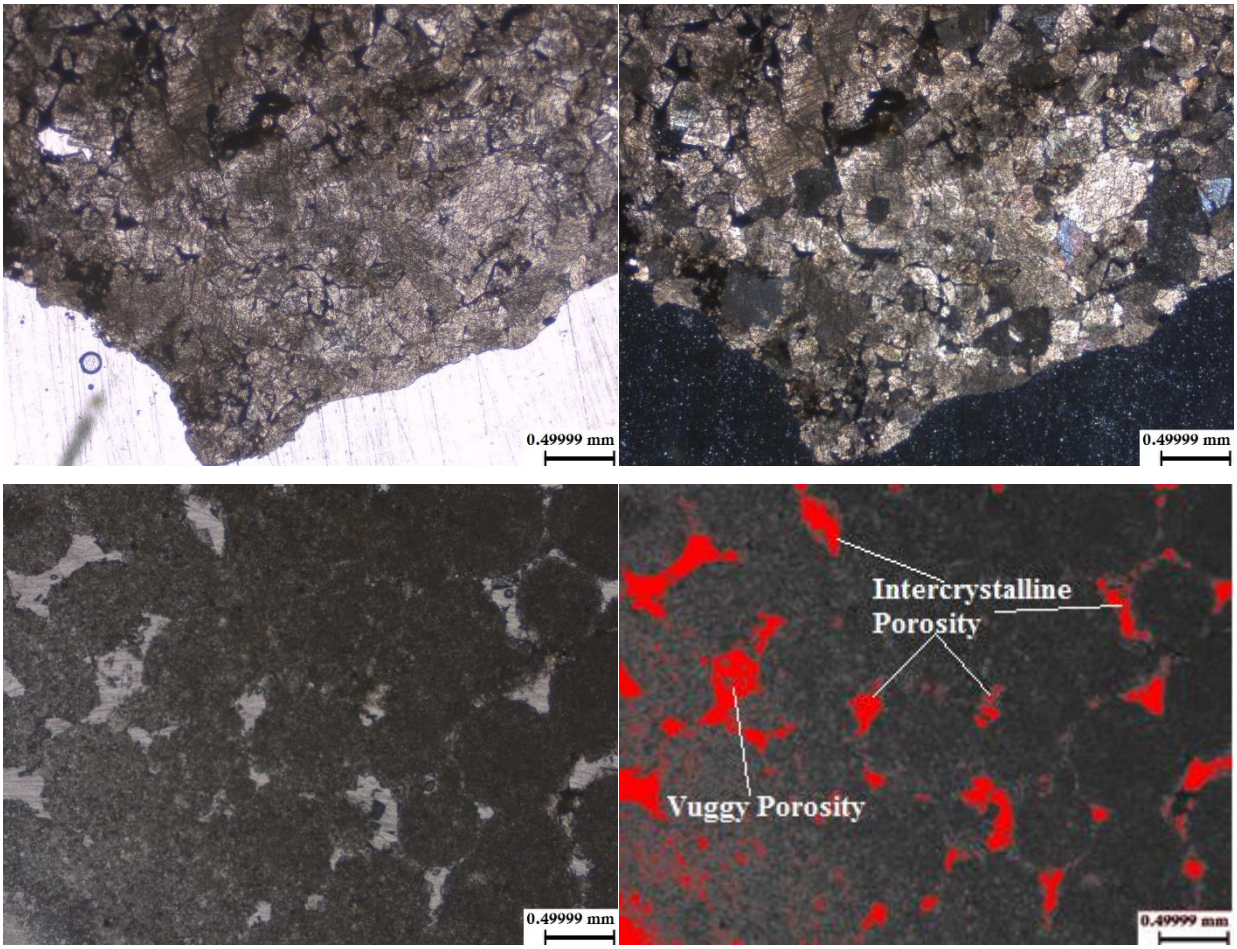

Figure 26: Optical PPL thin section (upper left), optical XPL thin section (upper right), optical PPL thin section (bottom left) and the corresponding ImageJ picture with threshold applied (bottom right) to estimate maximum porosity for Fearon 4 (2911 ft, 20 minutes circulation).

Well Name (Depth and Circulation Time)	Crystal Size	Texture	Porosity Type	ImageJ Porosity Estimate	Visual Porosity Count Estimate
Fearon 4 (2911 ft, 20 minutes)	Very Finely to Coarsely Crystalline	Euhedral to Anhedral	Intercrystalline, Fracture, Vuggy	7.3%	12%

Table 10: Table summarizing thin section observations as well as maximum ImageJ porosity estimate and visual porosity count estimate for Fearon 4 (2911 ft, 20 minutes circulation).

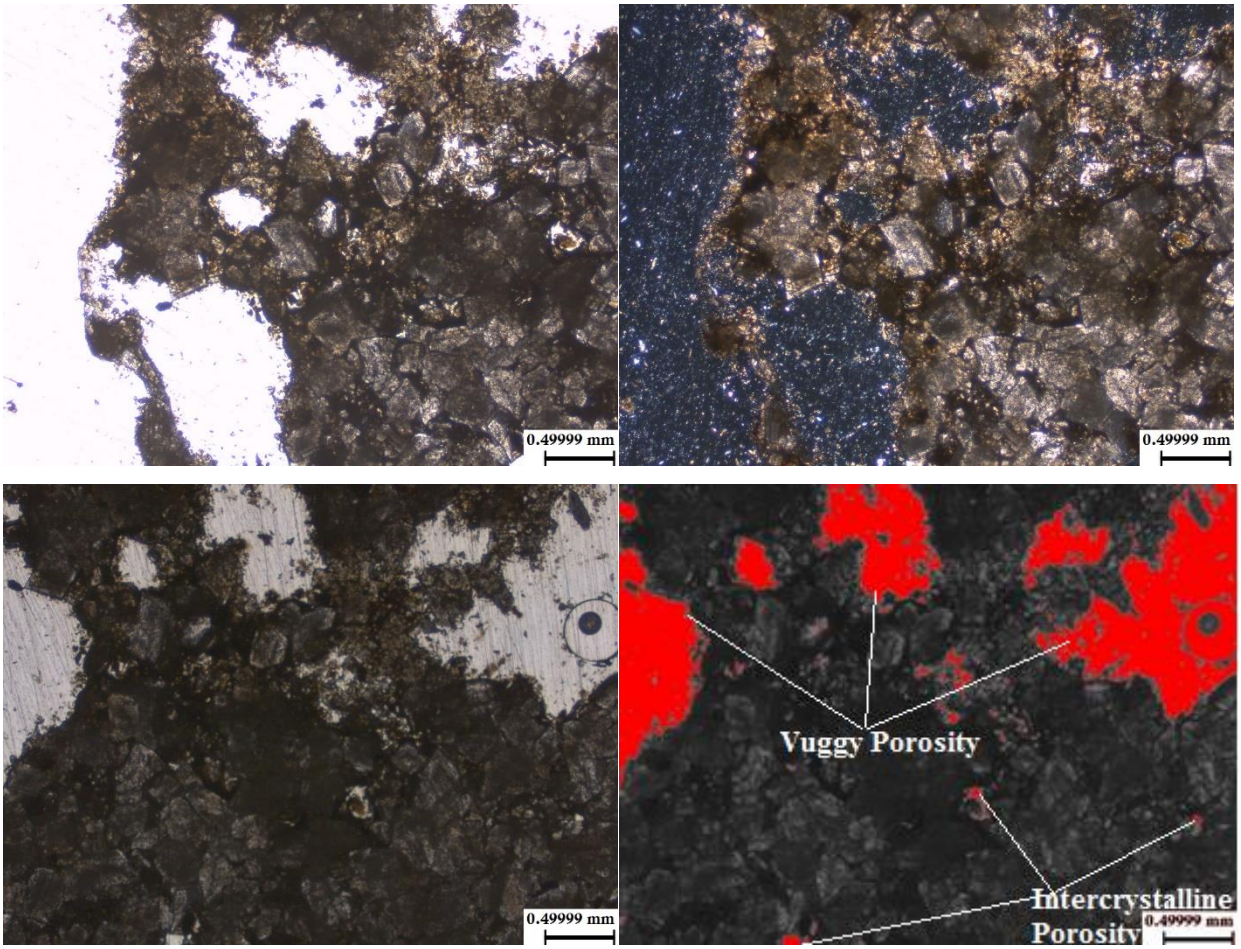

Figure 27: Optical PPL thin section (upper left), optical XPL thin section (upper right), optical PPL thin section (bottom left) and the corresponding ImageJ picture with threshold applied (bottom right) to estimate maximum porosity for Fearon 4 (2911 ft, 30 minutes circulation).

Well Name (Depth and Circulation Time)	Crystal Size	Texture	Porosity Type	ImageJ Porosity Estimate	Visual Porosity Count Estimate
Fearon 4 (2911 ft, 30 minutes)	Finely to Very Coarsely Crystalline	Euhedral to Anhedral	Intercrystalline, Vuggy	15.2%	20%

Table 11: Table summarizing thin section observations as well as maximum ImageJ porosity estimate and visual porosity count estimate for Fearon 4 (2911 ft, 30 minutes circulation).

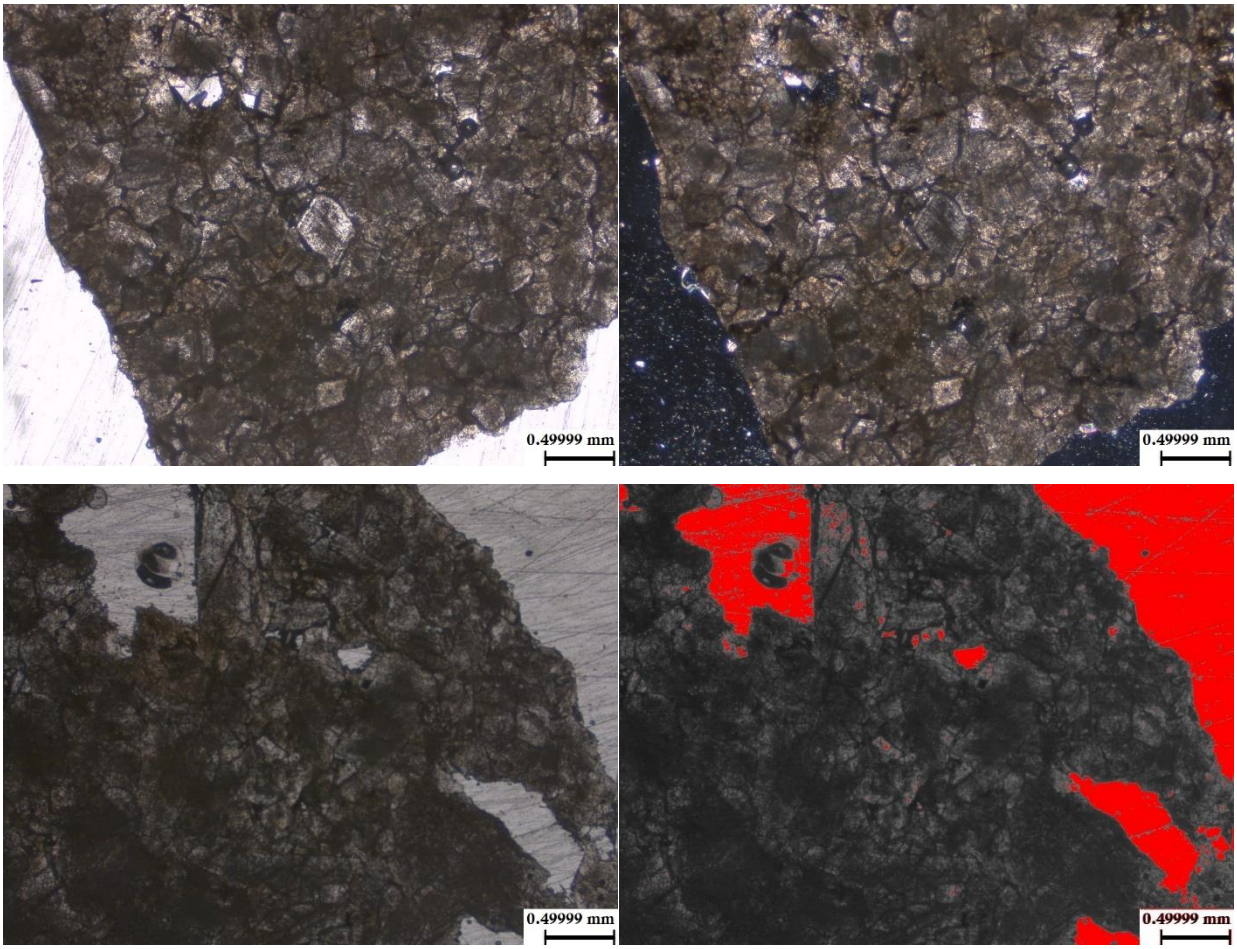

Figure 28: Optical PPL thin section (upper left), optical XPL thin section (upper right), optical PPL thin section (bottom left) and the corresponding ImageJ picture with threshold applied (bottom right) to estimate maximum porosity for Fearon 4 (2911 ft, 45 minutes circulation).

Well Name (Depth and Circulation Time)	Crystal Size	Texture	Porosity Type	ImageJ Porosity Estimate	Visual Porosity Count Estimate
Fearon 4 (2911 ft, 45 minutes)	Finely to Coarsely Crystalline,	Euhedral to Anhedral	Intercrystalline	7.4%	12%

Table 12: Table summarizing thin section observations as well as maximum ImageJ porosity estimate and visual porosity count estimate for Fearon 4 (2911 ft, 45 minutes circulation).

Fearon 5

Geologic reports for Fearon 5 oil and gas well indicate that the top of the Viola limestone is at 2872 feet, with the bottom of the hole at 2877 feet. Well cuttings for Fearon 5 oil and gas well were collected from 2877 feet at the 15, 30, and 45-minutes of circulation intervals based on the information disclosed in the geologic reports. Thin sections were created for each of the circulation time intervals and examined using a petrographic microscope. Medium to coarsely crystalline dolomite that is euhedral to subhedral was observed when the 15-minute circulation interval thin section was looked at under the petrographic microscope. Intercrystalline porosity is present with porosity estimated at 1.5%. The 30-minute circulation interval thin section is made up of medium to coarsely crystalline dolomite that is euhedral to subhedral. Porosity was estimated at 1.3% with porosity types present including: intercrystalline, vuggy, and moldic. Finally, medium to coarsely crystalline dolomite that is euhedral to subhedral was observed in the 45-minute circulation interval. Intercrystalline and vuggy porosity are present, and porosity was estimated at 2.3%.

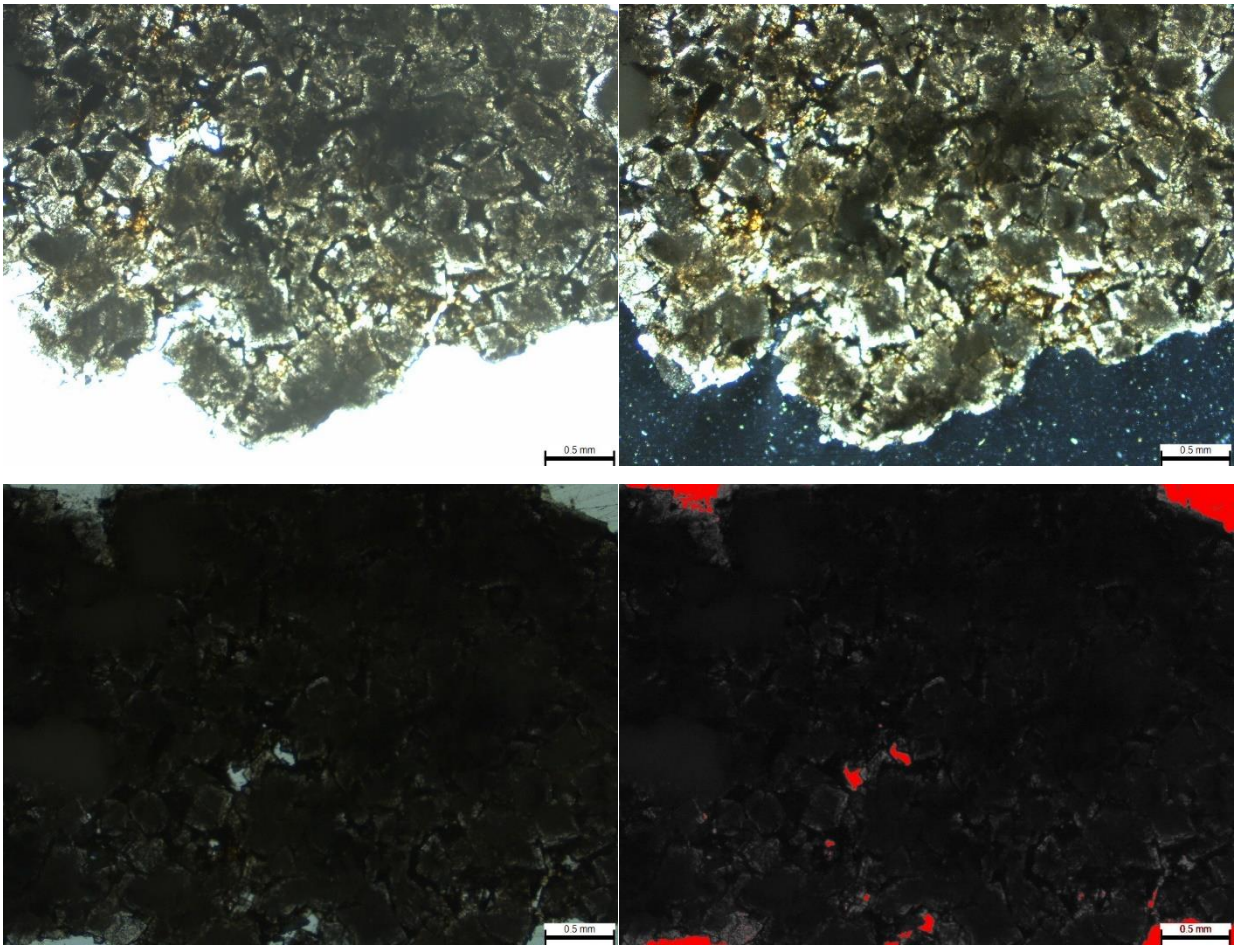

Figure 29: Optical PPL thin section (upper left), optical XPL thin section (upper right), optical PPL thin section (bottom left) and the corresponding ImageJ picture with threshold applied (bottom right) to estimate maximum porosity for Fearon 5 (2877 ft, 15 minutes circulation).

Well Name (Depth and Circulation Time)	Crystal Size	Texture	Porosity Type	ImageJ Porosity Estimate	Visual Porosity Count Estimate
Fearon 5 (2877 ft, 15 minutes)	Medium to Coarsely Crystalline	Euhedral to Subhedral	Intercrystalline	1.5%	2%

Table 13: Table summarizing thin section observations as well as maximum ImageJ porosity estimate and visual porosity count estimate for Fearon 5 (2887 ft, 15 minutes circulation).

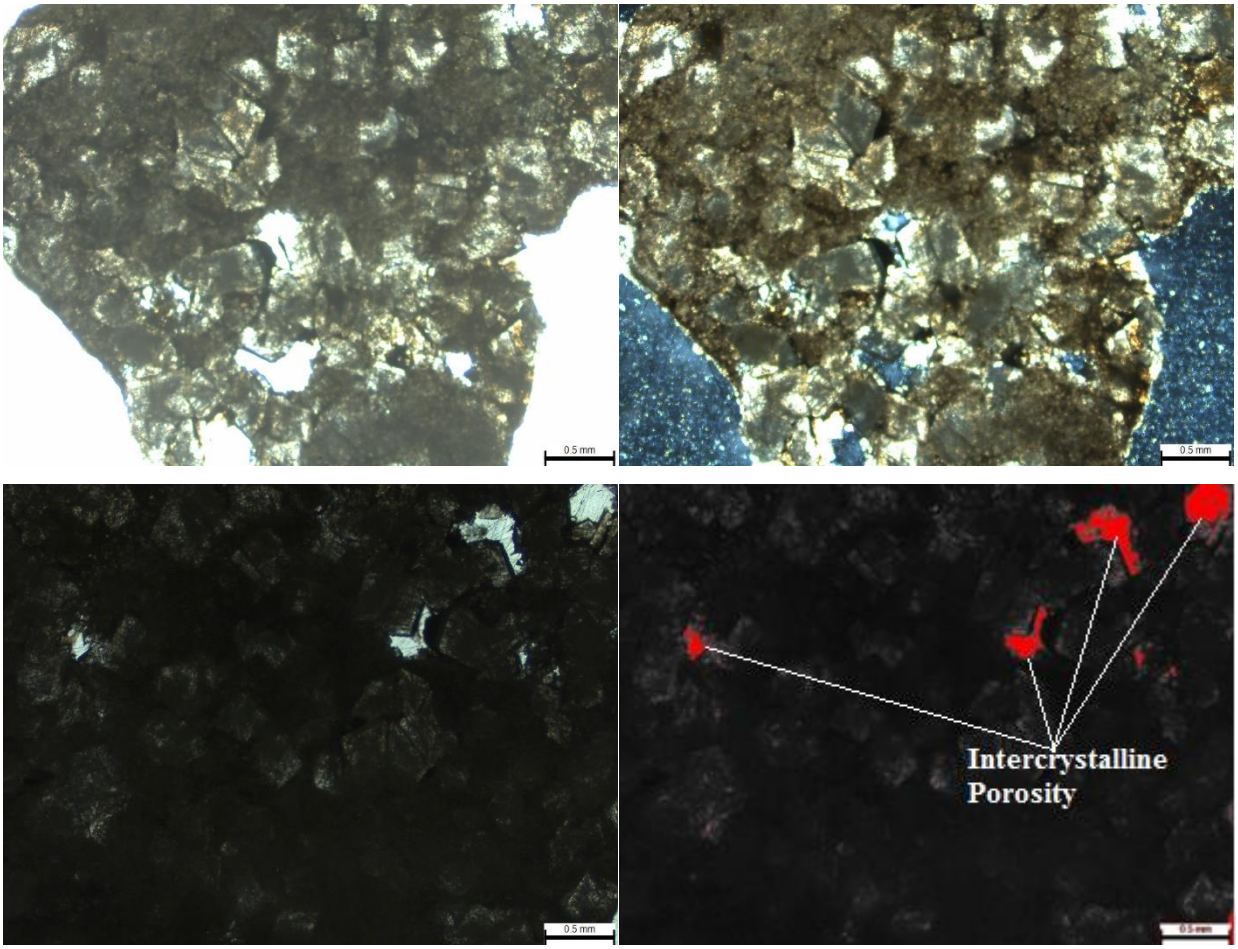

Figure 30: Optical PPL thin section (upper left), optical XPL thin section (upper right), optical PPL thin section (bottom left) and the corresponding ImageJ picture with threshold applied (bottom right) to estimate maximum porosity for Fearon 5 (2877 ft, 30 minutes circulation).

Well Name (Depth and Circulation Time)	Crystal Size	Texture	Porosity Type	ImageJ Porosity Estimate	Visual Porosity Count Estimate
Fearon 5 (2877 ft, 30 minutes)	Medium to Coarsely Crystalline,	Euhedral to Subhedral	Intercrystalline, Vuggy, Moldic	1.3%	3%

Table 14: Table summarizing thin section observations as well as maximum ImageJ porosity estimate and visual porosity count estimate for Fearon 5 (2887 ft, 30 minutes circulation).

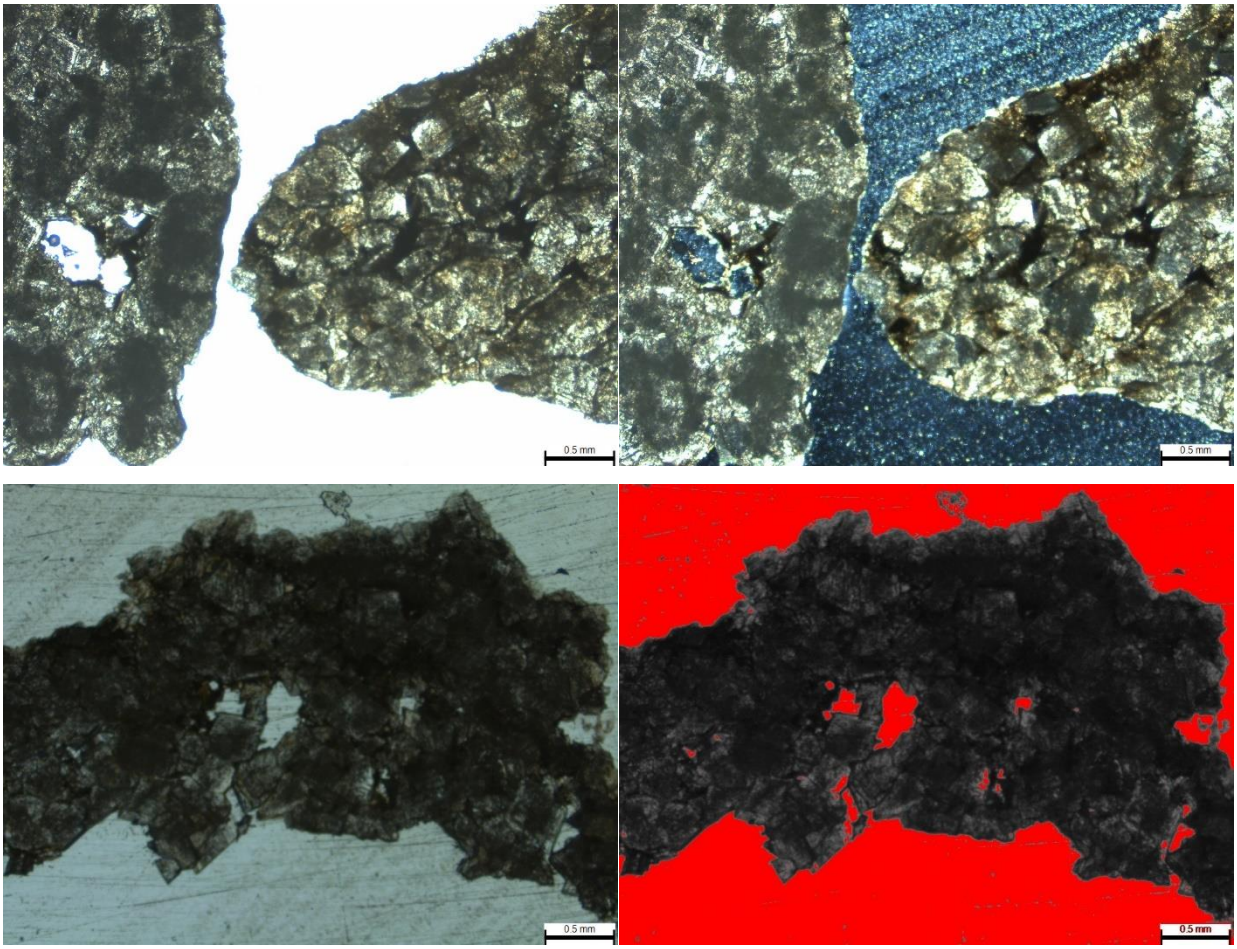

Figure 31: Optical PPL thin section (upper left), optical XPL thin section (upper right), optical PPL thin section (bottom left) and the corresponding ImageJ picture with threshold applied (bottom right) to estimate maximum porosity for Fearon 5 (2877 ft, 45 minutes circulation).

Well Name (Depth and Circulation Time)	Crystal Size	Texture	Porosity Type	ImageJ Porosity Estimate	Visual Porosity Count Estimate
Fearon 5 (2877 ft, 45 minutes)	Medium to Coarsely Crystalline	Euhedral to Subhedral	Intercrystalline, Vuggy	2.3%	5%

Table 15: Table summarizing thin section observations as well as maximum ImageJ porosity estimate and visual porosity count estimate for Fearon 5 (2887 ft, 45 minutes circulation).

Wagner M.C 1

The top of the Viola limestone is located at 2860 feet with the bottom of the hole at 2865 feet based on information presented in the geologic reports. Well cuttings for Wagner M.C 1 oil and gas well were collected, and thin sections were made from the interval of 2860 – 2865 feet and at 2865 feet at the 15, 30, and 45-minutes of circulation intervals. These intervals were chosen based on information disclosed in the geologic reports, as well as observations made while looking at cuttings. Medium to coarsely crystalline dolomite that is euhedral to subhedral was noted when analyzing the 2860 – 2865 feet interval thin section. Intercrystalline porosity is present and porosity was estimated at 1.5%. Looking at the 15-minute circulation interval thin section revealed heavy oil staining on finely to coarsely crystalline dolomite that is anhedral to euhedral. Porosity was estimated at 6.7% with vuggy and intercrystalline porosity types present. Finely to coarsely crystalline dolomite that is euhedral to subhedral comprises the 30-minute circulation interval thin section. Intercrystalline and vuggy porosity types were observed and a porosity estimate of 4.4% was obtained. The 45-minute circulation interval thin section contains finely to coarsely crystalline dolomite that is euhedral to anhedral. Intercrystalline porosity is observed under the petrographic microscope with porosity estimated at 4.2%.

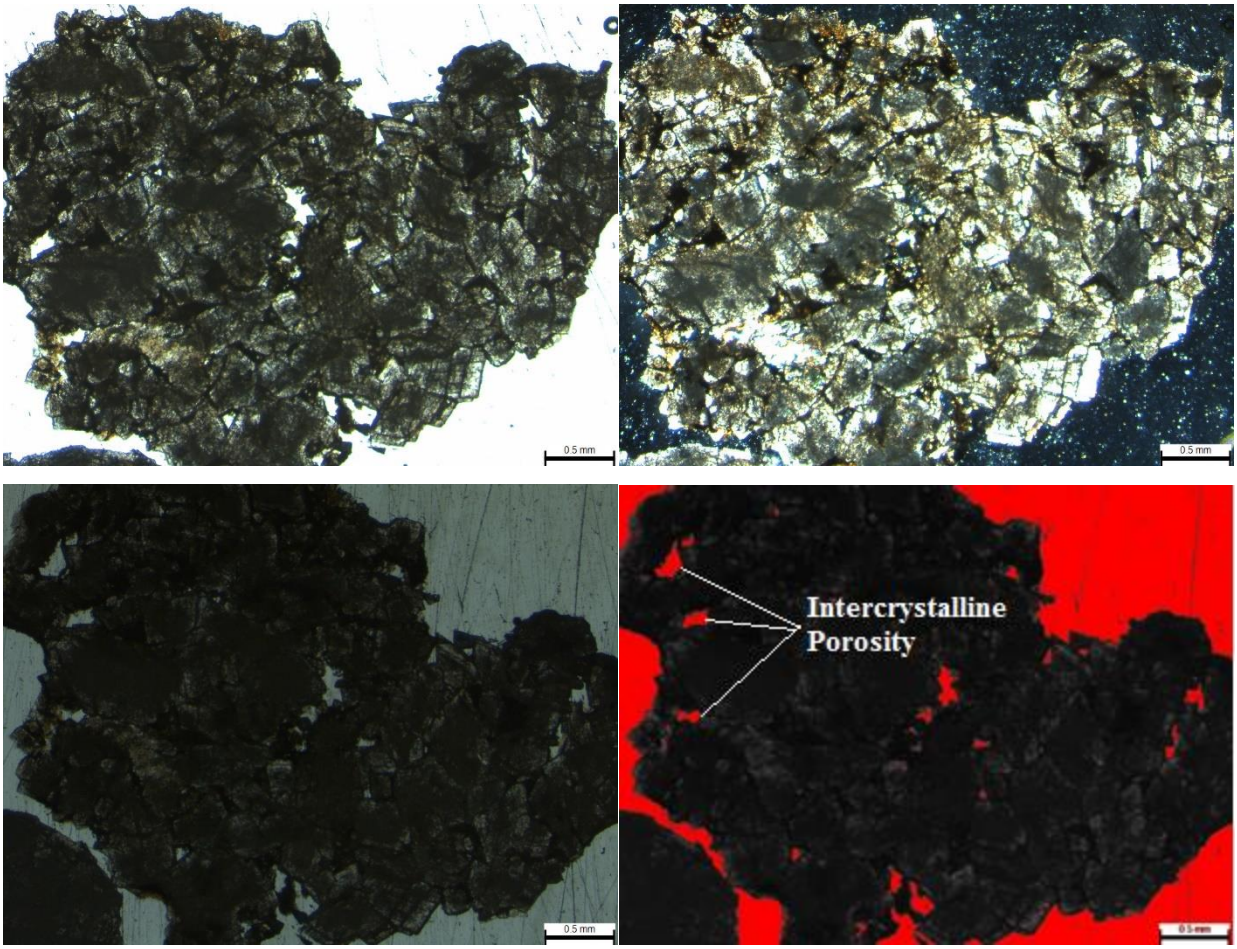

Figure 32: Optical PPL thin section (upper left), optical XPL thin section (upper right), optical PPL thin section (bottom left) and the corresponding ImageJ picture with threshold applied (bottom right) to estimate maximum porosity for Wagner M.C 1 (2860 - 2865 ft).

Well Name (Depth and Circulation Time)	Crystal Size	Texture	Porosity Type	ImageJ Porosity Estimate	Visual Porosity Count Estimate
Wagner M.C 1 (2860 – 2865 ft)	Medium to Coarsely Crystalline	Euhedral to Subhedral	Intercrystalline	1.5%	6%

Table 16: Table summarizing thin section observations as well as maximum ImageJ porosity estimate and visual porosity count estimate for Wagner M.C 1 (2860 - 2865 ft).

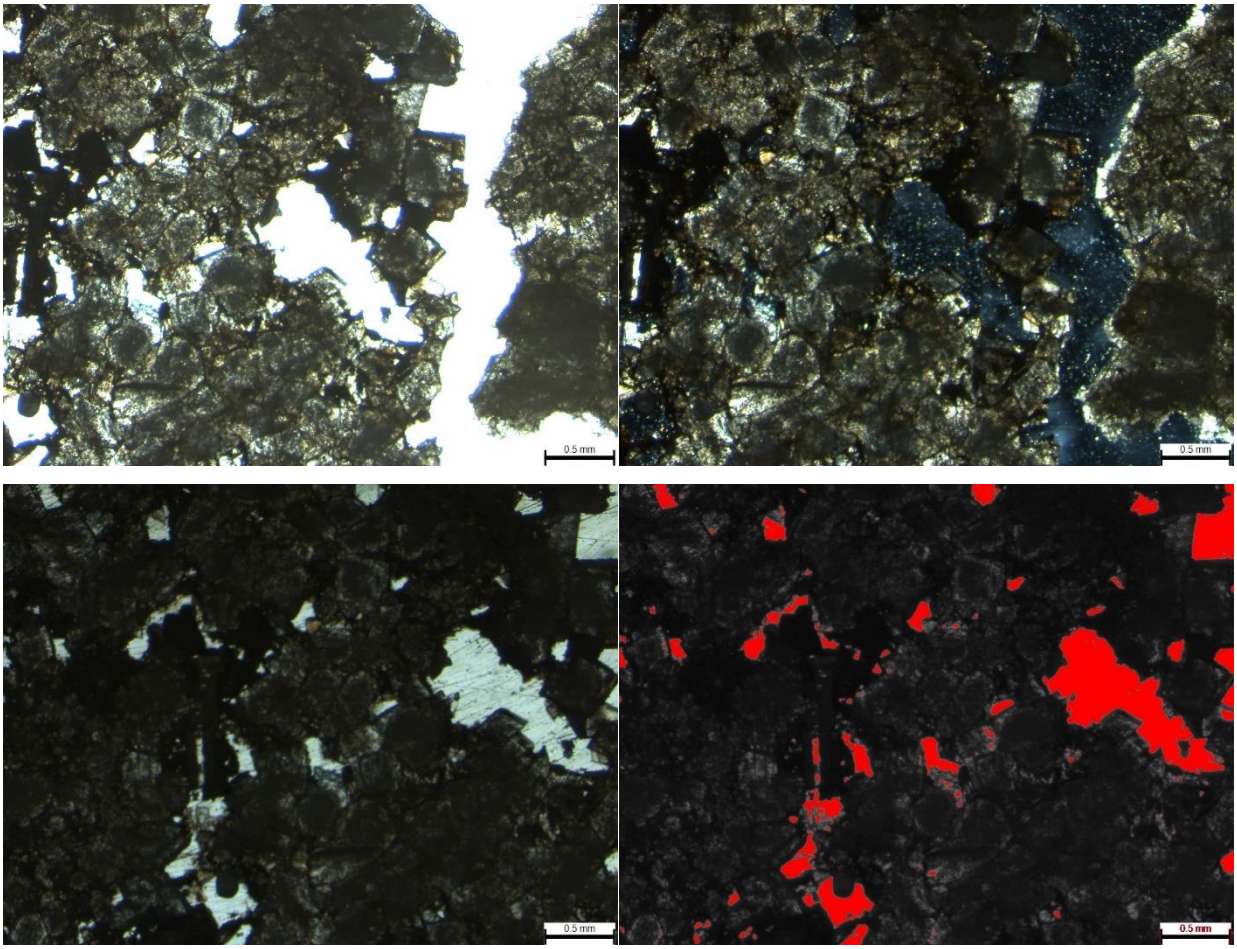

Figure 33: Optical PPL thin section (upper left), optical XPL thin section (upper right), optical PPL thin section (bottom left) and the corresponding ImageJ picture with threshold applied (bottom right) to estimate maximum porosity for Wagner M.C 1 (2865 ft, 15 minutes circulation).

Well Name (Depth and Circulation Time)	Crystal Size	Texture	Porosity Type	ImageJ Porosity Estimate	Visual Porosity Count Estimate
Wagner M.C 1 (2865 ft, 15 minutes)	Finely to Coarsely Crystalline	Euhedral to Anhedral	Intercrystalline, Vuggy	6.7%	13%

Table 17: Table summarizing thin section observations as well as maximum ImageJ porosity estimate and visual porosity count estimate for Wagner M.C 1 (2865 ft, 15 minutes circulation).

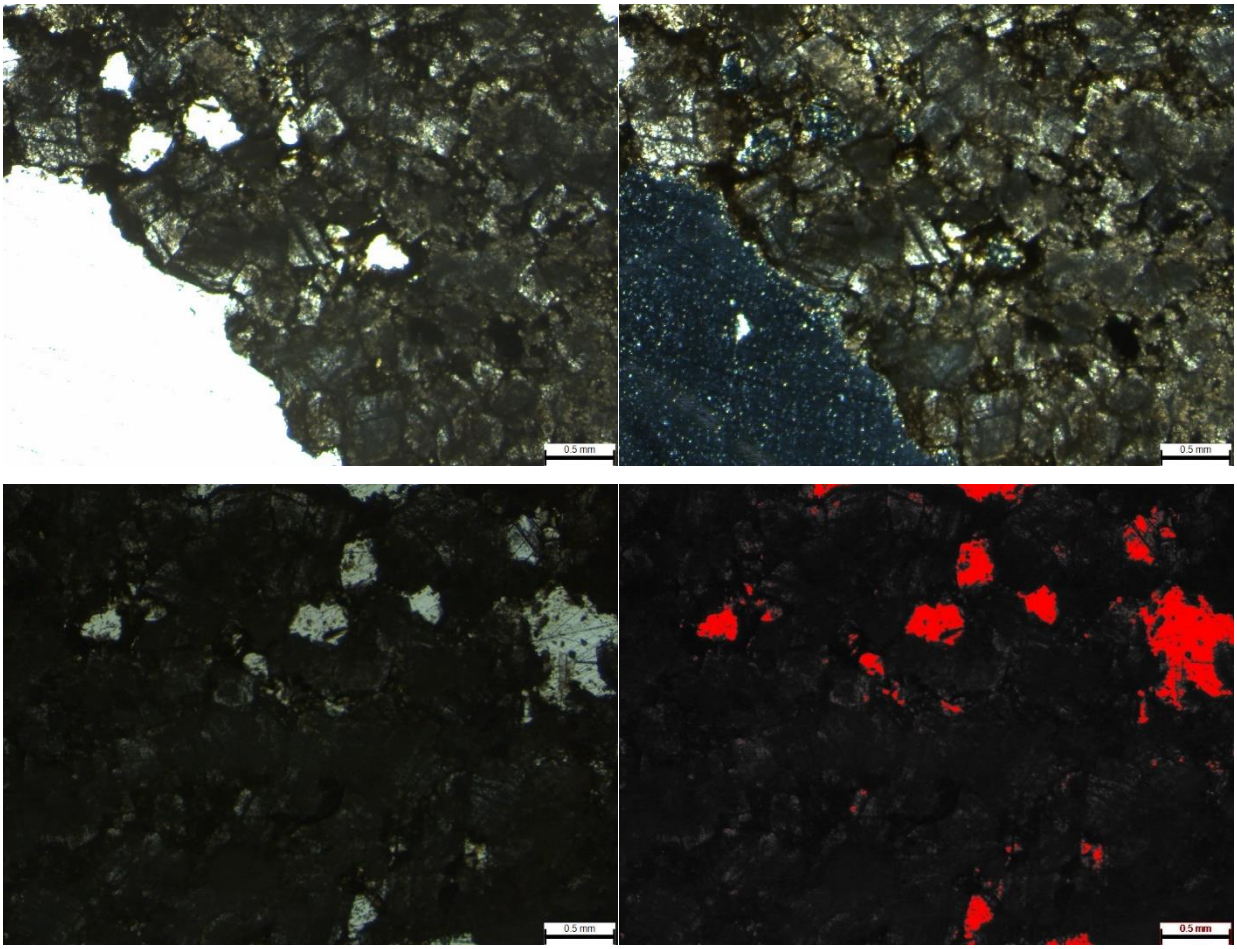

Figure 34: Optical PPL thin section (upper left), optical XPL thin section (upper right), optical PPL thin section (bottom left) and the corresponding ImageJ picture with threshold applied (bottom right) to estimate maximum porosity for Wagner M.C 1 (2865 ft, 30 minutes circulation).

Well Name (Depth and Circulation Time)	Crystal Size	Texture	Porosity Type	ImageJ Porosity Estimate	Visual Porosity Count Estimate
Wagner M.C 1 (2865 ft, 30 minutes)	Finely to Coarsely Crystalline	Euhedral to Subhedral	Intercrystalline, Vuggy	4.4%	8%

Table 18: Table summarizing thin section observations as well as maximum ImageJ porosity estimate and visual porosity count estimate for Wagner M.C 1 (2865 ft, 30 minutes circulation).

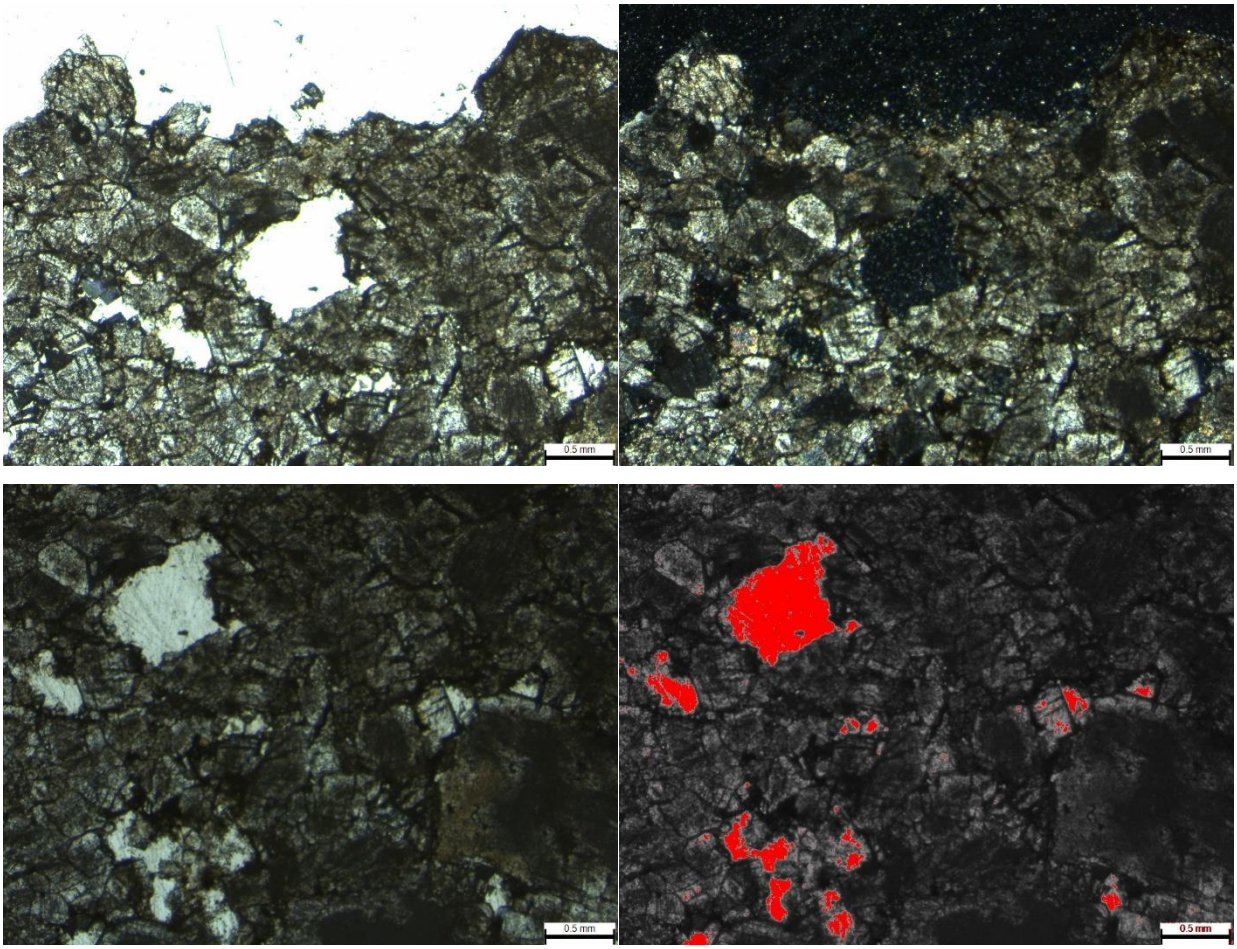

Figure 35: Optical PPL thin section (upper left), optical XPL thin section (upper right), optical PPL thin section (bottom left) and the corresponding ImageJ picture with threshold applied (bottom right) to estimate maximum porosity for Wagner M.C 1 (2865 ft, 45 minutes circulation).

Well Name (Depth and Circulation Time)	Crystal Size	Texture	Porosity Type	ImageJ Porosity Estimate	Visual Porosity Count Estimate
Wagner M.C 1 (2865 ft, 45 minutes)	Finely to Coarsely Crystalline	Euhedral to Anhedral	Intercrystalline	4.2%	7%

Table 19: Table summarizing thin section observations as well as maximum ImageJ porosity estimate and visual porosity count estimate for Wagner M.C 1 (2865 ft, 45 minutes circulation).

Wagner M.C 2

Geologic reports for Wagner M.C 2 oil and gas well indicate the top of the Viola limestone at 2884 feet, and the bottom of the hole at 2887 feet. Well cuttings for Wagner M.C 2 oil and gas well were collected from 2887 feet at the 15, 30, 45, and 60-minute circulation time intervals based on information found in the geologic reports. Thin sections were created for each of the circulation time intervals and analyzed using a petrographic microscope. Finely to very coarsely crystalline dolomite that is euhedral to anhedral was observed in the 15-minute circulation interval thin section. Intercrystalline and vuggy porosity are present with porosity estimated at 2.2% using ImageJ software. The 30-minute circulation interval thin section is comprised of finely to very coarsely crystalline dolomite that is euhedral to anhedral with intercrystalline and vuggy porosity. Porosity of the 30-minute circulation interval thin section was estimated at 1.9%. Analyzing the 45-minute circulation interval thin section revealed finely to very coarsely crystalline dolomite that is euhedral to anhedral. Porosity was estimated at 5.6% and is comprised of intercrystalline porosity. Lastly, finely to coarsely crystalline dolomite that is euhedral to anhedral is present in the 60-minute circulation interval thin section. Intercrystalline and vuggy porosity were observed with porosity estimated at 1.0%.

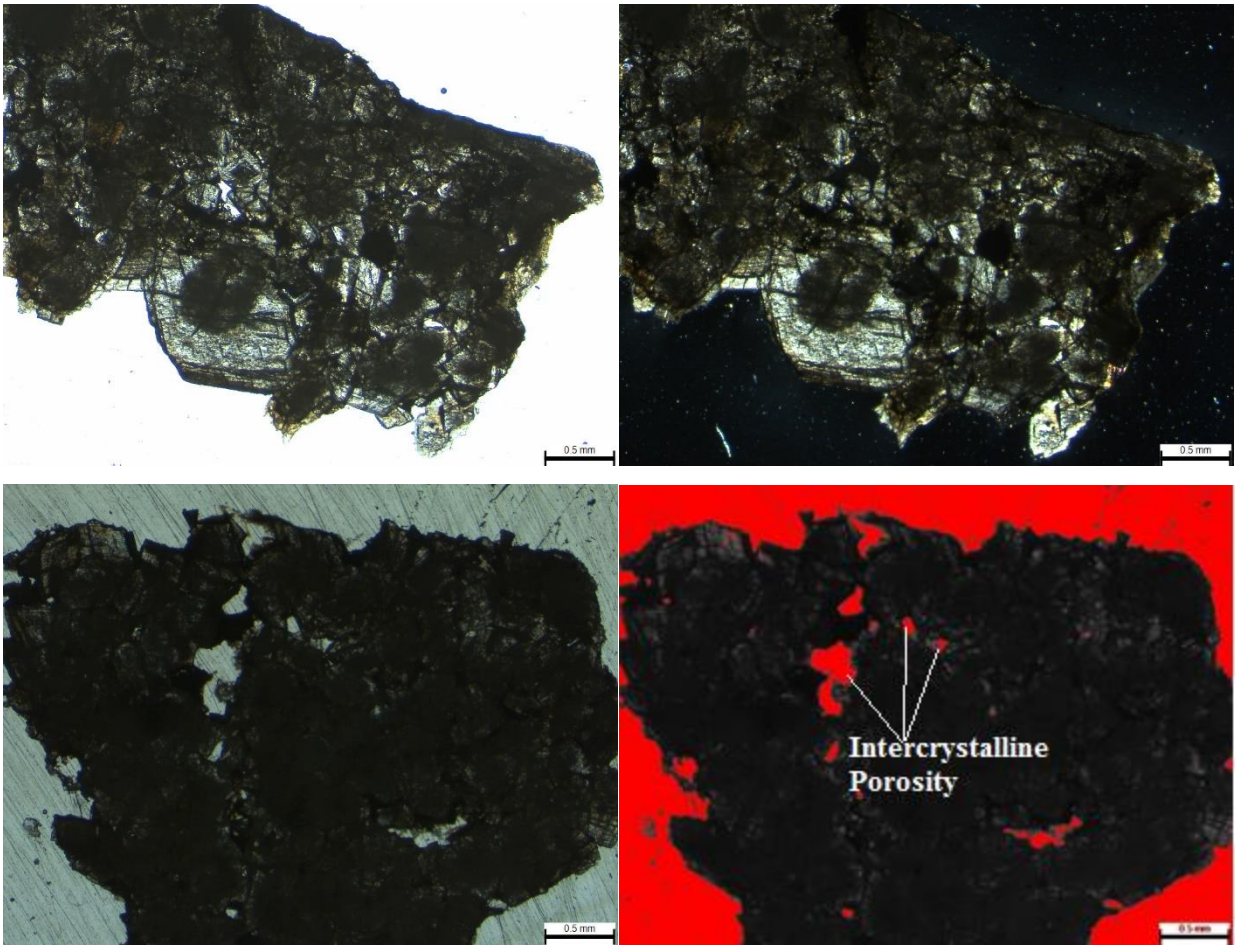

Figure 36: Optical PPL thin section (upper left), optical XPL thin section (upper right), optical PPL thin section (bottom left) and the corresponding ImageJ picture with threshold applied (bottom right) to estimate maximum porosity for Wagner M.C 2 (2887 ft, 15 minutes circulation).

Well Name (Depth and Circulation Time)	Crystal Size	Texture	Porosity Type	ImageJ Porosity Estimate	Visual Porosity Count Estimate
Wagner M.C 2 (2887 ft, 15 minutes)	Finely to Very Coarsely Crystalline,	Euhedral to Anhedral	Intercrystalline, Vuggy	2.2%	4%

Table 20: Table summarizing thin section observations as well as maximum ImageJ porosity estimate and visual porosity count estimate for Wagner M.C 2 (2887 ft, 15 minutes circulation).

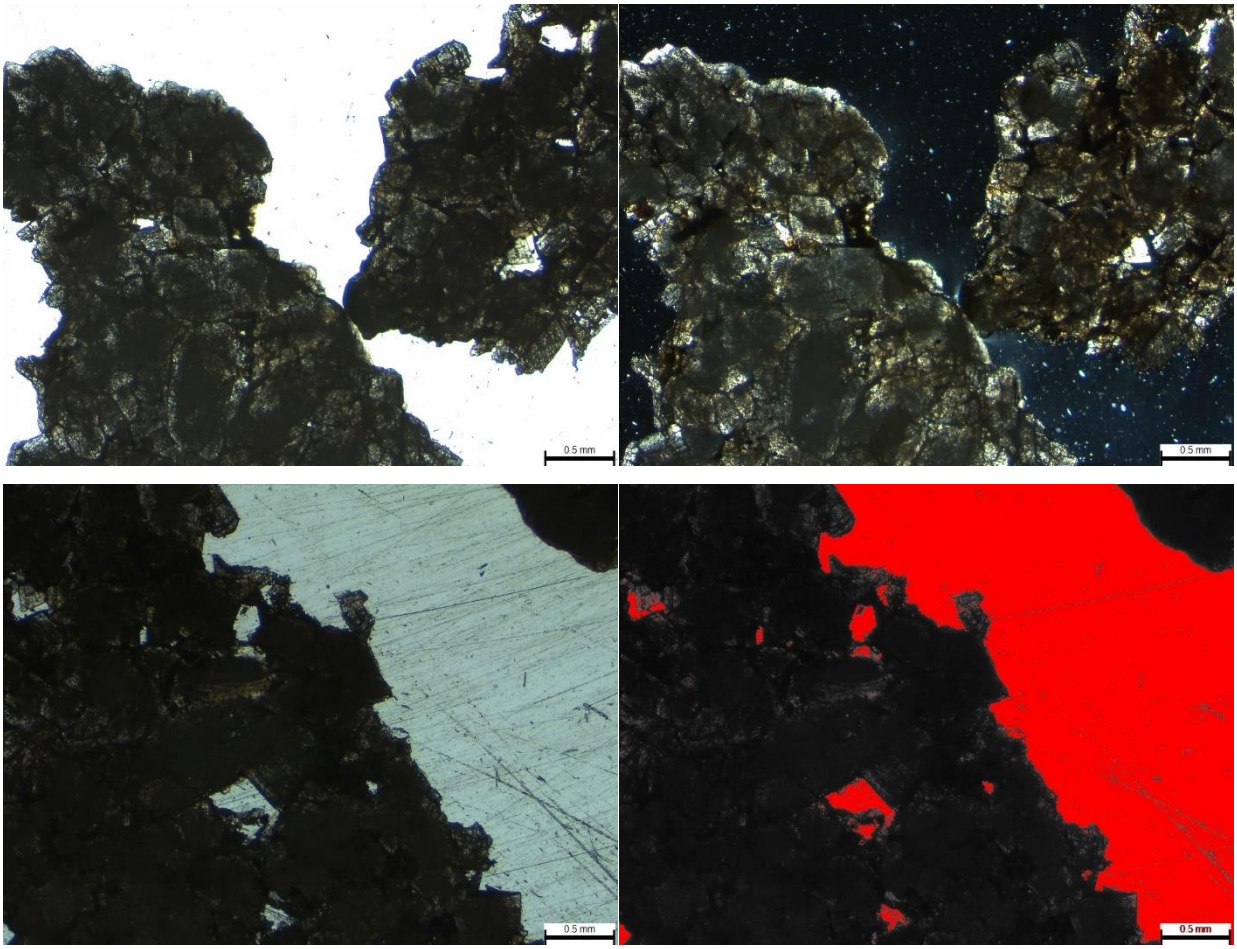

Figure 37: Optical PPL thin section (upper left), optical XPL thin section (upper right), optical PPL thin section (bottom left) and the corresponding ImageJ picture with threshold applied (bottom right) to estimate maximum porosity for Wagner M.C 2 (2887 ft, 30 minutes circulation).

Well Name (Depth and Circulation Time)	Crystal Size	Texture	Porosity Type	ImageJ Porosity Estimate	Visual Porosity Count Estimate
Wagner M.C 2 (2887 ft, 30 minutes)	Finely to Very Coarsely Crystalline	Euhedral to Anhedral	Intercrystalline, Vuggy	1.9%	4%

Table 21: Table summarizing thin section observations as well as maximum ImageJ porosity estimate and visual porosity count estimate for Wagner M.C 2 (2887 ft, 30 minutes circulation).

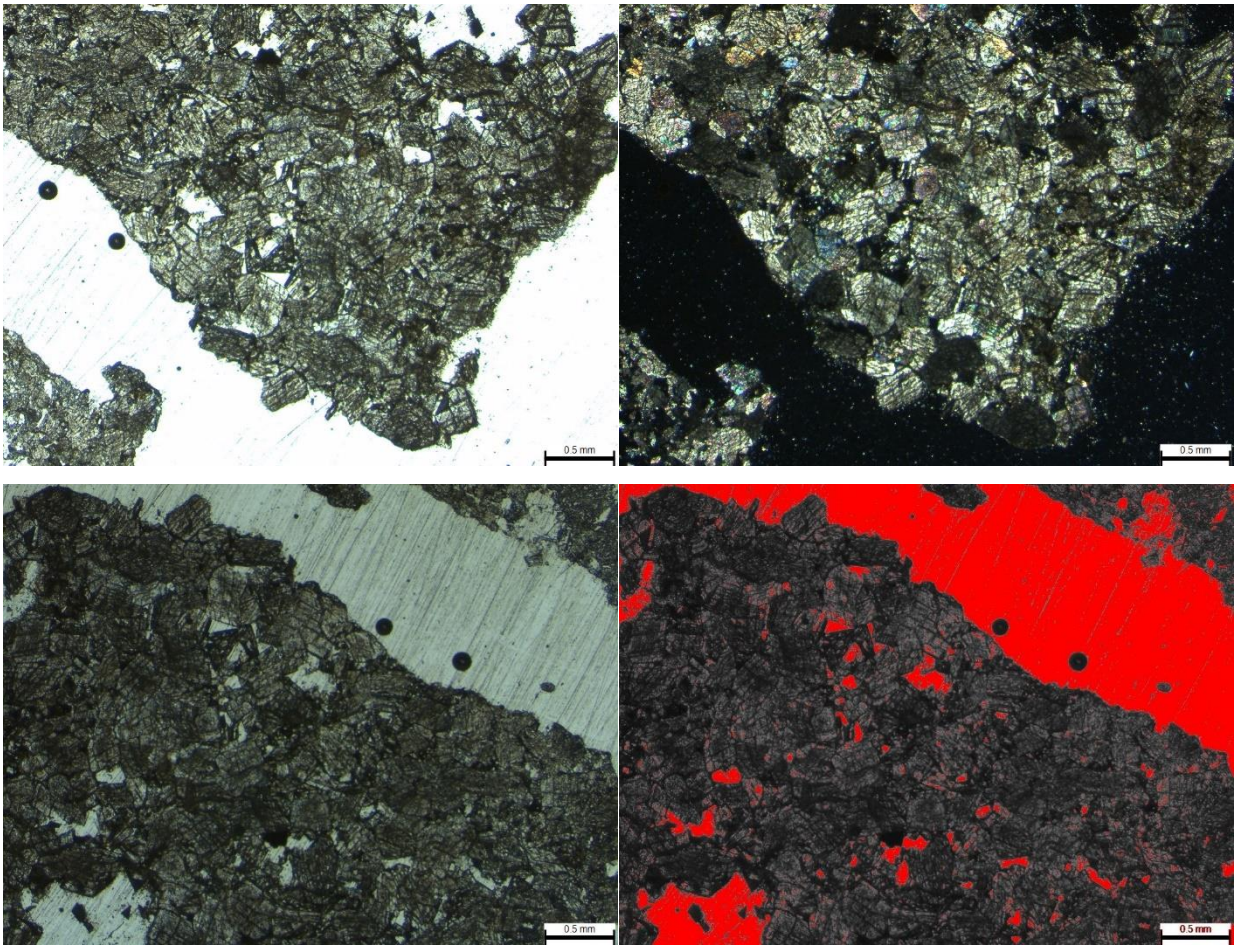

Figure 38: Optical PPL thin section (upper left), optical XPL thin section (upper right), optical PPL thin section (bottom left) and the corresponding ImageJ picture with threshold applied (bottom right) to estimate maximum porosity for Wagner M.C 2 (2887 ft, 45 minutes circulation).

Well Name (Depth and Circulation Time)	Crystal Size	Texture	Porosity Type	ImageJ Porosity Estimate	Visual Porosity Count Estimate
Wagner M.C 2 (2887 ft, 45 minutes)	Finely to Very Coarsely Crystalline	Euhedral to Anhedral	Intercrystalline	5.6%	8%

Table 22: Table summarizing thin section observations as well as maximum ImageJ porosity estimate and visual porosity count estimate for Wagner M.C 2 (2887 ft, 45 minutes circulation).

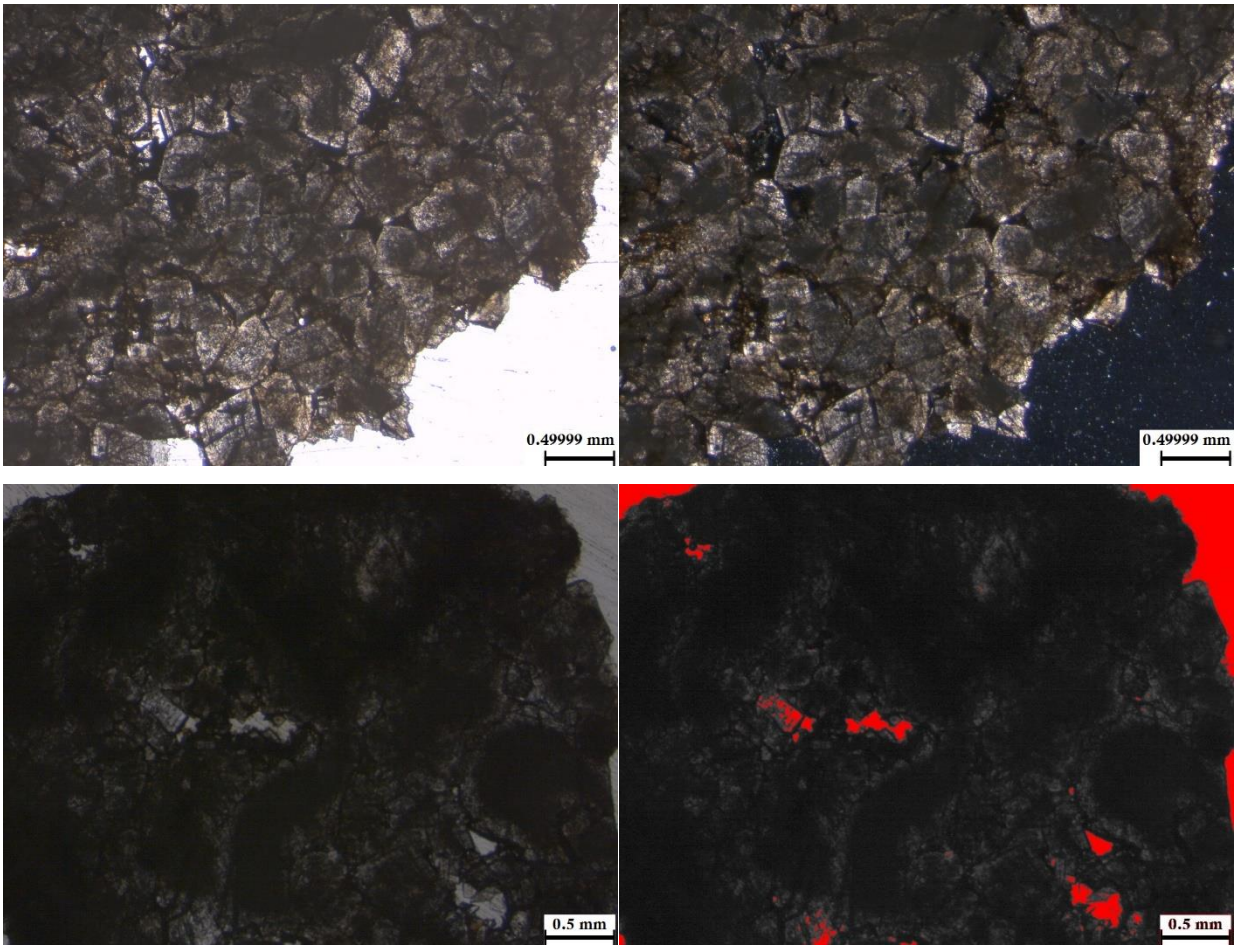

Figure 39: Optical PPL thin section (upper left), optical XPL thin section (upper right), optical PPL thin section (bottom left) and the corresponding ImageJ picture with threshold applied (bottom right) to estimate maximum porosity for Wagner M.C 2 (2887 ft, 60 minutes circulation).

Well Name (Depth and Circulation Time)	Crystal Size	Texture	Porosity Type	ImageJ Porosity Estimate	Visual Porosity Count Estimate
Wagner M.C 2 (2887 ft, 60 minutes)	Finely to Coarsely Crystalline	Euhedral to Anhedral	Intercrystalline, Vuggy	1.0%	3%

Table 23: Table summarizing thin section observations as well as maximum ImageJ porosity estimate and visual porosity count estimate for Wagner M.C 2 (2887 ft, 60 minutes circulation).

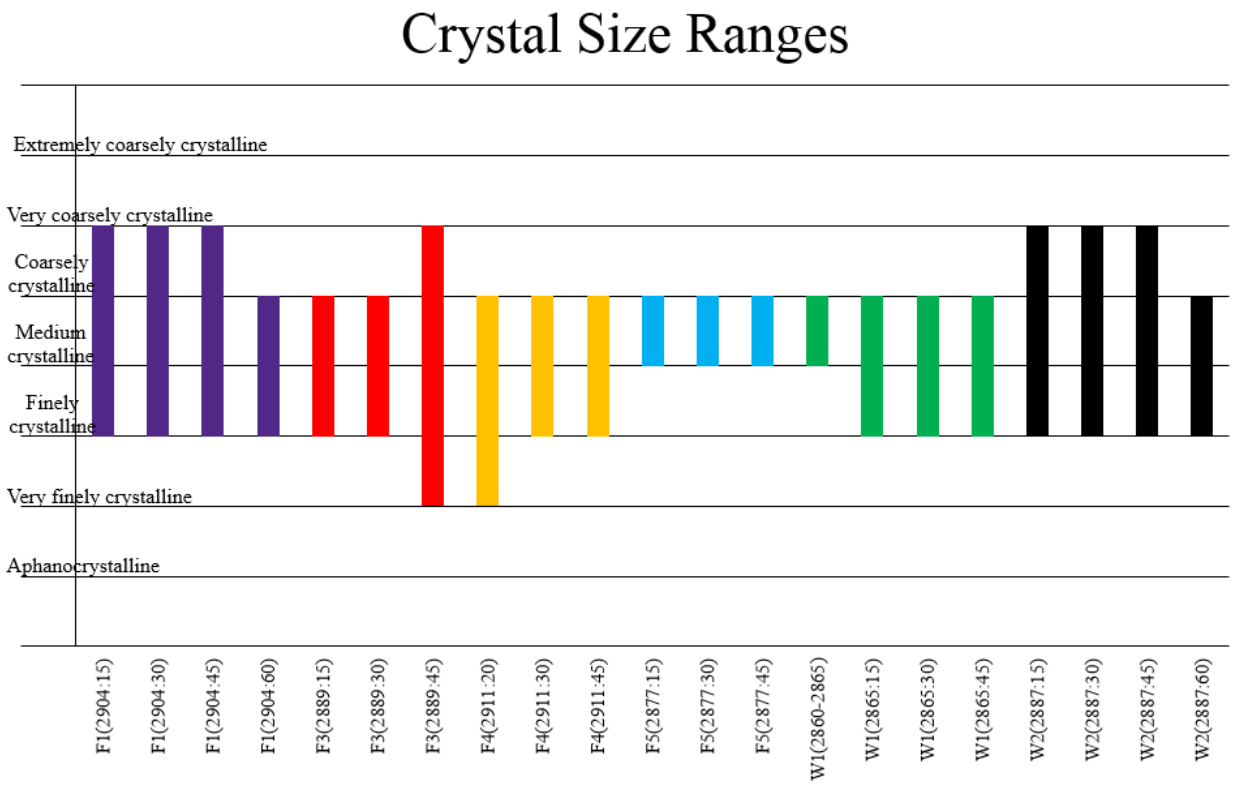

Figure 40: Floating bar graph showing the crystal size range observed for each thin section. Thin section samples are shown on the X-axis with F1 representing Fearon 1, F3 (Fearon 3), F4 (Fearon 4), F5 (Fearon 5), W1 (Wagner M.C 1), and W2 representing Wagner M.C 2. Crystal sizes are on the Y-axis. As an example of how to read the graph, the sample F1(2904:15) is a thin section created from the Fearon 1 well at 2904 feet and 15-minute circulation time interval. For this sample the graph shows that there is finely, medium, coarsely, and very coarsely crystalline dolomite present.

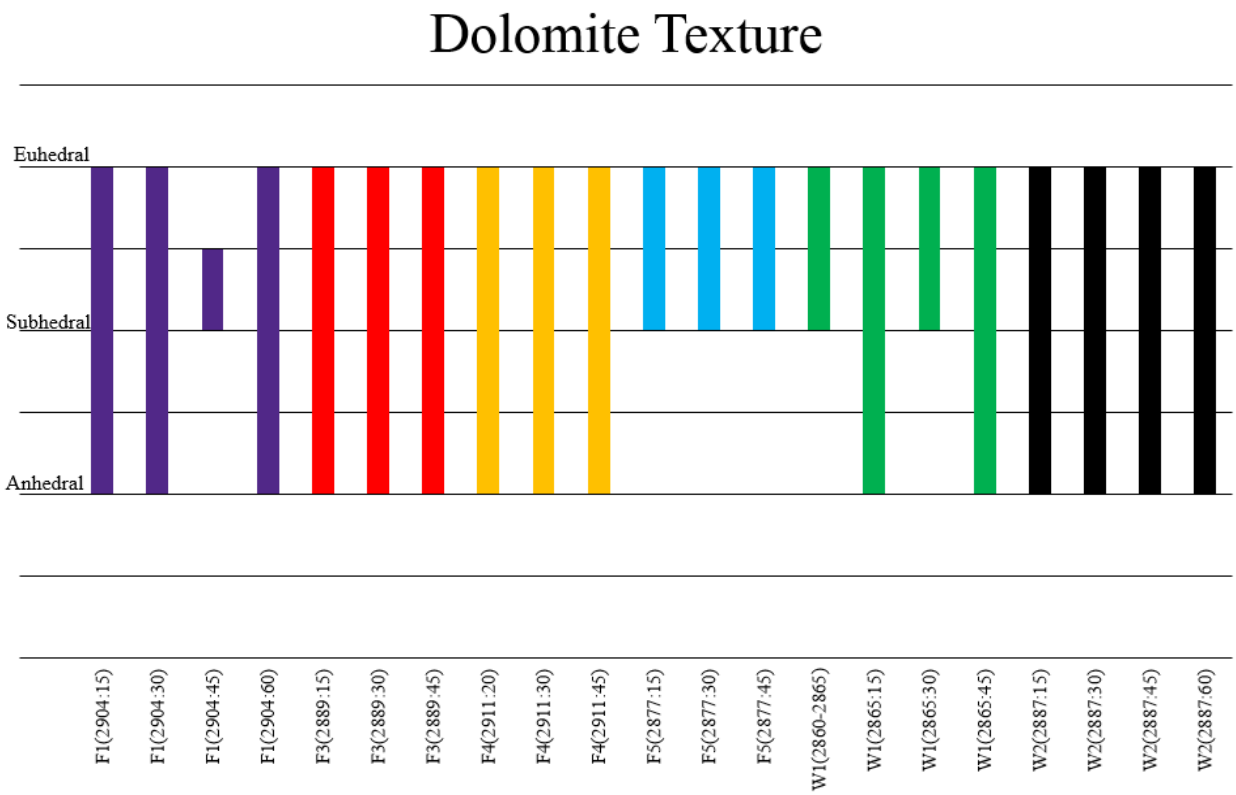

Figure 41: Floating bar graph showing the dolomite textures observed for each thin section. Thin section samples are shown on the X-axis with F1 representing Fearon 1, F3 (Fearon 3), F4 (Fearon 4), F5 (Fearon 5), W1 (Wagner M.C 1), and W2 representing Wagner M.C 2. Crystal sizes are on the Y-axis. As an example of how to read the graph, the sample F1(2904:15) is a thin section created from the Fearon 1 well at 2904 feet and 15-minute circulation time interval. For this sample the graph shows that there are anhedral, subhedral, and euhedral dolomite textures present.

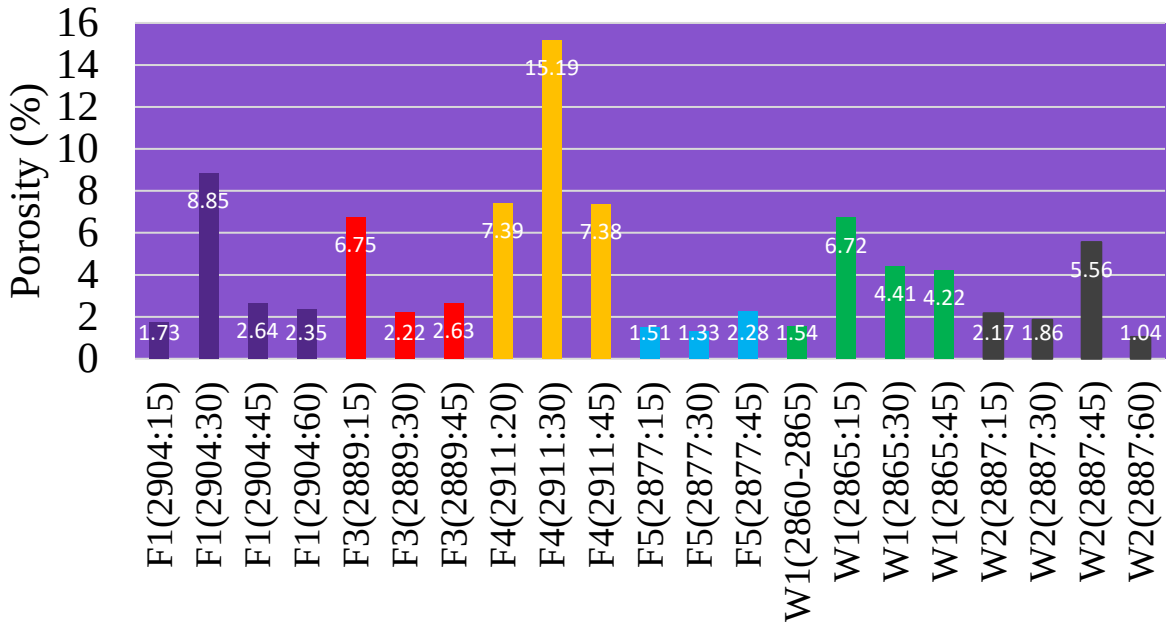

Figure 42: Graph showing ImageJ porosity estimations for each one of the thin sections. Thin section samples are shown on the X-axis with F1 representing Fearon 1, F3 (Fearon 3), F4 (Fearon 4), F5 (Fearon 5), W1 (Wagner M.C 1), and W2 representing Wagner M.C 2. As an example of how to read the graph, the sample F1(2904:15) is a thin section created from the Fearon 1 well at 2904 feet and 15-minute circulation time interval.

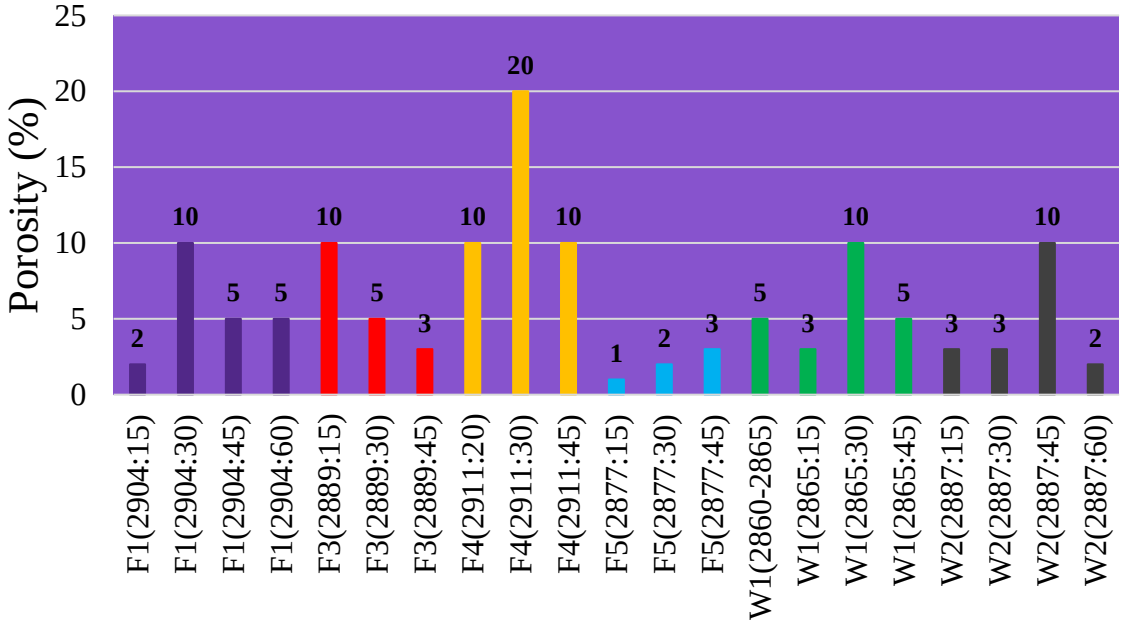

Figure 43: Graph showing visual porosity count estimations for each one of the thin sections. Thin section samples are shown on the X-axis with F1 representing Fearon 1, F3 (Fearon 3), F4 (Fearon 4), F5 (Fearon 5), W1 (Wagner M.C 1), and W2 representing

Wagner M.C 2. As an example of how to read the graph, the sample F1(2904:15) is a thin section created from the Fearon 1 well at 2904 feet and 15-minute circulation time interval.

Porosity Averages

ImageJ porosity estimates and visual porosity count estimates were averaged for all six wells using porosity estimates for all thin sections examined during this study. Average ImageJ porosity estimates and average visual porosity estimates are presented in the table below, with visual porosity count averages being higher than that of ImageJ porosity estimate averages (Table 24).

Well Name	ImageJ Average Porosity (%)	Visual Porosity Count Average (%)
Fearon 1	3.9	7.0
Fearon 3	3.9	7.7
Fearon 4	10.0	14.7
Fearon 5	1.7	3.3
Wagner M.C 1	4.2	8.5
Wagner M.C 2	2.7	4.8

Table 24: Table summarizing the average of ImageJ porosity estimates for each well.

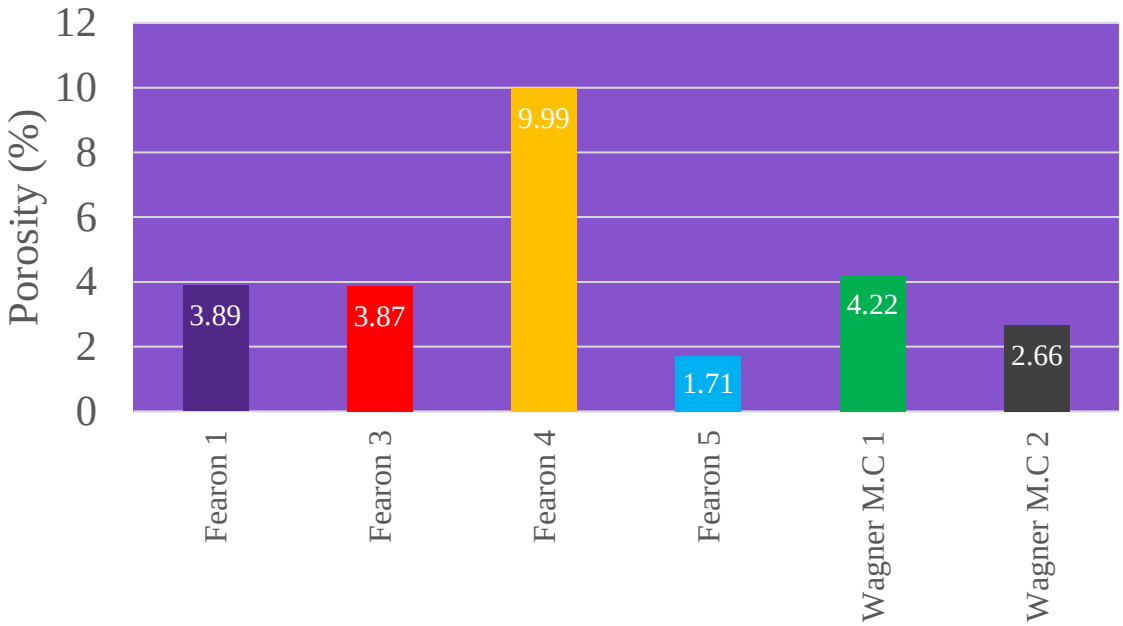

Figure 44: Graph showing the average porosity of each well using ImageJ porosity estimates.

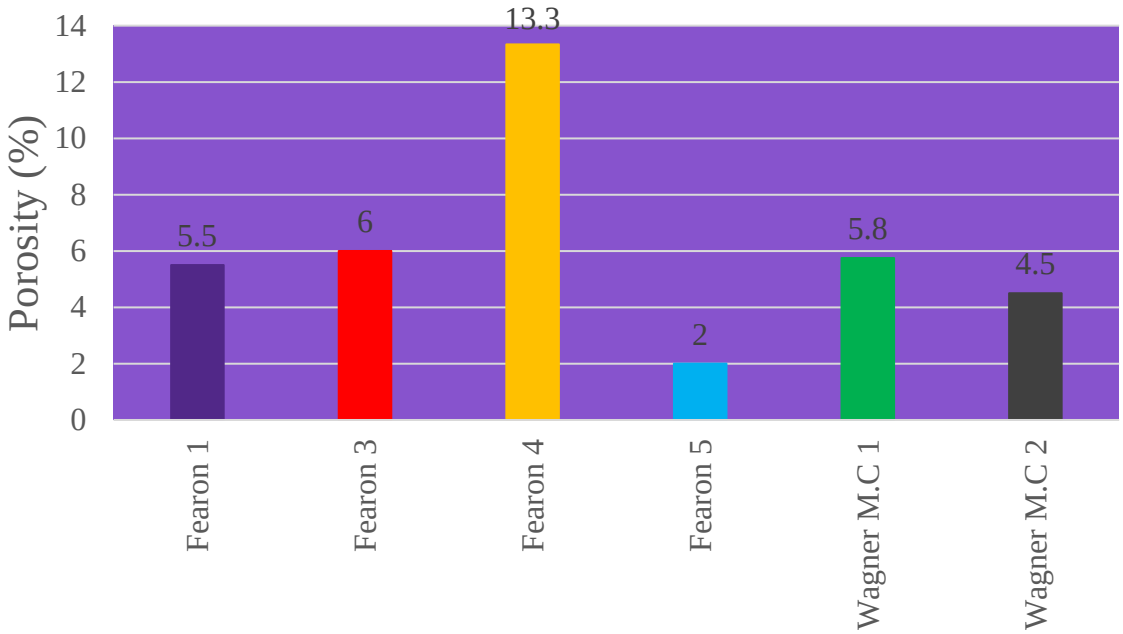

Figure 45: Graph showing the average porosity of each well using visual porosity count estimations.

Carbonate Mineralogy

Six thin sections were analyzed using alizarin iron cyanide red stain, of which none showed signs of staining, as summarized in Table 25 below. Meaning no limestone is present in the thin sections, but instead all of the cuttings are composed of dolomite.

Well Name (Depth and Circulation Time)	ImageJ Porosity Estimate	Staining Present or Not Present
Wagner M.C 2 (2887 ft, 60 minutes)	1.0%	Not Present
Fearon 5 (2877 ft, 30 minutes)	1.3%	Not Present
Wagner M.C 1 (2865 ft, 30 minutes)	4.4%	Not Present
Wagner M.C 2 (2887 ft, 45 minutes)	5.6%	Not Present
Fearon 1 (2904 ft, 30 minutes)	8.8%	Not Present
Fearon 4 (2911 ft, 30 minutes)	15.2%	Not Present

Table 25: Table summarizing the results of alizarin iron cyanide staining of selected thin sections.

Structure Map on Top of Viola

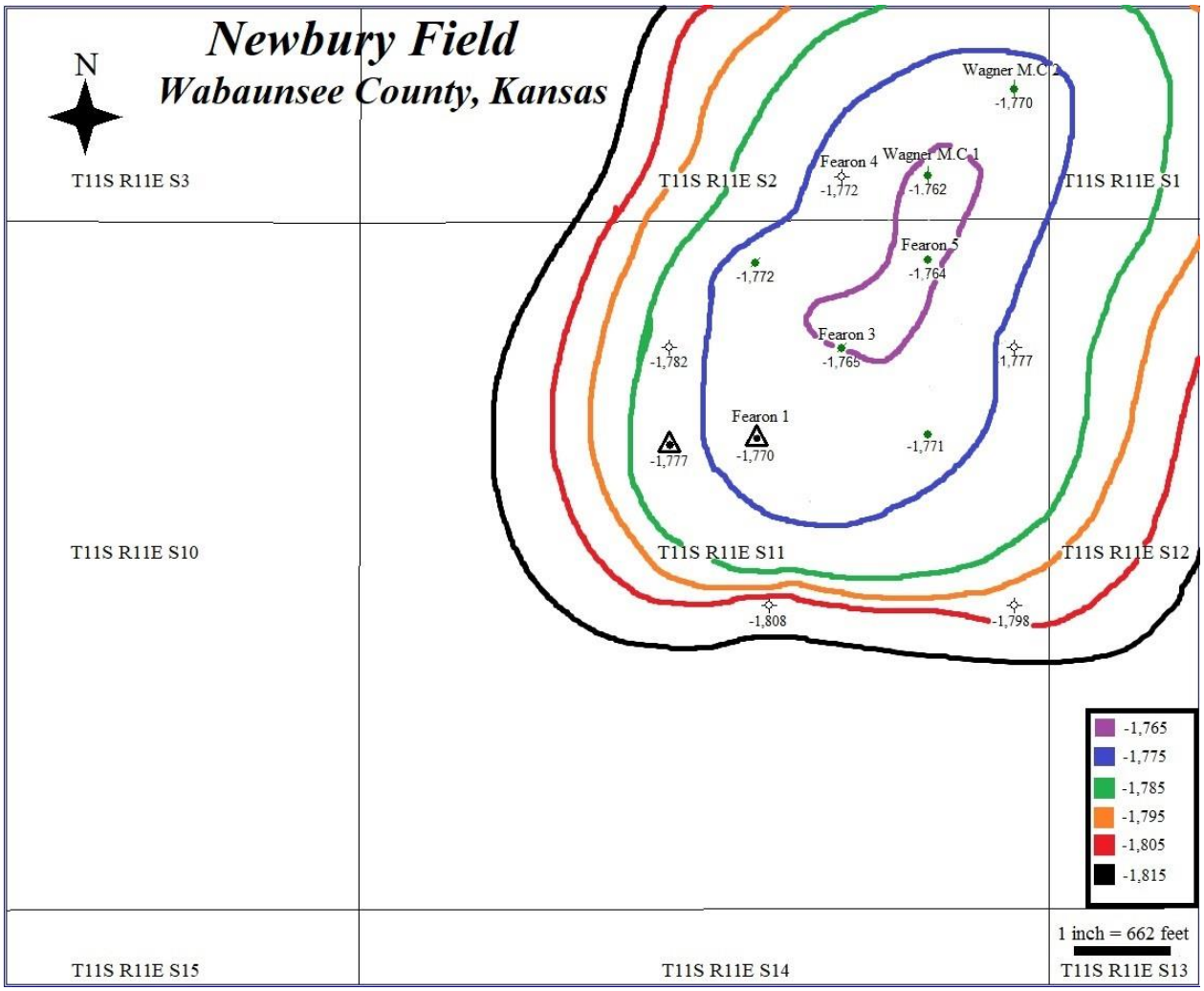

Figure 46: Structure map of the top of the Viola formation in Newbury field. The structure map depicts a concentric anticline with the highest point being at the center and lowest points along the flank of the anticline. The highest contour line is 1,765 feet below sea level, while the lowest contour line is 1,810 feet below sea level. Contour interval, the change in depth between each contour line, is five feet. Contour lines that are closely spaced represent rapid elevation change, while widely spaced contour lines represent areas with slow elevation change.

Oil Reserves

Due to the lack of resistivity logs, the oil-water contacts were derived by looking at drill stem tests and identifying the well with the deepest oil production, i.e. 1,780 feet below sea level, and adding five and 15 feet onto that depth. Five and 15 feet were added to the deepest production depth to act as a buffer because the oil-water contact cannot be accurately located. Using an estimated oil-water contact at 1,785 feet below sea level, volume of the reservoir was calculated to be 3,288.862 acre-feet. Reserves using a porosity of 4.27%, oil saturation of 24.25%, a recovery factor of 70%, and a volume of 3,288.862 acre-feet were calculated to be 184,940.95 barrels of oil. Using the same volume, oil saturation, and recovery factor, but a porosity of 7.56% returned a reserves calculation of 327,436.44 barrels of oil. Volume of the reservoir was calculated to be 7,084.596 acre-feet for an oil water contact 1,795 feet below sea level. Calculating oil reserves using a porosity of 4.27%, oil saturation of 24.25%, a recovery factor of 70%, and a volume of 7,084.596 acre-feet, gave a value of 398,384.58 barrels of oil. Keeping volume, oil saturation, and recovery factor the same, but changing the porosity to 7.56% yielded an oil reserves calculation of 705,336.64 barrels of oil. Using the average of porosity of each well using visual porosity counts at 6.20 %, returned oil reserve values of 271,577.74 barrels of oil for the 1,785 foot oil-water contact, and 578,450.68 barrels of oil for the 1,795 foot oil-water contact. Using the average of porosity observed at Davis Ranch field and John Creek field, 15.00%, as a proxy, returned oil reserve values of 649,675.47 barrels of oil for the 1,785 foot oil-water contact, and 1,399,477.46 barrels of oil for the 1,795 foot oil-water contact.

Oil Water Contact (Feet Below Sea Level)	Volume (Acre-Feet)	Porosity (%)	Oil Saturation (%)	Recovery Factor (%)	Recoverable Oil Reserves (Barrels)
1,785	3,288.862	4.27	24.25	70	184,940.95
1,785	3,288.862	6.20	24.25	70	271,577.74
1,785	3,288.862	7.56	24.25	70	327,436.44
1,785	3,288.862	15.00	24.25	70	649,675.47
1,795	7,084.596	4.27	24.25	70	398,384.58
1,795	7,084.596	6.20	24.25	70	578,450.68
1,795	7,084.596	7.56	24.25	70	705,336.64
1,795	7,084.596	15.00	24.25	70	1,399,477.46

Table 26: Table showing the different parameters used to do oil reserve calculations, and the results of each calculation in terms of recoverable oil reserves.

Chapter 5 - Discussion

Structure of Fields in the Forest City Basin of Northeast Kansas

The one consistent factor when looking at most oil fields that produce from the Viola formation in the Forest City basin is production from small structural traps that manifest themselves in the form of anticlines (Figure 47) (Wells, 1971). That is not to say that there are no other potential trapping mechanisms. Wells (1971) suggested that facies changes from limestone to dolomite in the upper portion of the Viola formation may cause areas of reduced porosity to be adjacent to rocks with favorable porosity, thus forming stratigraphic traps (Wells, 1971). The possibility of more than one trapping mechanisms existing within a single field could explain the wide variation in cumulative oil production between fields producing from the Viola formation in northeast Kansas.

Newbury field, like most other fields in the area, is a classic four-way closure anticlinal trap (Figure 46). Structural similarities of oil fields in the Forest City basin of northeastern Kansas allow for comparison between fields using volumetric values that give an insight into potential factors affecting oil production. The number of barrels produced per acre-foot of the Viola formation at Newbury field is comparable with that of Davis Ranch field, one of the most prolific fields in the Forest City basin of northeastern Kansas.

Area values determined as described in the methods section for oil reserve calculations, and oil column thicknesses were used in conjunction with Simpson's rule to determine the reservoir volume of Viola formation at both fields. Two volume values were calculated for Newbury field based on two separate oil column thickness hypotheses. Volumes of 3288.87 and 7084.60 acre-feet were calculated for the Viola formation at Newbury field using 23-foot and 33-foot oil columns, respectively. At Davis Ranch field the volume of the Viola formation reservoir

was determined to be 15498.09 acre-feet using an oil column thickness of 63 feet (Smith and Anders, 1951).

Historical production values for Newbury field and Davis Ranch field were divided by their respective volumes to obtain the barrels of oil produced per acre-feet of reservoir volume and to eliminate the effects of unequal reservoir dimensions. At an oil column thickness of 23 feet and historical production of 507,894 barrels of oil, Newbury field has produced 154.43 barrels of oil per acre-foot of Viola formation. When the oil column thickness was changed to 33 feet the number of barrels produced per acre-foot of Viola formation decreased to 71.69. Newbury field has produced less oil per acre-foot of Viola formation when compared to Davis Ranch field. Based on historical production values of 9,084,020 barrels of oil and an oil column thickness of 63 feet, 586.14 barrels of oil have been produced per acre-foot of Viola formation at Davis Ranch field.

Depending on the exact depth of the oil-water contact at Newbury field, the volume of the Viola formation above the oil-water contact at Davis Ranch field is roughly two to five times the volume of the Viola formation at Newbury field. But, the historical production of Davis Ranch field is over 17 times greater than Newbury field, meaning that Davis Ranch field produces more barrels per acre-foot of Viola formation. This can only be attributed to differences in porosity and permeability. So, production, for fields within the Forest City basin of northeastern Kansas is affected more by porosity and permeability than structure.

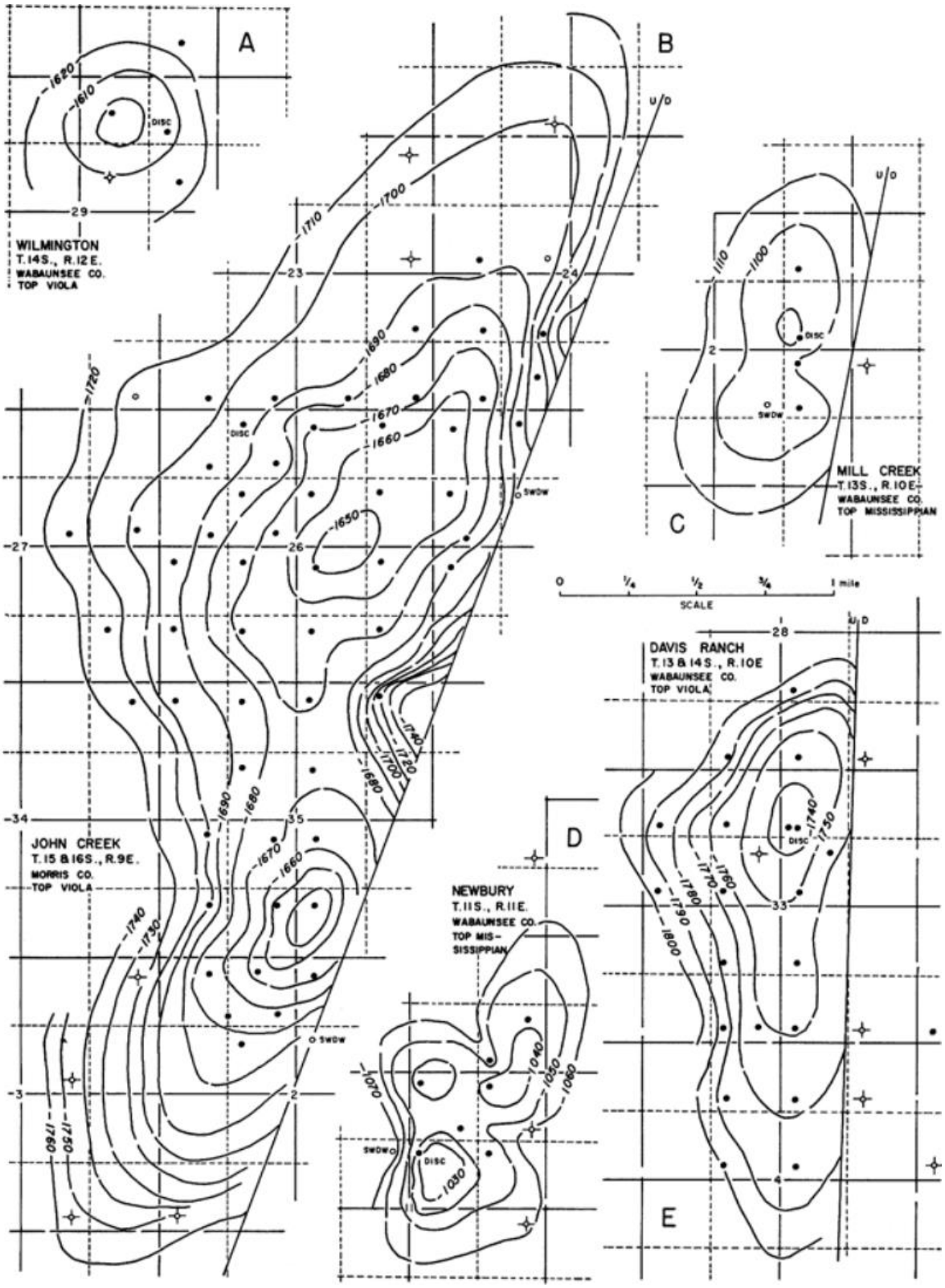

Figure 47: Structure maps of Newbury field, Wilmington field, Mill Creek field, Davis Ranch field, and John Creek field. These fields are in the Forest City basin of northeastern Kansas and manifest themselves as small anticlinal traps. Modified from Merriam (1955).

Crystal Size, Porosity, and Texture

Petrographic analysis was used to evaluate whether variations in crystal size, porosity or texture could explain the variations in production presented above. Unfortunately, there were no well cuttings present for any of the dry wells that were plugged and abandoned, so all the thin sections created and examined were of wells that were oil producers. Therefore, differences in porosity, texture, and crystal size between producing and dry wells could not be evaluated. However, it was possible to compare the porosity, texture, and crystal size of wells that are still producing through 2018 with oil wells that are now plugged and abandoned or inactive. It is worth noting, however, that an analysis of the effect of geologic controls on the production status of wells does not account for any effects that result from drilling failures, completion failures, or economics. In addition, although yearly production, initial production, and drill stem test data were available for the wells studied, the data set was limited by the low number of leases, as well as some inconsistencies and unexplainable variations in the data. Production inconsistencies arise when comparing drill stem tests with initial 24 hour production values. As an example, drill stem tests and initial 24 hour production are presented for Fearon 1 and Fearon 3 oil and gas wells. Drill stem tests for Fearon 1 were run for an hour and 50 minutes, recovering 910 feet of clean oil, and initial 24 hour production was 84.68 barrels of oil. Drill stem tests for Fearon 3 were run for an hour and 30 minutes, recovering 490 feet of clean oil, and initial 24 hour production was 1226 barrels of oil. Drill stem tests directly correlate to initial 24 hour production. If drill stem test results and initial 24 hour production are correctly measured and reported, then a drill stem test recovering more clean oil will produce more oil within the first 24 hours than a drill stem test with lower recovery. Either the drill stem test results, or the initial 24 hour barrel per day values were not accurately measured or were noted incorrectly for wells in Newbury field.

Petrographic analysis of thin sections from the selected wells in Newbury field revealed a large range of crystal sizes, textures, and porosity types. Crystal size ranged from very finely to very coarsely crystalline. Also, all three dolomite textures, euhedral, subhedral, and anhedral, were observed in thin section. Finally, thin sections were dominated by intercrystalline and vuggy porosity types but, fracture and moldic porosity were also observed. Below are discussions of the effects that crystal size, porosity, and texture have on production.

Crystal Size

All but four thin sections examined contained crystal sizes that ranged from either very finely or finely crystalline to coarsely or very coarsely crystalline, suggesting that there were possibly two separate dolomitizing events. Three of the four samples studied from the Fearon 5 well showed a more limited range of crystal sizes (Figure 40, Figure 48). The Wagner MC 1 well also showed a limited crystal size range within the 2860 – 2865 foot interval (Figure 40, Figure 48). These two wells, Fearon 5 and Wagner M.C 1, and their crystal size range limitations are of interest because they are both located at the center of the anticlinal structure and are the shallowest wells that have produced in Newbury field (Figure 43). Fearon 5, which has been recompleted as Reiners 5, is one of two wells still producing oil through 2018 (Yearly and Monthly Production Reiners Lease, 2018). On the other hand, the Wagner M.C 1 well was recompleted as Hund 1 and became inactive in 2009, making it the third longest producing well in Newbury field, with only Fearon 5 and Fearon 6, which was recompleted as Reiners 6, producing longer (Yearly and Monthly Production Reiners Lease, 2018). Unfortunately, cuttings do not exist for Fearon 6, so further analysis of the well was not possible. However, Wagner M.C 1, Fearon 5, and Fearon 6 are aligned along a north south array (Figure 43). The more

homogeneous crystal size range found in these wells may mean these locations were only exposed to fewer episodes or a shorter duration of dolomitization than the surrounding areas. Being subjected to fewer or shorter duration dolomitization events may mean the Viola formation did not surpass 95% dolomitization, and thus retained more effective porosity than areas subjected to more or longer duration dolomitizing events (Qing Sun, 1995). However, Wagner M.C 1 and Fearon 5, both located near the center of the structure and within the north to south array of inactive and active oil wells, have low ImageJ porosity estimates of 4.2% and 1.7% (Figure 50). By comparison, Fearon 4, which was plugged and abandoned after 10 years of production, has the best ImageJ average porosity of any wells studied at 10.0%. Fearon 4 contained very finely to coarsely crystalline dolomite, unlike the medium to coarsely crystalline dolomite found in wells that are still producing (Figure 49). So, it appears that the wells with larger variations in dolomite crystal size have greater porosity, but lower production longevity. This may be explained by quicker oil production due to the higher porosity, which causes faster encroachment of water toward the bore hole. Once enough water has made its way to the bore hole, it is no longer economical to transport the water produced per barrel of oil, so the holes are plugged and abandoned.

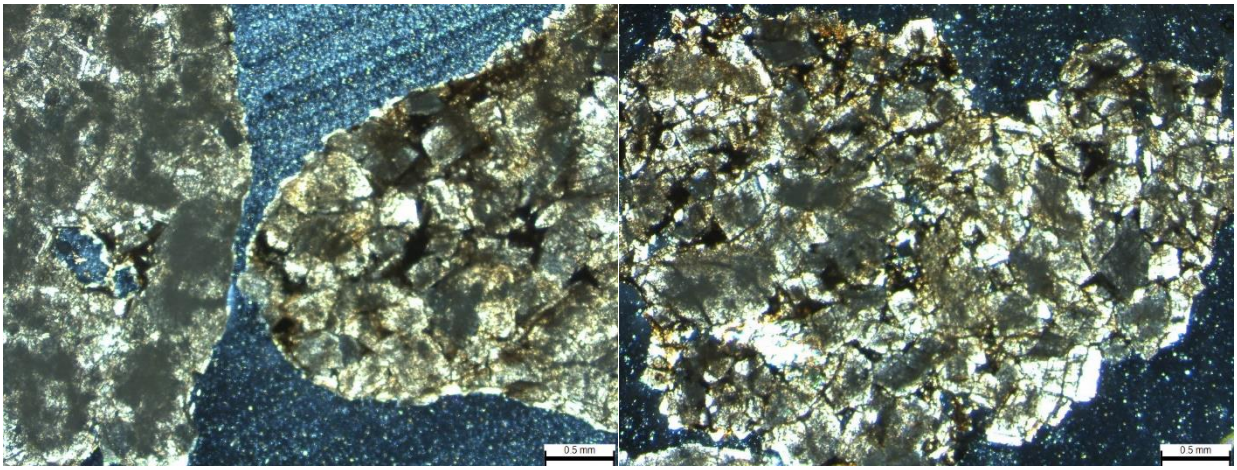

Figure 48: Image on the left is a thin section from Fearon 5, while the image on the right is from Wagner M.C 1. Both thin sections show a small variation in crystal size present, ranging from medium to coarsely crystalline.

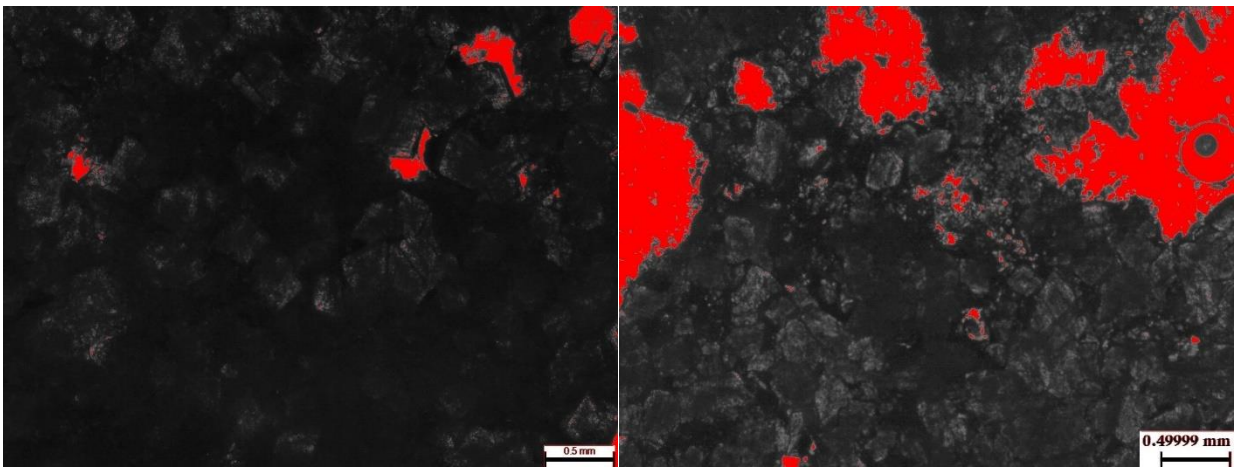

Figure 49: Images of Fearon 5 on the left and Fearon 4 on the right. The red coloration shows the contrast in porosity between the two wells. Fearon 5 has an ImageJ average porosity of 1.7% while Fearon 4 has an ImageJ average porosity of 10.00%. Differences in crystal size are also represented. Fearon 5 is composed of medium to coarsely crystalline dolomite and Fearon 4 is comprised of very finely to coarsely crystalline dolomite.

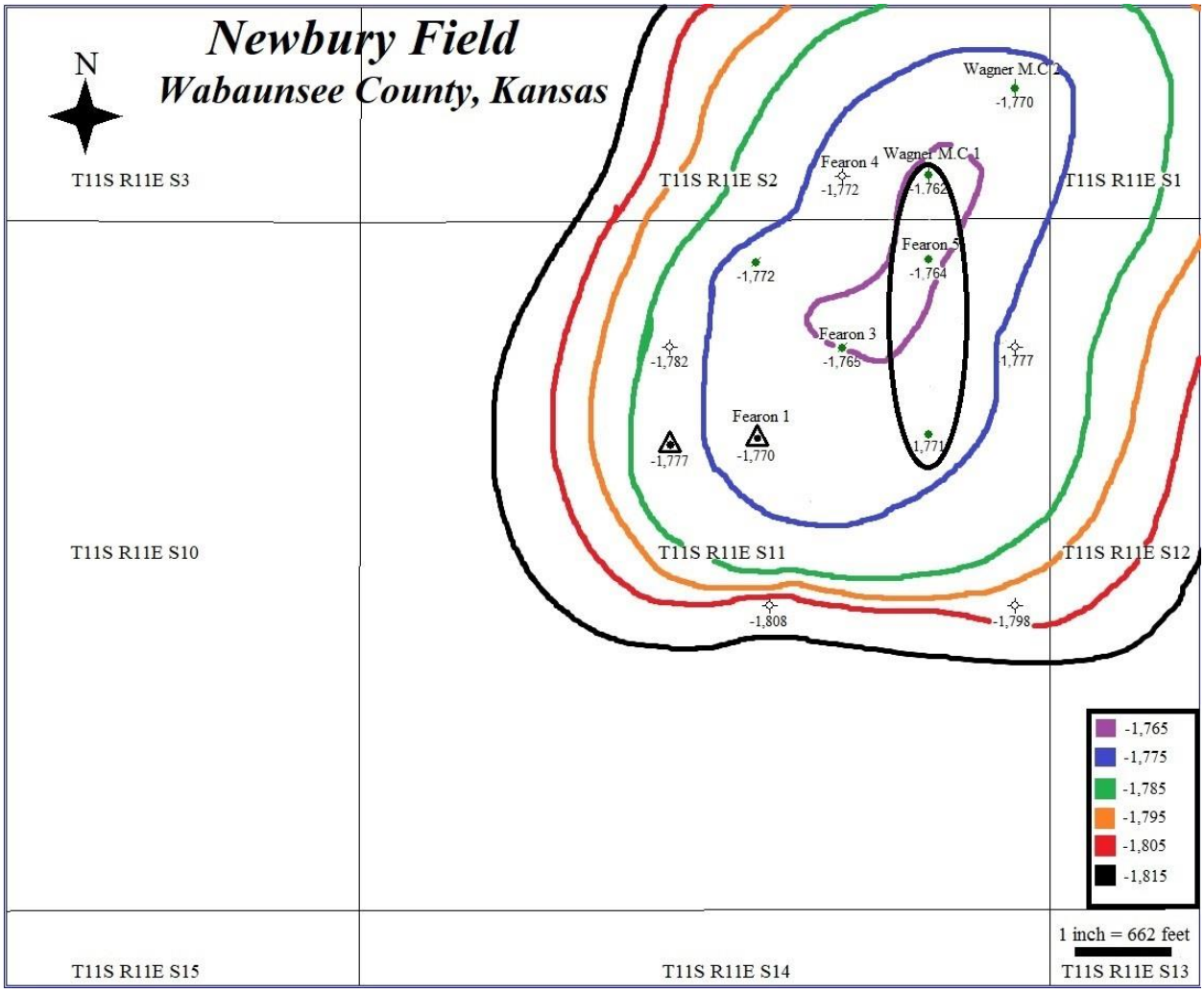

Figure 50: Structure map on top of the Viola formation showing Wagner M.C 1, Fearon 5, and Fearon 6 enclosed in the black circle, showing the north south array of the three wells.

Dolomite Texture

Examination of dolomite textures in thin section revealed that all three textures (euhedral, subhedral and anhedral) are present, but there is not a lot of variation between samples. All but one sample contained well-defined euhedral dolomite crystals combined with subhedral or anhedral dolomite crystals (Figure 41, Figure 51). With so little textural variation among the samples, it is difficult to determine whether texture influences Viola formation reservoir quality at Newbury field. An extensive in-depth study looking at the ratio of individual textures present

in thin sections would need to be conducted to determine whether a specific texture affects porosity and production.

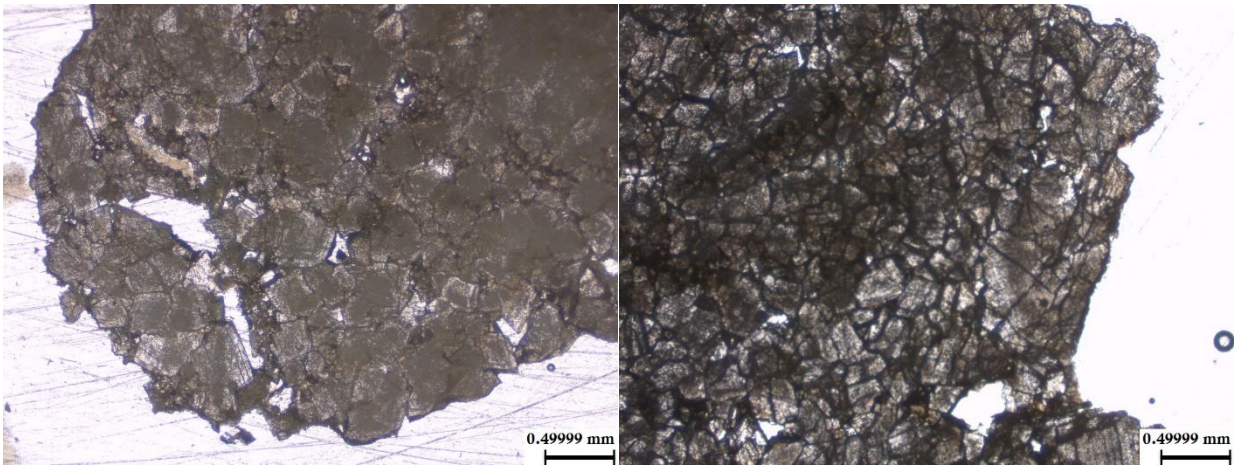

Figure 51: Thin section from Fearon 3 on the left showing euhedral, subhedral, and anhedral dolomite crystals all present in a single cutting, while only subhedral dolomite crystals are present in the thin section from Fearon 1 on the right.

Porosity

All four of the important dolomite porosity types were present during this study, but intercrystalline and vuggy porosity were the most prevalent. Fearon 5, the only active producer in the study, had the lowest overall porosity estimates based on the ImageJ analysis. The three thin sections created for Fearon 5 had an ImageJ average porosity of just 1.7% even though intercrystalline, vuggy, and moldic porosity were observed (Figure 44). Cutting samples may have contributed to the low porosity estimates as cuttings are not representative of any larger fracture porosity, or large vuggy porosity due to the small size of well cuttings. Unfortunately, with no core available, and only one porosity log penetrating the Viola formation, it was only possible to estimate porosity from the available well cuttings.

In contrast, Fearon 4 showed the highest average ImageJ porosity estimate at 10.0% (Figure 44). It was also the only well in which ooids were observed. With significant porosity

located between the ooids, these samples yielded the highest ImageJ porosity estimates at 15.2%. Thus, given that the Fearon 4 well, which is located away from the top of structure, exhibits high porosity, but no longer produces oil, demonstrates that porosity and permeability are not the only factors contributing to production, but crystal size and dolomite texture also have an effect on production.

Newbury Field Structure and Its Effect on Field Production

Classic anticlinal traps have production focused on the central high of the structure, with production fading off as wells approach the flanks. Within the central group of wells located on the anticlinal structure studied here, there is a wide range of current production variation (Table 27, Figure 41). There are four wells within this group that are either inactive or currently producing wells. These wells are: Fearon 5, Fearon 6, Wagner M.C 1, and Wagner M.C 2 (Figure 41). Wagner M.C 1 and Wagner M.C 2 are both inactive wells that were active up to the early to late 2000's (Kansas Geological Survey Interactive Oil and Gas Wells and Fields, 2018). Fearon 5 and Fearon 6 are both active wells, producing small amounts of oil after being put back on production in 2018 (Yearly and Monthly Production Reiners Lease, 2018). There are also two oil wells that were plugged and abandoned within the main group of wells (Figure 41). These plugged and abandoned oil and gas wells are Fearon 4 and Fearon 3 (Figure 41). Fearon 1 was previously an oil-producing well that was later converted to a saltwater disposal well (Figure 41). Lastly, Fearon 7, Margaret Hund 1, and Zeller 1 were all dry holes that were plugged and abandoned (Figure 41). Even at the center of the structure, production is variable: Fearon 5 is an active well; Wagner, M.C 1 is, an inactive well, and Fearon 3 was plugged and abandoned

(Figure 41). So, production, even at the center of structure is variable, meaning structure is not the only factor controlling production in Newbury field.

The idea that multiple factors control production is supported by the characteristics of Fearon 6 and Margaret Hund 1. Fearon 6 is producing oil from 1771 to 1775 feet, which is at the same or lower depth than Margaret Hund 1, but the latter is a dry well that was plugged and abandoned. If production was only affected by structure, then Margaret Hund 1 should have produced oil as well.

Comparing the characteristics of Fearon 5 to those of Wagner M.C 1, both located toward the top of the structure, reveals interesting petrographic differences between the two wells (Figure 48). Fearon 5 is comprised of medium to coarsely crystalline dolomite that exhibits euhedral to subhedral texture throughout the pay zone. Porosity ranges from intercrystalline at the top of the pay zone to intercrystalline, vuggy, and moldic toward the bottom of the pay zone. Wagner M.C 1 is made up of medium to coarsely crystalline dolomite at the top of the pay zone, which changes to finely to coarsely crystalline further down the pay zone. Dolomite texture alternates from euhedral to subhedral and euhedral to anhedral throughout the pay zone. Porosity type for Wagner M.C 1 varies between intercrystalline at the top and bottom of the pay zone, with intercrystalline and vuggy comprising the center of the pay zone. Despite the similarities in dolomite texture, average porosity for Fearon 5 determined by ImageJ is only 1.7%., whereas average porosity calculated using ImageJ for Wagner M.C 1 is 4.2%. Fearon 5 is currently producing oil, while Wagner M.C 1 is an inactive well. Therefore, these values do not support porosity being the only influence on production. Furthermore, the fact that both wells are located on the structural high with one producing and one being inactive means that some factor other than structure is controlling production. The data, therefore, suggest that a combination of factors

control production. One such possibility is that zones of extensive dolomitization destroyed effective porosity and permeability, preventing the migration of significant hydrocarbons into certain areas of the structure. But, more in-depth research would need to be done to determine this.

The lack of a significant number of wells in Newbury field made detailed analysis of the structure map difficult. Ideally, there would be more wells drilled all over the Viola structure at Newbury field, but there are not.

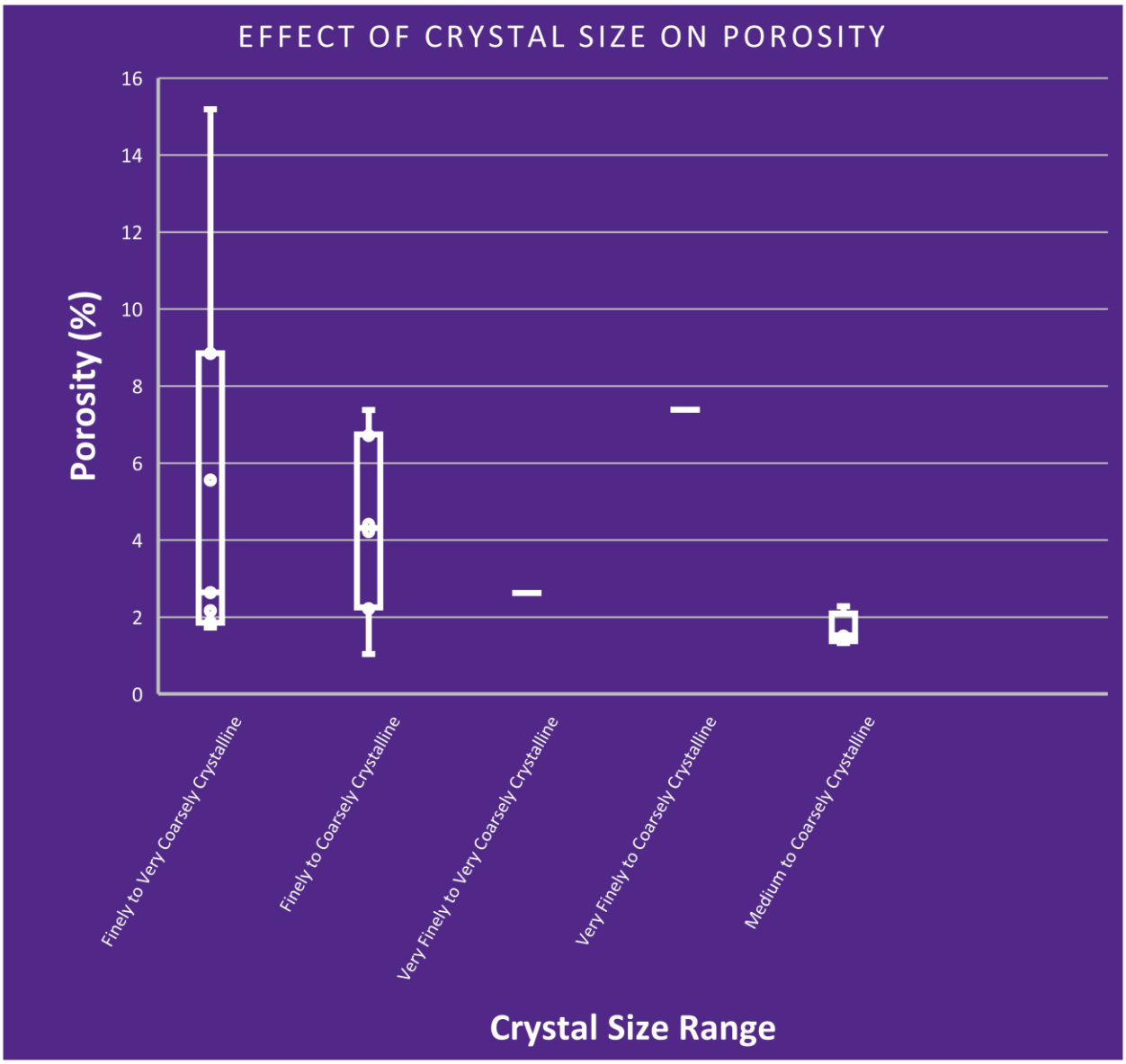

Figure 52: Box and whisker plot showing the porosity values associated with different crystal size ranges observed during the study. The porosity estimates used to make this graph came from ImageJ and underestimate the actual porosity found at Newbury field.

Well Name	Crystal Size Range	Texture	Porosity Types	ImageJ Average Porosity (%)	Production Status in 2019	Year of Completion and Year Production Stopped	Initial Production (Barrels of Oil Per Day)
Fearon 1	Finely to Very Coarsely Crystalline	Euhedral to Anhedral	Intercrystalline, Vuggy	3.9	Converted to Saltwater Disposal Well	1950-Unknown	84.68
Fearon 3	Very Finely to Very Coarsely Crystalline	Euhedral to Anhedral	Intercrystalline, Vuggy	3.9	Plugged and Abandoned	1951-1965	1226
Fearon 4	Very Finely to Coarsely Crystalline	Euhedral to Anhedral	Intercrystalline, Vuggy, Fracture	10.0	Plugged and Abandoned	1951-1961	360
Fearon 5	Medium to Coarsely Crystalline	Euhedral to Subhedral	Intercrystalline, Vuggy, Moldic	1.7	Producing	1951-N/A	529
Wagner M.C 1	Finely to Coarsely Crystalline	Euhedral to Anhedral	Intercrystalline, Vuggy	4.2	Inactive	1951-2008	323.64
Wagner M.C 2	Finely to Very Coarsely Crystalline	Euhedral to Anhedral	Intercrystalline, Vuggy	2.7	Inactive	1951-2008	77.22

Table 27: Table summarizing the geologic controls observed, 2019 production status, and initial production of each well.

Oil Reserves

Oil reserves were calculated to estimate the barrels of recoverable oil still in place at Newbury field. Knowing the recoverable reserves in place provides insight into how economical it would be to pursue further research and oil exploration at Newbury field. Looking at the results presented above, there are three reserve calculations that are lower than the 507,894 barrels of oil already produced at Newbury field, which is not possible if the parameters used in the calculations are accurate representations of the conditions at Newbury field (Table 26) (Newbury—Oil and Gas Production, 2018). According to the results, at an oil water contact of 1,785 feet below sea level and porosity values of 4.3%, from ImageJ, 6.2%, from visual porosity count, and 7.6%, Newbury field has already produced more oil, than the reserves calculated, i.e. 507,894 barrels actually produced vs 184,940.95, 271,577.74, and 327,436.44 barrels of oil, respectively (Table 26) (Newbury—Oil and Gas Production, 2018). From this it can be determined that either the oil-water contact is at a deeper depth, porosity is higher than the ImageJ porosity averages determined in this study, or the oil saturation is higher than the proxy used. When an oil-water contact of 1,795 feet below sea level was used in determining reserves, values of 398,384.58, 578,450.68, and 705,336.64 barrels of oil were determined using porosity values of 4.3%, 6.2%, and 7.6%, respectively (Table 26). Reserves calculated using the 4.3% porosity value is lower than the volume already produced, while the 7.6% porosity value is higher than the volume already produced at Newbury field. Therefore, actual porosity in the producing Viola intervals is likely higher than the 4.3% average that was determined using ImageJ for Newbury field in this study. It is thought that ImageJ returned low porosity averages for Newbury field due to the fact that cuttings do not represent large scale fracture and large vuggy porosity. Oil reserves calculated using 15.00% porosity, the average of porosity estimated

at Davis Ranch field and John Creek field, as a proxy returned reserve calculations of 649,675.47 barrels of oil for the 1,785 foot oil-water contact and 1,399,477.46 barrels of oil for the 1,795 foot oil-water contact (Table 26). Both reserve calculations using 15.00% porosity are higher than historical production at Newbury field. Showing that average porosity estimated using ImageJ and visual porosity counts are likely lower than the actual porosity representative of the Viola formation at Newbury field. Reserves lower than the historical production of Newbury field were calculated when using porosity values determined through ImageJ and visual porosity count estimates of cuttings, suggesting that only intercrystalline porosity was observed and studied. This means that Newbury field has to be comprised of additional large scale vuggy and fracture porosity in order to explain reserves that have already been produced from Newbury field.

Large-scale fracture and vuggy porosity could potentially explain the low porosity values determined for Newbury field during this study. Along the Nemaha Uplift there are expansive networks of fractures in the surrounding subsurface of the Forest City basin (Safley et al., 1998). Newbury field is close enough to the Nemaha Uplift that vertical fractures may be present beneath and into the Viola formation. These fractures can create or enhance migration pathways that allow larger accumulations of hydrocarbons to be deposited into the Viola formation (Safley et al., 1998). Fracture and vuggy porosity of a large scale, however, does not show up in drill cuttings and may cause porosity estimates to be lower than the actual effective porosity of the Viola formation at Newbury field. Future work studying fractures in the subsurface at Newbury field would need to be completed before this can be validated or rejected.

Comparison with Previous Studies

Both Jensik (2013) and Rennaker (2016) suggested that dolomite crystal size was related to porosity, which was a dominant control on oil production in the Leech and Soldier fields. Leach and Soldier field must contain hydrocarbons within intercrystalline porosity without significant vuggy or fracture porosity. The correspondingly lower reserves reflect this. It is not surprising that these studies came to similar conclusions, as the Leech field and Soldier field are near one another. The results of this study on the Newbury field concluded that samples with dolomite that exhibits a large range of crystal sizes (i.e. very finely or finely crystalline to coarsely or very coarsely crystalline) and that is subhedral to anhedral have higher porosity. In contrast, Jensik (2013) and Rennaker (2016) suggest that samples with larger dolomite crystals that are euhedral have higher porosity. The differences observed may be explained by the spatial distribution of the three fields in question. Solider field and Leech field are located close to one another, whereas Newbury field is located ~25 miles southwest of them.

Chapter 6 - Conclusions

Reservoir characterization can be accomplished using techniques such as well log analysis, core analysis, cuttings analysis, porosity analysis, petrographic analysis, geochemical analysis, seismic data analysis, basin analysis, structural analysis and many other methods. This study focused on cuttings, petrographic, and structural analysis to characterize the Viola formation of Newbury field in Wabaunsee County, Kansas. The objective of this study was to determine what factors, other than structure, were contributing to hydrocarbon production in the field. Newbury field produces a fraction of the oil that some of the largest fields within the Forest City basin produce, and this study aimed to gain insight into why Newbury field does not currently have the same potential as those larger fields. The study also investigated reasons for production variation between wells within Newbury field.

Cuttings were collected and turned into thin sections for six wells in Newbury field and analyzed using a petrographic microscope to determine porosity types present in the field, dolomite textures, and crystal shapes of the dolomite present. Photomicrographs were taken of each thin section and were used to obtain porosity estimates using ImageJ software. A subsurface structure map was created for the Viola formation in Newbury field and was used to locate wells on the structural high, and those on the flank of the anticlinal structure. Due to the complexity that occurred during analysis of the petrographic and porosity information, oil reserves were calculated to determine whether it is economical to pursue further research and exploration of Newbury field.

Variations in production between more prolific fields and Newbury field were determined to not only be controlled by structure alone, but also by porosity. Porosity values within the Viola formation vary largely with spatial distribution due to varying degrees of

dolomitization caused by differences in the number and duration of dolomitizing events that occurred within any given stratigraphic interval. This variation in production between fields may also be attributed to fracture networks in the subsurface around the Nemaha Uplift, but further research needs to be done to confirm this.

Production variation between wells in Newbury field seems to be controlled not only by structure, but also by porosity, crystal size, and crystal texture. Wells that exhibited large ranges of crystal size, such as very finely or finely crystalline to coarsely or very coarsely crystalline, and exhibited subhedral to anhedral texture had higher porosity. These wells appear to have produced oil but saw a fast decline in production (Table 27). Wells that had smaller crystal size ranges, such as medium to coarsely or very coarsely crystalline, and exhibited euhedral dolomite textures had lower porosity. These wells have low production, a combined 86 barrels of oil for the year of 2018 between Fearon 5 and Fearon 6, but have sustained production for a long period of time (Yearly and Monthly Production—Reiners Lease, 2018). This variation in longevity could be attributed to water encroachment causing the more prolific wells to become uneconomical and being plugged and abandoned faster than the slower producing wells.

Total production numbers for individual wells would need to be studied in the future to determine whether the fast or slow producing wells produce more oil over their lifetime to determine a proper exploration model for Newbury field and surrounding anticlinal fields in the immediate vicinity. The results of this study, therefore, are at odds with the findings of Jensik (2013) and Rennaker (2016). There does not seem to be a single exploration model that covers the entirety of fields within the Forest City basin along the western boundary of the basin and the Nemaha Uplift. Rather, there appear to be regions in which are dominated by intercrystalline

porosity, while others include significant vuggy and fracture porosity. The highest reserves are seen in fields that include vuggy and fracture porosity.

Chapter 7 - Bibliography

Adler, F. J., Henslee, H.T., Hicks, I.C., Larson, T.G., Rascoe Jr, B., Caplan, W.M., Carlson, M.P., Goebel, E.D., McCracken, M.H., Wells, J.S., Parker, M.C., and Schramm Jr, M.W., 1971, "Future petroleum provinces of the Midcontinent: An Overview." *AAPG Memoir 15*, v. 2, p. 985-1120. *AAPG Datapages.*

Adkinson, W.L., 1972, "Stratigraphy and Structure of Middle and Upper Ordovician Rocks in the Sedgwick Basin and Adjacent Areas, South-Central Kansas." *Geological Survey Professional Paper 702*, p. 1-33. *AAPG Datapages.*

Al-Awadi, M., Clark, W.J., Moore, W.R., Herron, M., Zhang, T., Zhao, W., Hurley, N., Kho, D., Montaron, B., Sadooni, F., 2009, "Dolomite: Perspectives on a Perplexing Mineral." *Oilfield Review Autumn 2009 3,* v. 21, p. 32-45.

Allan, J.R., Wiggins, W.D., 1993, "Dolomite Reservoirs: Geochemical Techniques for Evaluating Origin and Distribution." *AAPG Continuing Education Course Note Series 36*, p. 1-129. *AAPG Datapages.*

Anderson, K.H., Wells, J.S., 1968, "Forest City Basin of Missouri, Kansas, Nebraska, and Iowa." *AAPG Bulletin 2,* v. 52, p. 264-281. *AAPG Datapages.*

Baars, D.L., Watney, L.W., Steeples, D.W., and Brostuen, E.A., 1989, "Petroleum: A Primer for Kansas." *Kansas Geological Survey Education Series 7,* p. 9. *Kansas Geological Survey.*

Casey—Oil and Gas Production. 2018. *Kansas Geological Survey.* Retrieved from https://chasm.kgs.ku.edu/ords/oil.ogf4.IDProdQuery?FieldNumber=1000150505

Charpentier, R.R., 1995, “Forest City Basin Province (056).” *USGS.*

Choquette, P.W., Pray, L.C., 1970, “Geologic Nomenclature and Classification of Porosity in Sedimentary Carbonates.” *AAPG Bulletin 2,* v. 54, p. 207-250. *AAPG Datapages.*

Davis Ranch—Oil and Gas Production. 2018. *Kansas Geological Survey.* Retrieved from https://chasm.kgs.ku.edu/ords/oil.ogf4.IDProdQuery?FieldNumber=1000152582

Dolton, F.L., and Finn, T.M., 1989, “Petroleum Geology of the Nemaha Uplift, Central Mid-Continent.” p. 1-32. *AAPG Datapages.*

Gay Jr, S.P., 2003, “The Nemaha Trend-A System of Compressional Thrust-Fold, Strike-Slip Structural Features in Kansas and Oklahoma, Part 1.” *The Shale Shaker 1,* v. 54, p. 9-17. *AAPG Datapages.*

Hartmann, D.J., and Kieke, E.M., 1973, “Scanning Electron Microscope Application to Formation Evaluation.” *Transactions-Gulf Coast Association of Geological Societies,* vol. XXIII, p. 60-67. *AAPG Datapages.*

Hatch, J.R., Newell, K.D., 1999, “Geochemistry of Oils and Hydrocarbon Source Rocks from the Forest City Basin, Northeastern Kansas, Northwestern Missouri, Southwestern Iowa, and Southeastern Nebraska.” *Kansas Geological Survey, Technical Series 13.*

Hyne, N.J., 2001, “Nontechnical Guide to Petroleum Geology, Exploration, Drilling, and Production.” Chapter 25. *Google Books.*

James, A., King, C., Lewis, J. P., 1960, "Kansas Oil and Gas Fields Volume III Northeastern Kansas with Special Contributions Covering SE Nebraska and NW Missouri." p. 49-55. *AAPG Datapages.*

Jensik, C., 2013, "Geologic Controls on Reservoir Quality of the Viola Limestone in Soldier Field, Jackson County, Kansas." *Thesis. Kansas State University, Department of Geology. K-State Research Exchange.*

John Creek—Oil and Gas Production. 2018. *Kansas Geological Survey.* Retrieved from https://chasm.kgs.ku.edu/ords/oil.ogf4.IDProdQuery?FieldNumber=1000149927

Kansas Geological Survey Interactive Oil and Gas Wells and Fields. 2018. *Kansas Geological Survey*. Retrieved from http://maps.kgs.ku.edu/oilgas/index.cfm

Leach—Oil and Gas Production. 2018. *Kansas Geological Survey.* Retrieved from https://chasm.kgs.ku.edu/ords/oil.ogf4.IDProdQuery?FieldNumber=1000149118

Lee, Wallace., 1943, "The Stratigraphy and Structural Development of the Forest City Basin in Kansas." *Kansas Geological Survey Bulletin 51,* p. 1-7. *Kansas Geological Survey.*

Lewis, J.P., 1960, "Newbury Field." *Kansas Oil and Gas Fields: Northeastern Kansas with Special Contributions Covering SE Nebraska and NW Missouri,* v. 3. *AAPG Datapages.*

Malvic, T., Rajic, R., Slavinic, P., Zelenika, K.N., 2014, "Numerical Integration in Volume Calculation of Irregular Anticlines." *Rudarsko Geolosko Nftni Zboornik,* v. 29, p. 1-8, *ResearchGate.*

Mazzulo, S., J., 2004, "Overview of Porosity Evolution in Carbonate Reservoirs." *Kansas Geological Society Bulletin,* v. 79. *AAPG Datapages.*

McClain—Oil and Gas Production. 2018. *Kansas Geological Survey*. Retrieved from https://chasm.kgs.ku.edu/ords/oil.ogf4.IDProdQuery?FieldNumber=1000149995

Merriam, D.F., 1955, "Structural patterns in western Kansas." *Kansas Geological Society 18th Field Conference Guidebook,* p. 80-87, *Kansas Geological Survey.*

Newbury—Oil and Gas Production. 2018. *Kansas Geological Survey*. Retrieved from https://chasm.kgs.ku.edu/ords/oil.ogf4.IDProdQuery?FieldNumber=1000152587

Newel, D.K., Watney, L.W., Stephens, P.B., Hatch, R.J., 1987, "Hydrocarbon Potential in Forest City Basin." *Oil and Gas Journal,* v. 88, p. 58-62.

Newell, D.K., Watney, L.W., Cheng, S.W.L., Brownrigg, R.L., 1987, "Stratigraphic and Spatial Distribution of Oil and Gas Production in Kansas." *Kansas Geological Survey, Subsurface Geology Series 9,* p. 2. *Kansas Geological Survey.*

Paxico—Oil and Gas Production. 2018. *Kansas Geological Survey.* Retrieved from https://chasm.kgs.ku.edu/ords/oil.ogf4.IDProdQuery?FieldNumber=1000152589

Powers, R.B., 1989, "Petroleum Exploration Plays and Resource Estimates, 1989, Onshore United States—Region 7, Mid-Continent." *U.S. Department of the Interior, U.S. Geological Survey.*

Powers, R.W., 1962, "Arabian Upper Jurassic Carbonate Reservoir Rocks." *Classification of Carbonate Rocks; A Symposium,* p. 122-192. *AAPG Datapages.*

Qing Sun, S., 1995, "Dolomite Reservoirs: Porosity Evolution and Reservoir Characteristics." *AAPG Bulletin 2,* v. 79, p. 186-204. *AAPG Datapages.*

Rennaker, J., 2016, "Geologic Controls on Reservoir Quality of the Hunton and Viola Limestones in the Leach field, Jackson County, Kansas." *Thesis. Kansas State University, Department of Geology*. *K-State Research Exchange.*

Richardson, M., 2016, "A Reservoir Characterization of a Portion of the Aldrich Oil Field in Ness County, Kansas: Possible Candidate for Enhanced Recovery." *Thesis. Kansas State University, Department of Geology.*

Safley, L.E., Reeves, T.K., Spakiewicz, M., Guo, G., Volk, L., Banerjee, S., Jordan, J., Johnson, W., Fite, J., George, S., 1998. "Basin Analysis and Exploration Methodologies for the South-Central Mid-Continent Region," *Eight International Williston Basin Symposium,* p. 141-146. *AAPG Datapages.*

Scholle, P.A., Ulmer-Scholle, D.S., 2003, "A Color Guide to the Petrography of Carbonate Rocks: Grains, Textures, Porosity, Diagenesis." *AAPG.* Print.

Sibley, D.F., Gregg, J.M, 1987, "Classification of Dolomite Rock Textures." *Journal of Sedimentary Petrology 6,* v. 57, p. 967-975. *AAPG Datapages.*

Solider—Oil and Gas Production. 2018. *Kansas Geological Survey.* Retrieved from https://chasm.kgs.ku.edu/ords/oil.ogf4.IDProdQuery?FieldNumber=1000149120

Smith, K.R., Anders, E.L., 1951, "The Geology of the Davis Ranch Oil Pool, Wabaunsee County, Kansas." *Kansas Geological Survey Bulletin 90, Part 2. Kansas Geological Survey.*

Steeples, D.W., 1982, "Structure of the Salina-Forest City Interbasin Boundary from Seismic Studies." *Geophysics in Kansas: Kansas Geological Survey Bulletin 226,* p. 31-52. *Kansas Geological Survey.*

U.S. Geological Survey National Oil and Gas Resource Assessment Team, 1995, "1995 National Assessment of United States Oil and Gas Resources: Overview of the 1995 National Assessment of Potential Additions to Technically Recoverable Resources of Oil and Gas—Onshore and State Water of the United States." *U.S. Geological Survey Circular 1118.*

Wells, J.S., 1971, "Petroleum Potential of the Forest City Basin." *AAPG Memoir 15,* v. 2, p. 1098-1103. *AAPG Datapages.*

Weyl, P.K., 1960, "Porosity Through Dolomitization: Conservation-of-Mass Requirements." *Journal of Sedimentary Petrology 1,* v. 30, p. 85-90. *AAPG Datapages.*

Yearly and Monthly Production Reiners Lease. 2018. *Kansas Geological Survey.* Retrieved from https://chasm.kgs.ku.edu/ords/oil.ogl5.MainLease?f_lc=1001109726

Zeller, D.E., 1968, "The Stratigraphic Succession in Kansas." *Kansas Geological Survey Bulletin 189,* p. 6. *Kansas Geological Survey.*